# NAVAL POSTGRADUATE SCHOOL
## Monterey, California






# THESIS

DESIGN, SIMULATION, AND EXPERIMENTAL VERIFICATION OF A COMPUTER MODEL AND ENHANCED POSITION ESTIMATOR FOR THE NPS AUV II

by

David C. Warner

DECEMBER 1991

Thesis Advisor: Fotis Papoulias



Approved for public release: Distribution is unlimited

Unclassified

SECURITY CLASSIFICATION OF THIS PAGE

## REPORT DOCUMENTATION PAGE

Form Approved OMB No. 0704-0188

| | |
|---|---|
| 1a. REPORT SECURITY CLASSIFICATION: Unclassified | 1b. RESTRICTIVE MARKINGS |
| 2a. SECURITY CLASSIFICATION AUTHORITY | 3. DISTRIBUTION/AVAILABILITY OF REPORT: Approved for public release: Distribution is unlimited |
| 2b. DECLASSIFICATION/DOWNGRADING SCHEDULE | |
| 4. PERFORMING ORGANIZATION REPORT NUMBER(S) | 5. MONITORING ORGANIZATION REPORT NUMBER(S) |
| 6a. NAME OF PERFORMING ORGANIZATION: Naval Postgraduate School; 6b. OFFICE SYMBOL (If applicable): ME | 7a. NAME OF MONITORING ORGANIZATION: Naval Postgraduate School |
| 6c. ADDRESS (City, State, and ZIP Code): Monterey, CA 93943-5000 | 7b. ADDRESS (City, State, and ZIP Code): Monterey, CA 93943-5000 |
| 8a. NAME OF FUNDING SPONSORING ORGANIZATION; 8b. OFFICE SYMBOL (If applicable) | 9. PROCUREMENT INSTRUMENT IDENTIFICATION NUMBER |
| 8c. ADDRESS (City, State, and ZIP Code) | 10. SOURCE OF FUNDING NUMBER: PROGRAM ELEMENT NO. / PROJECT NO. / TASK NO. / WORK UNIT ACCESSION NO. |

11. TITLE (Include Security Classification)
DESIGN, SIMULATION, AND EXPERIMENTAL VERIFICATION OF A COMPUTER MODEL AND ENHANCED POSITION ESTIMATOR FOR THE NPS AUV II

12. PERSONAL AUTHORS
DAVID C. WARNER

| 13a. TYPE OF REPORT | 13b. TIME COVERED FROM ____ TO ____ | 14. DATE OF REPORT (Year, Month, Day) | 15. PAGE COUNT |
|---|---|---|---|
| Engineer's Thesis | | DECEMBER 1991 | 130 |

16. SUPPLEMENTARY NOTATION
The views expressed are those of the author and do not reflect the official policy or position of the Department of Defense or the U.S. Government

| 17. COSATI CODES: FIELD | GROUP | SUB-GROUP | 18. SUBJECT TERMS (Continue on reverse if necessary and identify by block numbers) |
|---|---|---|---|
| | | | autonomous underwater vehicles, computer simulation, marine vehicle dynamics |
| | | | |

19. ABSTRACT (Continue on reverse if necessary and identify by block numbers)

A full six-degree-of-freedom computer model of the Naval Postgraduate School Autonomous Underwater Vehicle (NPS AUV II) is developed. Hydrodynamic Coefficients are determined by geometric similarity with an existing swimmer delivery vehicle and analysis of initial open loop AUV II trials. Comparisons between simulated and experimental results demonstrate the validity of the model and the techniques used. A reduced order observer of lateral velocity was produced to provide an input for an enhanced position estimator. Results are presented which show that the position estimator can be calibrated using AUV II run data to provide a real-time accurate estimate of position.

| 20. DISTRIBUTION/AVAILABILITY OF ABSTRACT | 21. ABSTRACT SECURITY CLASSIFICATION |
|---|---|
| XX UNCLASSIFIED/UNLIMITED __ SAME AS RPT __ DTIC USERS | unclassified |

| 22a. NAME OF RESPONSIBLE INDIVIDUAL | 22b. TELEPHONE (Include Area Code) | 22c. OFFICE SYMBOL |
|---|---|---|
| Fotis Papoulias | (408) 646-3381 | ME/Pa |

DD Form 1473, JUN 86 — Previous editions are obsolete. S/N 0102-LF-014-6603

SECURITY CLASSIFICATION OF THIS PAGE
Unclassified

Approved for public release: Distribution is unlimited

Design, Simulation, and Experimental Verification
of a Computer Model and Enhanced Position Estimator
for the NPS AUV II

by

David C. Warner
Commander, United States Navy
M.S., Northwestern University, 1978

Submitted in partial fulfillment of the
requirements for the degree of

MASTER OF SCIENCE
IN MECHANICAL ENGINEERING

and

MECHANICAL ENGINEER

from the

NAVAL POSTGRADUATE SCHOOL

DECEMBER 1991

Author: _____
David C. Warner

Approved by: _____
Fotis Papoulias, Thesis Advisor

_____
A.J. Healey, Chairman
Department of Mechanical Engineering

## ABSTRACT

A full six-degree-of-freedom computer model of the Naval Postgraduate School Autonomous Underwater Vehicle (NPS AUV II) is developed. Hydrodynamic Coefficients are determined by geometric similarity with an existing swimmer delivery vehicle and analysis of initial open loop AUV II trials. Comparisons between simulated and experimental results demonstrate the validity of the model and the techniques used. A reduced order observer of lateral velocity was produced to provide an input for an enhanced position estimator. Results are presented which show that the position estimator can be calibrated using AUV II run data to provide a real-time accurate estimate of position.

## TABLE OF CONTENTS

## LIST OF TABLES

## LIST OF FIGURES

# I. INTRODUCTION

## A. GENERAL

During the past three decades there has been an increasing interest by the U.S. Navy in the use of unmanned underwater vehicles (UUVs) [Ref. 1]. These vehicles can be either tethered vehicles (TUVs), controlled by a cable, or completely autonomous (AUV). Beginning in mid 1960s the U.S. Navy has used an AUV mobile submarine simulator (MOSS) as a submarine decoy on ballistic missile submarines. In 1988 the U.S. Navy and Charles Stark Draper Laboratory in Cambridge, Massachusetts, initiated a study to determine how UUVs could be employed to meet specific Navy missions. [Ref. 2]

Within the Navy, possible missions for AUVs include submarine, anti-submarine warfare wherein the AUV could conduct surveillance of or act as a decoy to enemy vessels. In a mine warfare roll an AUV could be employed to map an enemy mine field to provide friendly forces with information they could use to find a safe transit of the field. AUVs could be employed to conduct surveillance of harbor activity using a variety of sensors.

Applications of AUV technology are not limited to military missions. AUVs could be programmed to explore areas of the ocean where manned vehicles cannot travel, or where their endurance is limited by fuel and or food supplies.

AUVs could be used in salvage operations to inspect the area prior to employing manned submersibles.

Interest in the applications of AUV technology is evidenced by the growing number of conferences and workshops dedicated to the subject [Ref. 3] [Ref. 4]. The design and operation of AUVs present unique challenges due to the vessel's required ability to operate without human intervention. The control, guidance, and mission control software architectures are exceptionally complex and represent the state-of-the-art in real-time "intelligent" computer control software design.

## B. OVERVIEW OF NAVAL POSTGRADUATE SCHOOL AUV PROJECT

The AUV program at the Naval Postgraduate School (NPS) began in 1987 with the sponsorship of the Naval Surface Weapons System [Ref. 5]. The project is a joint effort of the Mechanical Engineering, Computer Science, and Electrical and Computer Engineering Departments. The research involves an integrated approach to mission planning and execution including navigation, collision avoidance, obstacle recognition, vehicle dynamics and control, and real-time onboard control software. Within the Mechanical Engineering Department efforts have focused in the areas of vehicle configuration and construction, vehicle dynamics and control, with experimental and computer simulation [Ref. 6].

## 1. Vehicle Configuration and Construction

The first autonomous underwater vehicle built at NPS, AUV NPS I, was built and studied by Brunner [Ref. 7]. In addition to designing and building a vehicle, the use of sensor devices such as gyros, inertial sensors, and pressure cells to measure vehicle performance were investigated. Brunner developed a technique to obtain required vehicle performance data from the vehicle, and designed a control system that could be employed to test depth changes of the vehicle in a testing tank.

The AUV I was a 30-inch long, seven-inch wide, and four-inch high, self-propelled, remotely controlled vehicle. The small size was a constraint imposed by available testing facilities. Onboard the vehicle were rate gyro sensors for pitch and yaw, pressure cells to measure speed and depth, two DC motors to power the two propellers, and a data acquisition system. Size restrictions required the use of a tether to transmit control signals and provide power from an external power source. The AUV I testing program successfully showed the feasibility of developing a controller that would provide accurate depth keeping control of an autonomous vehicle.

The second generation autonomous underwater vehicle built at NPS was designed by Good [Ref. 8]. The larger AUV II was designed using Total Ship Systems Engineering techniques. This integrated approach involved an iterative (design spiral) approach with the following subsystems: Hull, Energy Storage and Power Plant, Vehicle Motion Control, Sensor Suite, Obstacle

Avoidance, Navigation and Guidance, Mission Planning, and Machinery Monitoring. Figure 1.1 shows the configuration of the AUV II and internal equipment arrangement.

The AUV II contains its own power supply of rechargeable batteries, and an onboard computer that can be programmed prior to test runs. The larger size has eliminated the need for an external tether. In-water testing of the AUV II in the NPS swimming pool began in March 1991. The basic hull performance characteristics predicted by Good have been validated. The 7000 $ft^2$, 7½ ft deep swimming pool enables relatively complex test runs to be performed to test control methods and sensor systems.

## 2. Vehicle Control

The AUV guidance system consists of an autopilot and associated guidance law. The auto pilot is responsible for stabilizing vehicle motion dynamics in terms of speed, course, and depth. The guidance law will combine commands for the path or position for the vehicle to achieve with navigational estimates of true position and orientation to generate speed, course, and depth commands for the autopilot.

Boncal [Ref. 9] investigated the use of a model based controller for accurate path keeping of an underwater vehicle. The Swimmer Delivery Vehicle (SDV Mark 9) [Ref. 10] model hydrodynamic coefficients were used in this study. Linearized equations of motion were used as the bases for the feedforward and feedback elements of a depth controller. Results demonstrated

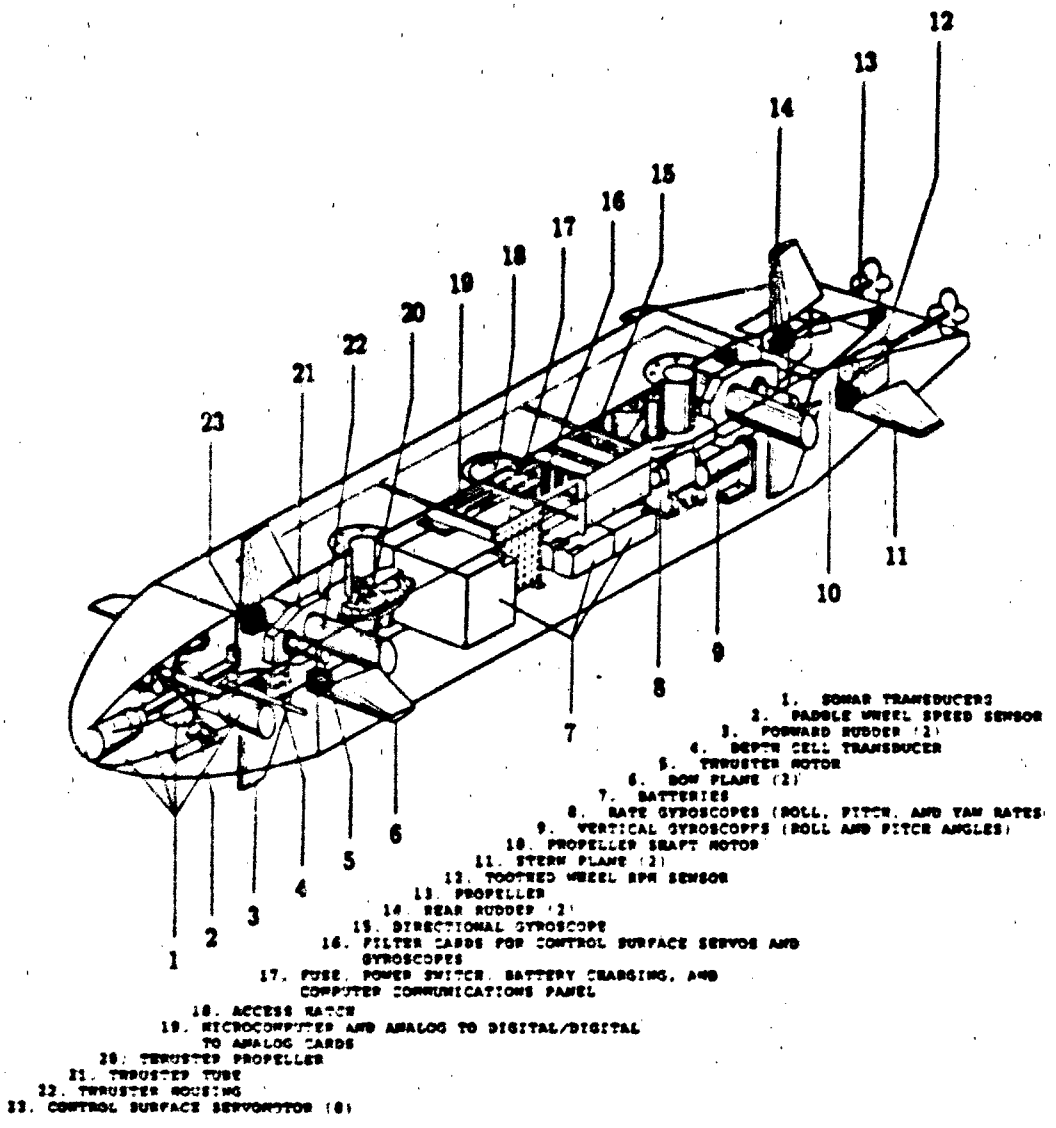


**Figure 1.1** AUV II, Transparent View Showing Internal Equipment Arrangement (Drawn by David Marco)

that, for depth changing maneuvers, accurate tracking of the planned path could be achieved for a considerable range of speeds.

McDonald [Ref. 11] combined the work of Boncal in controller design and applied it to the AUV I model. Only vehicle depth was available from the AUV I data acquisition system. Consequently, both state estimation of pitch and pitch rate and disturbance estimation/compensation techniques were used. A successful closed loop controller was developed using these methods. Sur [Ref. 12], continuing research on the AUV I depth control problem designed a sliding-mode compensator for depth control. Computer simulations using a full six-degree-of-freedom model and non-linear equations proved the method was successfully able to provide accurate depth control for an autonomous underwater vehicle.

Lienard [Ref. 13] demonstrated that sliding mode control provides a robust controller for underwater vehicles. Because the hydrodynamic forces on a vehicle can not be precisely measured problems may occur in predicting and controlling vehicle motion. Using the SDV Mark 9 as the base vehicle, Lienard used independent control of linearized motion equations for longitudinal and vertical planes, and coupled them together. Lienard used a Line-of-Sight guidance scheme. In this method the onboard navigator generates a geographic "way point" ahead of the AUV, and then aims the AUV at this point, and attempts to drive through it. By successive use of way points the AUV proceeds to its destination. Though the navigation control law can't be verified

to be stable, the tracking system as a whole is very robust. This control scheme will place the vehicle on the desired way point, but it may not always be going in the direction desired.

Building on this, Papoulias and Healey [Ref. 14] and Chism [Ref. 15] investigated a guidance scheme in which cross-track error is minimized. This method is analogous to driving an automobile down a roadway; the goal is to stay in the traffic lane, i.e., minimize deviation from the intended track. In this method, the navigator senses the lateral location of the AUV relative to the desired track between two way points.

This method of control is also robust, and generally keeps the vehicle closer on track than the LOS method. The tradeoff to staying close to the ordered track at all times is a lot of small maneuvering by control surfaces/thrusters. If a number of way points are located too close, as might happen if the vehicle has to maneuver into a harbor, the vehicle response may become excessively oscillatory.

The control schemes described so far approached the AUV control problem as a single input/single output (SISO) system. Hawkinson [Ref. 16] approached the AUV control problem by applying multiple input/multiple output (MIMO) sliding mode control theory. Use of a MIMO control method combined both a LOS and cross track error steering controller with a linear quadratic regulator for the depth controller. The speed controller developed by Lienard was also used.

Using the SDV Mark 9 vehicle characteristics, Hawkinson proved the superior performance of the MIMO sliding mode controller as compared to SISO controllers. Though the depth, speed and steering controllers were designed separately, the effectively simultaneously controlled the vehicle.

Papasotiriou [Ref. 17] investigated the use of a "moving aim point" or pursuit autopilot control scheme. This method is also similar to driving down the road wherein the driver is actually aiming at a point at some finite distance in front of the vehicle. Similarly, with this method the AUV II is always driving toward a moving aim point a few ship lengths ahead. The moving aim point is traveling down the line-of-sight toward the next way point.

This control scheme is almost as robust as the Line-of-Sight method. Both the guidance and control schemes must be designed together in order to avoid a loss of stability. This method has an advantage over the Line-of-Sight method in that it keeps the vehicle closer to the track.

Clothier [Ref. 18] investigated the application of a cubic spiral guidance method to autonomous vehicle guidance. This method minimizes cross track errors subject to the rate of change of path curvature. Heading commands are generated based on the cross track error, the path curvature rate, and the difference between desired and actual vehicle heading. This method has the advantage of placing the vehicle at a given waypoint at a certain heading.

### 3. Associated Initiatives

Farren [Ref. 19] and Lohrhammer [Ref. 20] performed preliminary work on the design of the AUV II sonar system. The AUV II is capable of detecting obstacles in its path, and determining an appropriate avoidance course. A high-resolution sonar suite employing four ultrasonic transducers has been installed and successfully tested on the AUV II by Floyd [Ref. 21].

To permit precise positioning the AUV II will employ four tube thrusters. Two will be vertically oriented, and two will be installed athwartships. Research on thrusters for the AUV II was begun by Saunders [Ref. 22] and continued by McLean [Ref. 23]. Thrusters are scheduled to be installed and tested in the AUV II during the first half on 1992.

A significant amount of research has been conducted by the Computer Science and Computer and Electrical Engineering Departments in the areas of mission planning, situation assessment through artificial intelligence, fuzzy logic controllers, and fault tolerant controllers. Appendix D contains a bibliography of all theses associated with the AUV research program.

## C. SCOPE OF THIS THESIS

This research makes the transition from motion control research based on the AUV I and SDV Mark 9 vehicles to a combination of computer simulation and experimental investigation into the vehicle dynamics of the AUV II. The initial

focus of this project was the development of a lateral motion control law for use in initial closed loop operation of the AUV II. Chapter II describes how the hydrodynamic coefficients in the yaw and sway motion equations for the AUV II were determined. Chapter III discusses the refinements to the initial hydrodynamic coefficient estimates, and presents the development of the control law used in the early stages of AUV II trials.

Computer simulations will play a significant role in furtl.er research on the AUV II. To enable new control and guidance laws to be tested and evaluated without actually using the AUV II, a full six-degree-of-freedom computer model of the AUV II was developed. Chapter IV describes how this model was developed, and compares the model performance to actual results.

The final phase of this project involved the design of an enhanced position estimation algorithm. Instrumentation and size restrictions limit the amount of motion information able to be determined on board the AUV II. Determining a vehicle's lateral velocity is a key factor in precise position estimation. Chapter V discusses the development of the reduced order observer for lateral velocity. The performance of the enhanced position estimator is compared against simulated and experimental AUV II trials. Finally, Chapter VI presents recommendations for further research and refinement of the six-degree-of-freedom computer model and position estimator for the AUV II.

## II. LATERAL MOTION HYDRODYNAMIC COEFFICIENT DEVELOPMENT

### A. GENERAL LATERAL MOTION EQUATIONS

The design of the AUV II control system begins with identifying the equations of motion. The generalized equations of motion for lateral motion and yaw for a submerged vehicle [Ref. 10] are shown in Equations (2.1) and (2.2). Variables are referenced to a right-hand orthogonal axis system fixed in the body center as shown in Figure 2.1. Table I defines the parameters used; a dot (·) over a quantity indicates a derivative with respect to time. Because the AUV II has two rudders, the equations of motion separately account for their effect.

$$
\begin{aligned}
m[\dot{v} + ur - wp + x_G(pq + \dot{r}) - y_G(p^2 + r^2) + z_G(qr - \dot{p})] = \\
+ \frac{\rho}{2} l^4 [Y_{\dot{p}}\dot{p} + Y_{\dot{r}}\dot{r} + Y_{pq}pq + Y_{qr}qr] \\
+ \frac{\rho}{2} l^3 [Y_{\dot{v}}\dot{v} + Y_{up}up + Y_{ur}ur + Y_{vq}vq + Y_{wp}wp + Y_{wr}wr] \\
+ \frac{\rho}{2} l^2 [Y_{uv}uv + Y_{vw}vw + Y_{\delta_s u^2}\delta_{rb} + Y_{\delta_s u^2}\delta_{rs}] \qquad (2.1) \\
\frac{\rho}{2} \int_{-x_{aft}}^{x_{fore}} [C_{Dy} h(x)(v + xr)^2 + C_{Dz} b(x)(w - xq)^2] \frac{(v + xr)}{U_{cf}(x)} x\,dx \\
(W - B)\cos\theta\sin\phi
\end{aligned}
$$

**Sway Equation of Motion**

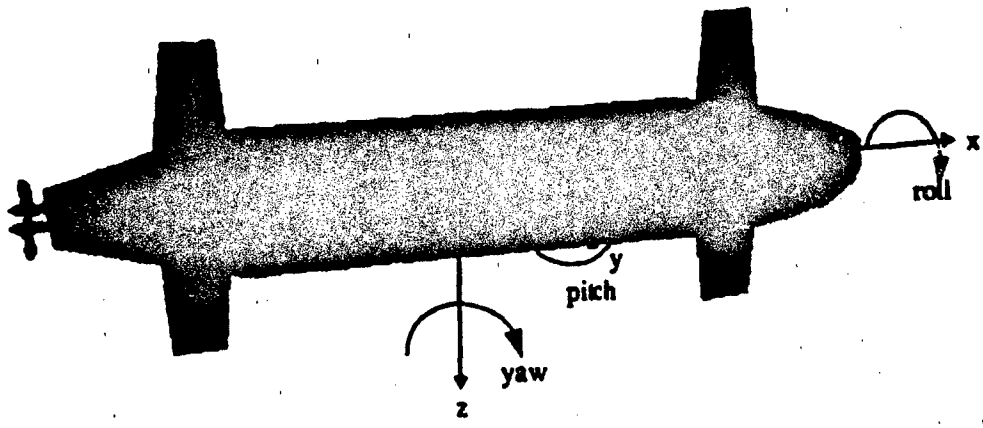


**Figure 2.1** **AUV II Axis System**

$$
\begin{aligned}
&I_z\dot{r} + (I_y - I_x)pq - I_{xy}(p^2 - q^2) - I_{yz}(pr + \dot{q}) + \\
&I_{xz}(qr - \dot{p}) + m[x_G(\dot{v} + ur - wp) - y_G(\dot{u} - vr + wq)] = \\
&\frac{\rho}{2}l^5[N_{\dot{p}}\dot{p} + N_{\dot{r}}\dot{r} + N_{pq}pq + N_{qr}qr] \\
&+ \frac{\rho}{2}l^4[N_{\dot{v}}\dot{v} + N_{up}up + N_{ur}ur + N_{vq}vq + N_{wp}wp + N_{wr}wr] \\
&+ \frac{\rho}{2}l^3[N_{uv}uv + N_{vw}vw + N_{\delta_{rs}}u^2\delta_{rs} + N_{\delta_{rb}}u^2\delta_{rb}] \qquad \textbf{(2.2)} \\
&- \frac{\rho}{2}\int_{x_{aft}}^{x_{bow}} [C_{Dy}h(x)(v + xr)^2 + C_{Dz}b(x)(w - xq)^2]\frac{(v + xr)}{U_{cf}(x)}x\,dx \\
&+ (x_G W - x_B B)\cos\theta\sin\phi + (y_G W - y_B B)\sin\theta + \frac{\rho}{2}l^3u^2N_{prop}
\end{aligned}
$$

**Yaw Equation of Motion**

## TABLE I. EQUATIONS OF MOTION VARIABLES

| Variable | Description |
|---|---|
| x,y,z | Distance along the principal axes |
| u,v,w | Velocity components of body axis system relative to fluid along body axes |
| p,q,r | Angular velocity components of body relative to inertial reference system along body axes |
| X,Y,Z | Hydrodynamic force components along body axes |
| K,M,N | Hydrodynamic moment components along body axes |
| $\Psi,\theta,\phi$ | Yaw, pitch, and roll angles (Euler angles) |
| m | Mass of the AUV II (including the fluid in the floodable sonar dome) |
| W | Weight of the AUV II (=gm) |
| $\nabla$ | Displacement volume of the AUV II |
| B | Buoyancy force acting on the AUV II ($=g\rho\nabla$) |
| $x_G,y_G,z_G$ | Coordinates of the Center of Gravity in the body axis system. These depend on the mass distribution of the vehicle |
| $x_B,y_B,z_B$ | Coordinates of the Center of Buoyancy in the body axis system. These are independent of the mass distribution of the vehicle |
| $I_x,I_y,I_z$ | Moments of inertia about the body system axes |
| $I_{xy},I_{xz},I_{yz}$ | Products of inertia about the body system axes |
| $\rho$ | Mass density water |
| l | Reference length used to nondimensionalize the hydrodynamic coefficients |
| b(x), h(x) | Width and height of the AUV II in the xy and xz planes, respectively, measured in the body axis system shown in Figure (2.1) |
| $x_{nose},x_{tail}$ | Coordinates of the vehicle nose and tail as measured in body axis system |
| $U_{cf}(x)$ | Total crossflow velocity on AUV II at position x |
| $\delta_{rb},\delta_{rs}$ | Bow and Stern rudder deflection angles in radians |
| $C_{Dy},C_{Dz}$ | Drag coefficients along the y and z axes of the body system axes. |

## B. LINEAR, SIMPLIFIED LATERAL MOTION EQUATIONS

The general equations of motion are extremely non-linear which makes their direct use in developing a control law very difficult. By using the following assumptions and specific physical characteristics of the AUV II, the equations were linearized and simplified:

1. The angular velocities about the x-axis (p) and y-axis (q) are zero. The associated accelerations $\dot{p}$ and $\dot{q}$ are also zero.
2. The AUV II is neutrally buoyant: W=B.
3. The AUV II is symmetrically loaded in the transverse and longitudinal directions: $y_g$, $y_b$, $x_g$, and $x_b$ are zero.
4. The counter-rotating propellers produce no yaw moment ($N_{prop}$=0).
5. The non-linear drag force term is small in value compared to other terms in the equation, and can be eliminated. For hovering analysis this term will have to be included in the simplified equations of motion.

Equations (2.3) and (2.4) are the simplified, linear equations of motion used for the initial development of the lateral motion control law.

$$m(\dot{v} + ur + x_G\dot{r}) = \frac{\rho}{2}l^4 Y_{\dot{r}}\dot{r} + \frac{\rho}{2}l^3 Y_{\dot{v}}\dot{v} + \frac{\rho}{2}l^3 Y_r ur + \frac{\rho}{2}l^2 Y_v uv + \frac{\rho}{2}l^2 Y_{\delta_m} u^2 \delta_{rs} + \frac{\rho}{2}l^2 Y_{\delta_m} u^2 \delta_{rb} \quad (2.3)$$

**Linear, Simplified Sway Equation of Motion**

$$I_z\dot{r} + mx_G\dot{v} + mx_G ur = \frac{\rho}{2}l^5 N_{\dot{r}}\dot{r} + \frac{\rho}{2}l^4 N_{\dot{v}}\dot{v} + \frac{\rho}{2}l^4 N_r ur + \frac{\rho}{2}l^3 N_v uv + \frac{\rho}{2}l^3 N_{\delta_m} u^2 \delta_{rs} + \frac{\rho}{2}l^3 N_{\delta_m} u^2 \delta_{rb} \quad (2.4)$$

**Linear, Simplified Yaw Equation of Motion**

## C. DETERMINATION OF HYDRODYNAMIC COEFFICIENTS

The next step in developing the lateral motion control law was the determination of hydrodynamic coefficients ($Y_{\dot{v}}$, $Y_v$, $Y_{\dot{r}}$, $Y_r$, $N_{\dot{v}}$, $N_v$, $N_{\dot{r}}$, and $N_r$) appearing in Equations (2.3) and (2.4). The coefficients for the SDV were used as a starting point. Though similar in geometry to the AUV II, the SDV has a large fin on the stern in which a third propeller for surfaced operations is located. The effect of this fin on the hydrodynamic coefficients was estimated and subtracted from the original SDV hydrodynamic coefficient values.

Table II lists the SDV hydrodynamic coefficients, the calculated fin effects, and the final "Finless SDV" values. Computations and details of the fin effect on the hydrodynamic coefficients are contained in Appendix A.

**TABLE II. SDV HYDRODYNAMIC COEFFICIENTS**

| | Given SDV | Fin Effect | Finless SDV |
|---|---|---|---|
| $Y_v$ | -0.05550 | -0.01965 | -0.03585 |
| $Y_v$ | -0.09310 | -0.01660 | -0.07650 |
| $Y_r$ | 0.00124 | 0.00756 | -0.00633 |
| $Y_r$ | 0.02970 | 0.00639 | 0.02331 |
| $N_v$ | 0.00124 | 0.00756 | -0.00632 |
| $N_v$ | -0.00742 | 0.00639 | -0.01381 |
| $N_r$ | -0.00340 | -0.00291 | -0.00049 |
| $N_r$ | -0.01640 | -0.00246 | -0.01394 |

The signs of the hydrodynamic coefficients $Y_r$, $Y_r$, $N_v$, and $N_v$ depend upon whether the vehicle is bow or stern dominant. The SDV, with the large fin at the rear, is stern dominant. The signs of all the SDV hydrodynamic coefficients except for $N_v$ and $N_v$ agree with predicted values [Ref. 24]. $N_v$ and $Y_r$ should be small numbers, either positive or negative. $N_v$ should be positive, but the given value of $N_v$ for the SDV is negative.

The hydrodynamic coefficients of the bow-dominant Finless SDV all have signs consistent with theoretical predictions. $Y_r$ remains positive, but has a smaller magnitude. $Y_r$ and $N_v$ become positive. $N_v$ remains negative, which it should be for a bow-dominant vehicle.

The Finless SDV still differs geometrically from the AUV II. Table III summarizes the geometric characteristics of the Finless SDV and the AUV II. Due to the significant differences in geometric characteristics, a better estimate of the AUV II hydrodynamic coefficients was needed.

**TABLE III. FINLESS SDV AND AUV GEOMETRIC CHARACTERISTICS**

| | Finless SDV | AUV II |
|---|---|---|
| Length (L) | 209.1[1] | 87.625 |
| Draft (T) | 31.8 | 10.125 |
| Beam (B) | 75.7 | 16.25 |
| $C_B$ | 0.77 | 0.83 |
| T/L Ratio | 0.1514 | 0.1155 |
| B/L Ratio | 0.3713 | 0.1854 |
| B/T Ratio | 2.4528 | 1.6049 |

[1] Actual SDV length is 229.0 inches, but the characteristic length used in all calculations is 209.1. Actual and characteristic length for the AUV II is 87.625 inches.

Clarke, Gedling, and Hine [Ref. 25] used a multiple regression analysis to estimate a marine vehicle's hydrodynamic coefficients. Thirty-six sets of data from rotating arm experiments and 36 sets of data from planar motion experiments were obtained, and then normalized using $(T/L)^2$. The predictor variables used were: $C_B$, L./B, L/T B/L, T/L, and T/B. Only the terms which tended to zero were used in the regression to assure stability. The resulting equations for the hydrodynamic coefficients are:

$$
\begin{aligned}
Y_{\dot{v}} &= -\pi\left(\frac{T}{L}\right)^2\left[1.0 + 0.16C_B\left(\frac{B}{T}\right) - 5.1\left(\frac{B}{L}\right)^2\right] \\
Y_{\dot{r}} &= -\pi\left(\frac{T}{L}\right)^2\left[1.0 + 0.4C_B\left(\frac{B}{T}\right)\right] \\
Y_r &= -\pi\left(\frac{T}{L}\right)^2\left[0.67\left(\frac{B}{L}\right) - 0.0033\left(\frac{B}{T}\right)^2\right] \\
Y_v &= -\pi\left(\frac{T}{L}\right)^2\left[-0.5 + 2.2\left(\frac{B}{L}\right)0.08\left(\frac{B}{T}\right)\right] \\
N_{\dot{v}} &= -\pi\left(\frac{T}{L}\right)^2\left[1.1\left(\frac{B}{L}\right) - 0.041\left(\frac{B}{T}\right)\right] \\
N_{\dot{r}} &= -\pi\left(\frac{T}{L}\right)^2\left[0.5 + 2.4\left(\frac{T}{L}\right)\right] \\
N_r &= -\pi\left(\frac{T}{L}\right)^2\left[0.083 + 0.017C_B\left(\frac{B}{T}\right) - 0.33\left(\frac{B}{L}\right)\right] \\
N_v &= -\pi\left(\frac{T}{L}\right)^2\left[0.25 + 0.039\left(\frac{B}{T}\right) - 0.56\left(\frac{B}{L}\right)\right]
\end{aligned}
\tag{2.5}
$$

### Hydrodynamic Coefficient Regression Equations

The hydrodynamic coefficient values obtained for the Finless SDV using the regression equations are listed in the second column of Table IV as "Regression SDV." The results obtained for the AUV II are listed under "Regression AUV II." All of the hydrodynamic coefficients of the Regression SDV are negative except for $N_r$, which also should be negative for a bow-dominant vehicle. All the hydrodynamic coefficients of the Regression AUV II are negative.

## TABLE IV. DETERMINATION OF AUV II HYDRODYNAMIC COEFFICIENTS

| | Finless SDV | Regression SDV | Reg. SDV/ Finless SDV (Conversion) | Regression AUV II | Regression AUV II/ Conversion |
|---|---|---|---|---|---|
| $Y_v$ | -0.03585 | -0.04551 | 1.269 | -0.04353 | -0.03430 |
| $Y_v$ | -0.07650 | -0.12624 | 1.650 | -0.06430 | -0.03896 |
| $Y_r$ | -0.00633 | -0.01632 | 2.578 | -0.00486 | -0.00189 |
| $Y_r$ | 0.02331 | -0.00775 | 0.332[1] | -0.00925 | unreliable |
| $N_v$ | -0.00633 | -0.02192 | 3.463 | -0.00579 | -0.00167 |
| $N_v$ | -0.01381 | -0.06309 | 4.568 | -0.03260 | -0.00714 |
| $N_r$ | -0.00049 | 0.00039 | 0.73469 | -0.00188 | unreliable |
| $N_r$ | -0.01394 | -0.01020 | 0.73171 | -0.00875 | -0.01196 |

[1] Due to inconsistencies between expected and actual hydrodynamic coefficient values for $Y_r$ and $N_r$ these conversion factors were not used to obtain estimates for the AUV II values as explained in the text.

The ratios between the hydrodynamic coefficient values of the Finless SDV and Regression SDV (Table IV, column 3) were used as scaling factors to adjust the corresponding Regression AUV II values. The resulting AUV II hydrodynamic coefficients are listed in column 5 of Table IV. Because the values of $Y_r$ and $N_r$ for the Finless SDV and the Regression SDV were not consistent, a different method to determine the AUV II values was used.

As shown in Appendix A, the effect of a fin on hydrodynamic coefficients is the same for $Y_r$ and $Y_v$. The ratio between the Finless SDV and AUV II/ Conversion values of $Y_v$, 1.9641, was divided into the Finless SDV value of $Y_r$ to obtain an estimate of $Y_r$ for the AUV II. As was observed for the Finless SDV, the

sign of $Y_r$ is positive, though a negative value had been expected based on an assumed bow dominant vessel geometry. Similarly, the effect of a fin is the same for $N_r$ and $Y_v$. The ratio between the Finless SDV and AUV II/Conversion values of $Y_v$, 1.05, was divided into the Finless SDV value of $N_r$ to obtain an estimate of $N_r$ for the AUV II.

An additional modification to the initial estimates of the AUV II hydrodynamic coefficients was made. The given SDV values of $Y_r$ and $N_v$ were the same, 0.00124, as were the calculated fin effect corrections. It was therefore reasonable to assume that the values of $Y_r$ and $N_v$ for the AUV II should be the same. The AUV II/Conversion values for $Y_r$ and $N_v$ were averaged, and the average was used for the $Y_r$ and $N_v$ AUV II Estimate 1 values.

## D. DETERMINATION OF RUDDER FORCE HYDRODYNAMIC COEFFICIENT $Y_\delta$

The y-direction component of the total rudder force is

$$Y_\delta \delta = Y_{rudder} = \pm(L\cos\beta_r + D\sin\beta_r) \qquad \textbf{(2.6)}$$

where $\beta_r$ = rudder drift angle
L = rudder lift
D = rudder drag

This expression assumes there is no interaction between the pressure field around the rudder and the adjacent ship. In most cases there is a significant interaction which results in the total y-direction force on the vessel being larger than predicted by Equation (2.6). By expressing the lift and drag forces in

nondimensional form, standard figures can be used for a given shape/section of rudder. The nondimensional forms of lift and drag forces are given by Equations (2.7) and (2.8).

$$\text{Lift Coefficient} \qquad C_L = \frac{L}{(\rho/2)A_T u^2} \tag{2.7}$$

$$\text{Drag Coefficient} \qquad C_D = \frac{D}{(\rho/2)A_T u^2} \tag{2.8}$$

where $A_T$ = control surface profile area.

The rudders on the AUV II are of a NACA 0015 foil section. Figure 2.2 shows the characteristics of a NACA 0015 section. By using this figure, $C_L$ was determined to be $3.1515\delta$, where $\delta$ is the rudder deflection in radians. For small drift angles $C_D\sin(\beta_r)$ is much smaller in magnitude than $C_L\cos(\beta_r)$. Eliminating the drag term from Equation (2.6), approximating $\cos(\beta_r)=1$, and writing the total rudder force in nondimensional form yields

$$\left(\frac{\rho}{2}\right)l^2 u^2 Y_\delta \delta = L\cos\beta_r = \left(\frac{\rho}{2}\right)A_T u^2 3.1515\delta \tag{2.9}$$

Solving for $Y_\delta$, with l=87.625 inches, and $A_T$=28.57in$^2$, yields $Y_\delta$=0.01173. Because there are two identical control surfaces at both forward and aft rudders, the actual value of $Y_\delta$ for the AUV II is 0.02345.

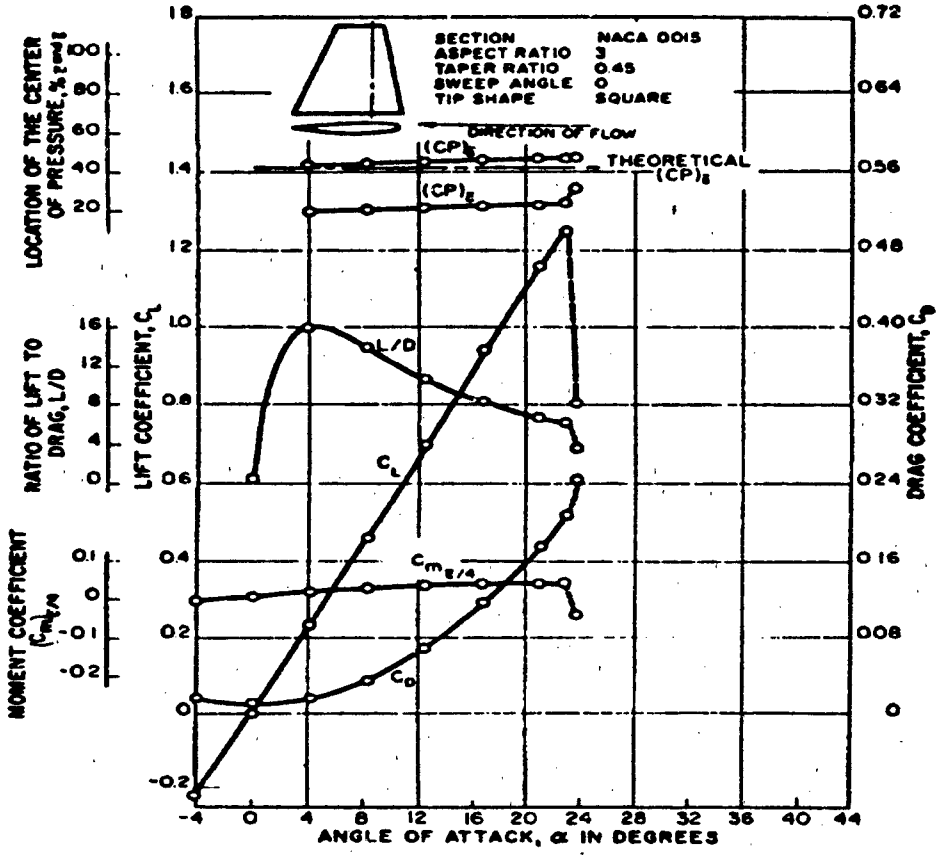


Figure 2.2 NACA 0015 Fin Characteristics [Ref. 24]

## E. AUV II GEOMETRY AND ESTIMATE/COEFFICIENT SUMMARY

Table V summarizes the AUV II Estimate 1 hydrodynamic coefficient and geometric properties used to in the initial open and closed loop simulations.

The mass moment of inertia, $I_z$, was calculated using the equation

$$\frac{M}{12}(B^2 + L^2) \qquad \textbf{(2.10)}$$

Equation (2.10) assumes that the mass within the vehicle is distributed homogeneously. To account for the actual non-homogeneous mass distribution,

$I_z$ for the SDV was calculated using Equation (2.10), and the ratio between the SDV computed and actual $I_z$ [Ref. 10] values was applied to the computed AUV II $I_z$ value to obtain the number appearing in Table V.

**TABLE V. AUV II GEOMETRIC PROPERTIES AND ESTIMATE 1 HYDRODYNAMIC COEFFICIENTS**

| | | | |
|---|---|---|---|
| $Y_v$ | -0.03430 | m (slugs) | 435/32.17 |
| $Y_{\dot{v}}$ | -0.03896 | $I_Z$ ($lb_f$-ft-$s^2$) | 45 |
| $Y_r$ | -0.00178 | $\rho$ (slugs/$ft^3$) | 1.94 |
| $Y_{\dot{r}}$ | 0.01187 | $x_B$ (ft) | +0.125/12 |
| $N_v$ | -0.00178 | $x_{rs}$[1] | -0.377 |
| $N_{\dot{v}}$ | -0.00714 | $x_{rb}$[1] | 0.283 |
| $N_r$ | -0.00047 | $l_{reference}$ (ft) | 87.625 |
| $N_{\dot{r}}$ | -0.01196 | $N_{\delta rs}=x_{rs}Y_{\delta rs}$ | |
| $Y_{\delta rs}$ | 0.02345 | $N_{\delta rb}=x_{rb}Y_{\delta rb}$ | |
| $Y_{\delta rb}$ | 0.02345 | | |

[1] $X_{rs}$ and $X_{rb}$ are expressed in fraction of vehicle length.

# III. INITIAL AUV II CLOSED LOOP SURFACED OPERATION

## A. STATE-SPACE SYSTEM REPRESENTATION

The state of a dynamic system, such as the AUV II, is defined by a set of physical quantities that uniquely determine the condition of the system. The state-space approach uses only dynamic variables and their first derivatives with respect to time. Thus, the condition of a physical system can be described with a set of first order differential equations.

The general form of state-space system representation is:

$$\dot{\mathbf{x}} = \mathbf{A}\mathbf{x} + \mathbf{B}\mathbf{u}$$
$$\mathbf{y} = \mathbf{C}\mathbf{x} \qquad (3.1)$$

where
- $x$ = state vector (nx1)
- $u$ = external input vector (rx1)
- $y$ = output/observation vector (mx1)
- $\mathbf{A}$ = open loop dynamic matrix (nxn)
- $\mathbf{B}$ = control distribution matrix (nxr)
- $\mathbf{C}$ = output/calibration matrix (mxn)

The state vector chosen for the AUV II lateral motion model was:

$$\mathbf{x} = \begin{bmatrix} \psi \\ v \\ r \end{bmatrix} = \begin{bmatrix} \text{Yaw angle} \\ \text{Lateral (crosstrack) velocity} \\ \text{Yaw rate} \end{bmatrix}$$

In a closed loop system the system output is fed back to the input. For example, the simplest form of feedback is u=-kx, where k is a gain vector of size (1xn).

Substituting u=-kx into Equation (3.1) yields a general closed loop state space system representation

$$\dot{\mathbf{x}} = [\mathbf{A} - \mathbf{B}\mathbf{k}]\mathbf{x}$$

Many different forms of feedback can be used, as will be shown later in this chapter.

## B. STEADY STATE PERFORMANCE

When a system is in steady state, the derivatives of state variables associated with velocities equal zero. This makes the system analysis simpler. Analysis of the AUV II lateral motion began by assuming steady state conditions (e.g., and equal zero). During initial testing the AUV II rudders operated together, i.e., they both moved the same amount, though in opposite directions ($\delta_{rb}$=-$\delta_{rs}$).

The linear, simplified equations of motion (Equations (2.3) and (2.4)) can be solved simultaneously to produce an explicit steady-state expression for the yaw (turning) rate, r, and approximate turning radius, R.

$$r = \frac{Y_v \frac{\rho}{2} l^3 u (N_{\delta rs} - N_{\dot{v}rb})\delta}{Y_v (m x_G - \frac{\rho}{2} l^4 N_r) - N_v l (m - \frac{\rho}{2} l^3 Y_r)} \qquad \textbf{(3.2)}$$

$$R = \frac{u}{r}$$

An exact expression for the turning radius R is $R=\frac{\sqrt{v^2+u^2}}{r}$. Equation (3.2) assumes that the lateral velocity, v, is small when compared with the forward velocity.

During the AUV II's "maiden voyage," the propellers turned at a speed corresponding to a forward velocity of two feet per second. The rudders were manually set at the maximum values (23°). The AUV II was observed to turn at a rate of approximately 9°/min in a turning radius of two vehicle lengths. These values were used as the baseline for determining the accuracy with which Equation (3.2) predicted the AUV II motion.

Table VI shows the Estimate 1 steady state hydrodynamic coefficients and the corresponding turning rate and turning radius. The Estimate 1 hydrodynamic coefficients did not produce a sufficiently fast turning rate. The effect of each hydrodynamic coefficient on the turning rate was analyzed to determine which coefficients should be modified, and by what amount.

The sensitivity of the turning rate to a change in a hydrodynamic coefficient is given by the slope of a curve of the turning rate versus the coefficient in question. Expressed mathematically, this equals $\frac{\partial r}{\partial HC}$, where HC is the hydrodynamic coefficient in question. Treating turning rate as a function of $Y_v$, $Y_r$, $N_v$, and $N_r$, the turning rate sensitivities are:

**TABLE VI. STEADY-STATE, SURFACED AUV II PERFORMANCE**

| | Estimate 1 | Estimate 2 | |
|---|---|---|---|
| $Y_v$ | -0.03896 | -0.03896 | -0.03896 |
| $Y_r$ | 0.01187 | 0.01187 | 0.01187 |
| $N_v$ | -0.00714 | -0.00769 | -0.00769 |
| $N_r$ | -0.01196 | -0.01022 | -0.01022 |
| $Y_{\delta rs}$, $Y_{\delta rb}$ | 0.02345 | 0.02345 | 0.02345 |
| u (ft/sec) | 2.0 | 2.0 | 1.5 |
| δ (degrees) | 23.0 | 23.0 | 23.0 |
| r (deg/sec) | 6.39 | 8.79 | 6.6 |
| R (vehicle lengths) | 2.45 | 1.79 | 1.79 |

$$\frac{\partial r}{\partial Y_v} = \frac{(\frac{\rho}{2}l^3(N_{\delta rs} - N_{\delta rb})u\delta)DEN + NUM(\frac{\rho}{2}l^4N_r - mx_G)}{(Y_v(mx_G - \frac{\rho}{2}l^4N_r) - N_v l(m - \frac{\rho}{2}l^3Y_r))^2}$$

$$\frac{\partial r}{\partial Y_r} = \frac{-NUM\frac{\rho}{2}l^4N_v}{(Y_v(mx_G - \frac{\rho}{2}l^4N_r) - N_v l(m - \frac{\rho}{2}l^3Y_r))^2}$$

$$\frac{\partial r}{\partial N_v} = \frac{-NUM(\frac{\rho}{2}l^3Y_r - m)l}{(Y_v(mx_G - \frac{\rho}{2}l^4N_r) - N_v l(m - \frac{\rho}{2}l^3Y_r))^2}$$

$$\frac{\partial r}{\partial N_r} = \frac{NUM\frac{\rho}{2}l^4Y_v}{(Y_v(mx_G - \frac{\rho}{2}l^4N_r) - N_v l(m - \frac{\rho}{2}l^3Y_r))^2}$$

where

$$NUM = \frac{\rho}{2} l^3 (N_{\delta rs} - N_{\delta rb}) Y_v u \delta$$

$$DEN = Y_v (m x_G - \frac{\rho}{2} l^4 N_r) - N_v l (m - \frac{\rho}{2} l^3 Y_r)$$

These equations are cumbersome to work with. Directly plotting the predicted turning rate against different values of the hydrodynamic coefficients provided an easier method by which to determine which coefficients most affected the turning rate. Figure 3.1 shows a plot of turning rate versus the hydrodynamic coefficients as they were individually varied from 50% to 150% of their Estimate 1 value.

The hydrodynamic coefficients associated with the moment of the vehicle due to yaw and lateral velocity, $N_v$ and $N_r$, had the largest affect on turning rate. For this reason, it was decided to adjust the values of $N_v$ and $N_r$, to values listed as Estimate 2 in Table VI.

The results obtained using the Estimate 2 values were deemed close enough to use for additional modeling for various reasons. Since exact values of yaw rate and turning radius were not known, it was unreasonable to obtain "exact" matching with the observed values. It should be noted that the AUV II did slow down during turns. Simulations using an average forward velocity of 1.5 feet/second also yielded results reasonably close to observed values.

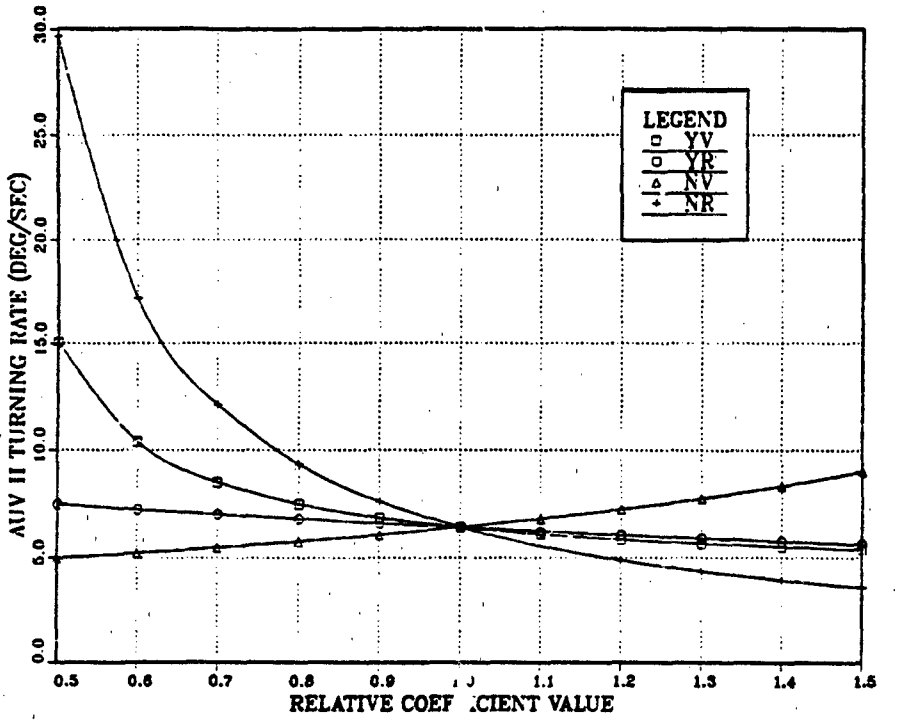


**Figure 3.1 AUV II Turn Radius Sensitivity**

## C. AUV II LATERAL MOTION REPRESENTATION

The general form of the state space equations describing the AUV II lateral motion are

$$\dot{\psi} = r$$

$$\dot{v} = a_{11}uv + a_{12}ur + b_{11}u^{2}\delta_{rs} + b_{12}u^{2}\delta_{rb} \qquad (3.3)$$

$$\dot{r} = a_{21}uv + a_{22}ur + b_{21}u^{2}\delta_{rs} + b_{22}u^{2}\delta_{rb}$$

or, in matrix notation

$$\begin{bmatrix}\dot{\psi}\\ \dot{v}\\ \dot{r}\end{bmatrix}=\begin{bmatrix}0 & 0 & 1\\ 0 & a_{11} & a_{12}\\ 0 & a_{21} & a_{22}\end{bmatrix}\begin{bmatrix}\psi\\ v\\ r\end{bmatrix}+\begin{bmatrix}0 & 0\\ b_{11} & b_{12}\\ b_{21} & b_{22}\end{bmatrix}\begin{bmatrix}u^2\delta_{rb}\\ u^2\delta_{rs}\end{bmatrix} \qquad (3.4)$$

The coefficients in Equations (3.3) and (3.4) were determined by simultaneously solving the linear, simplified equations of motion (Equations (2.3) and (2.4)) for $\dot{v}$ and $\dot{r}$, and are listed below.

$$a_{11}=\left[\frac{A_4B_2-A_2B_4}{A_1B_2-A_2B_1}\right] \qquad a_{12}=\left[\frac{A_3B_2-A_2B_3}{A_1B_2-A_2B_1}\right]$$

$$a_{21}=\left[\frac{A_4B_1-A_1B_4}{A_2B_1-A_1B_2}\right] \qquad a_{22}=\left[\frac{A_3B_1-A_1B_3}{A_2B_1-A_1B_2}\right]$$

$$b_{11}=\left[\frac{A_5B_2-A_2B_5}{A_1B_2-A_2B_1}\right] \qquad b_{12}=\left[\frac{A_6B_2-A_2B_6}{A_1B_2-A_2B_1}\right]$$

$$b_{21}=\left[\frac{A_5B_1-A_1B_5}{A_2B_1-A_1B_2}\right] \qquad b_{22}=\left[\frac{A_6B_1-A_1B_6}{A_2B_1-A_1B_2}\right]$$

where, expressing the hydrodynamic coefficients in non-dimensional form,

$$A_1=m-Y_{\dot{v}} \qquad B_1=mx_G-N_{\dot{v}}$$

$$A_2=mx_G-Y_{\dot{r}} \qquad B_2=Iz-N_{\dot{r}}$$

$$A_3=Y_r-m \qquad B_3=N_r-mx_G$$

$$A_4=Y_v \qquad B_4=N_v$$

$$A_5=Y_{\delta rs} \qquad B_5=+N_{\delta rs}$$

$$A_6=Y_{\delta rb} \qquad B_6=+N_{\delta rb}$$

In this form, the open loop dynamic matrix is singular, and one pole will always be located at zero. An alternative form of defining the system would only include the rows associated with lateral velocity and yaw rate. In addition, the system as defined contains two inputs, the bow and stern rudder angles. During initial operation of the AUV II, the rudders were not operated independently. Thus, Equation (3.4) simplifies to

$$\begin{bmatrix} \dot{v} \\ \dot{r} \end{bmatrix} = \begin{bmatrix} a_{11} & a_{12} \\ a_{21} & a_{22} \end{bmatrix} \begin{bmatrix} v \\ r \end{bmatrix} + \begin{bmatrix} b_1 \\ b_2 \end{bmatrix} u^2 \delta \qquad (3.5)$$

where $\delta_{rs} = \delta$
$\delta_{rb} = -\delta$
$b_1 = +b_{11} - b_{12}$
$b_2 = +b_{21} - b_{22}$

## D. CLOSED LOOP SYSTEM CONTROL DEVELOPMENT

### 1. Transfer Function Formulation

A marine vessel is steered to a required heading ($\psi$) by using the rudders. For this reason, the relationship, or transfer function, between $\psi$ and $\delta$ is of primary concern when developing a control law. The solid lines in Figure 3.2 show the block diagram representing the AUV II steering plant as expressed by Equation (3.5).

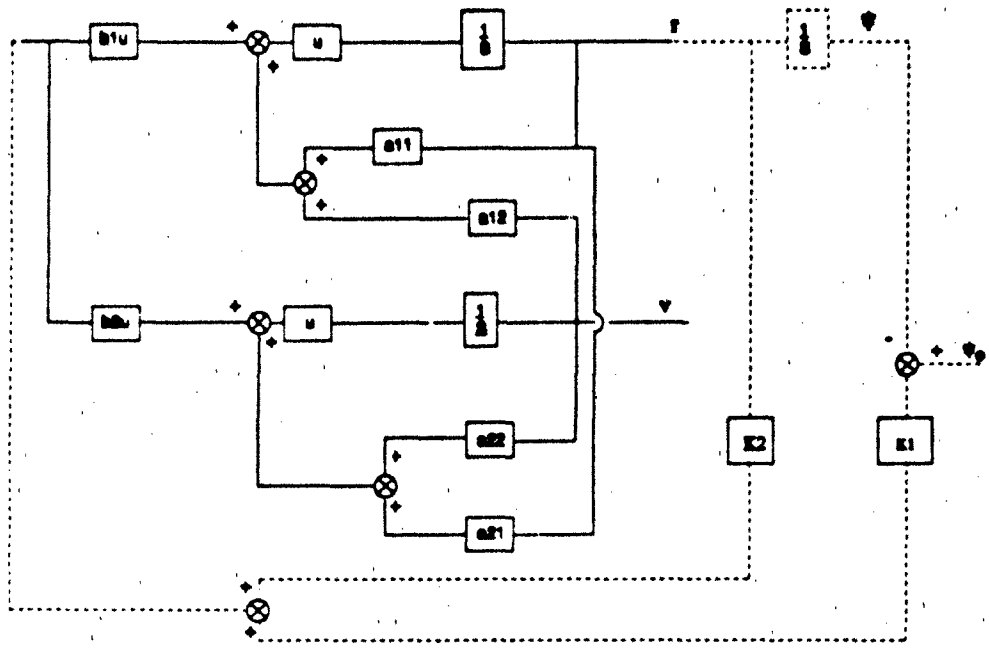

**Figure 3.2** **Simple Proportional/Derivative Controller**

Simultaneously solving the above equations yields the transfer function between $\psi$ and $\delta$

$$\ddot{\psi} - (a_{11} + a_{22})u\dot{\psi} + (a_{11}a_{22} - a_{12}a_{21})u^2\psi = b_2u^2\delta + (a_{21}b_1 - a_{11}b_2)u^3\delta$$

Expressed in the "s," or Laplace domain, the transfer function becomes

$$\frac{\psi}{\delta} = \frac{b_2u^2s + (a_{21}b_1 - a_{11}b_2)u^3}{s[s^2 - (a_{11} + a_{22})us + (a_{11}a_{22} - a_{12}a_{21})u^2]} \qquad (3.6)$$

Up to this point only the open loop situation has been addressed, i.e. provide a given rudder angle, $\delta$, and observe the change in heading, $\psi$. In

practice, the AUV II must maintain an ordered heading, $\psi_o$. This requires the use of a closed loop controller.

A simple proportional/derivative controller of the form

$$\delta = K_1\psi_e + K_2\psi, \text{ where } \psi_e = \psi_o - \psi \qquad (3.7)$$

was chosen for the initial form of the AUV II lateral motion controller. This form of controller is easy to implement in a situation such as this where the rate of change of heading (and thus rate of change of heading error) is able to be determined explicitly from the output of the "plant." It also has the added advantage of providing a more rapid and better damped system response than a controller that uses only the actual value of the heading error.

Since $\psi$=r, Equation (3.6) can be integrated to obtain a transfer function strictly between r and $\delta$

$$\frac{r}{\delta} = \frac{n_1 s + n_0}{s^2 + d_1 s + d_0} \qquad (3.8)$$

where $n_0 = (a_{21} b_1 - a_{11} b_2)\, u^3$
$n_1 = b_2 u^2$
$d_0 = (a_{11} a_{22} - a_{12} a_{21})\, u^2$
$d_1 = -(a_{11} + a_{22})\, u$

By combining Equation (3.8) with the control law of Equation (3.7), an expression for the transfer function between $\psi_o$ and $\psi$ can be determined

$$\frac{\psi}{\psi_o} = \frac{K_1(n_1 s + n_o)}{(K_1 + K_2 s)(n_1 s + n_o) - s(s^2 + d_1 s + d_o)} \qquad (3.9)$$

The denominator of Equation (3.9) is the characteristic equation of the AUV II lateral motion performance model subjected to a step input ($\psi_o$). Through analysis techniques such as an s-plane pole and zero plot, the desired response of the AUV II can be established.

## 2. Second Order System Response

The AUV II lateral motion system as represented by Equation (3.8) is a second order system. In general, a second order system can be represented is the s-domain by

$$C(s) = \frac{\omega_n^2}{(s^2 + 2\zeta\omega_n + \omega_n^2)} R(s) \qquad \textbf{(3.10)}$$

where
- $C(s)$ = output($\psi$)
- $R(s)$ = input($\psi_o$)
- $\omega_n$ = system natural frequency
- $\zeta$ = damping ratio

When the input, R(s), is a unit step input, such as a normalized ordered heading ($\psi_o$), Equation (3.10) becomes

$$C(s) = \frac{\omega_n^2}{s(s^2 + 2\zeta\omega_n + \omega_n^2)} \qquad \textbf{(3.11)}$$

for which the transient output is

$$c(t) = \psi(t) = 1 - \frac{1}{\beta} e^{-\zeta\omega_n t} \sin(\omega_n \beta t + \theta)$$

where $\beta = \sqrt{1 - \zeta^2}$ and $\theta = \tan^{-1}(\beta / \zeta)$.

The transient output of the system is defined by the swiftness of response as measured by rise time ($T_r$) and time to peak value ($T_p$), and the closeness of response to the desired peak value ($M_p$) and settling time ($T_s$). When analyzing the response of system to a step input, the most common parameters used are settling time and percent overshoot (P.O.) which is related to rise time and time to peak value. The settling time is the length of time required for the system response to stabilize within a certain percentage, usually 2%, of the final system value. For a second order system with a damping constant of $s\omega_n$, the response will remain within 2% after four time constants:

$$T_s = 4\tau = \frac{4}{\zeta\omega_n}$$

Percent overshoot, using the ordered course, $\psi_o$, as the input, is defined by

$$P.O. = \frac{M_p - \psi_o}{\psi_o} \times 100\%$$

The response of a second order system depends strongly upon the value of the damping ratio ($\zeta$). If $\zeta$ is low, the system will respond more rapidly (decreasing $T_r$ and $T_p$), but oscillate more around the final value, increasing peak value of the output as well as the settling time. A system with a large value of $\zeta$ will respond slower (longer $T_r$ and $T_p$), but it won't oscillate as much.

### 3. Gain Determination

Figure 3.2 can be simplified into the "reduced" form of Figure 3.3 in which the entire AUV II "plant" is represented as one block.

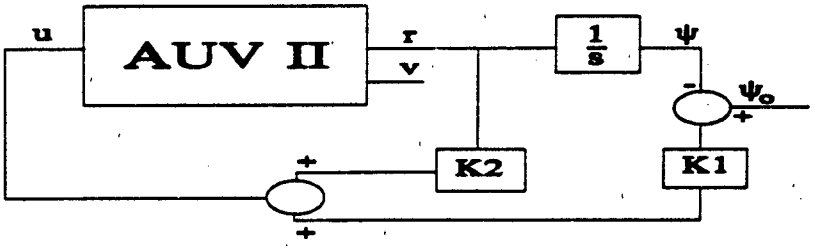


**Figure 3.3 "Reduced" Representation of Proportional/Derivative Controller**

The transfer function between the ordered course ($\psi_o$) and the actual heading ($\psi$) is given by Equation (3.9). The denominator of Equation (3.9) forms the characteristic equation

$$s^3 + (d_1 - K_2 n_1)s^2 + (d_o - K_2 n_0 - K_1 n_1)s - K_1 n_0 = 0 \qquad \textbf{(3.12)}$$

which can be analyzed using root locus techniques. First, Equation (3.12) is rearranged to separate $K_1$

$$1 + K_1 \frac{(-n_1 s + n_0)}{s^3 + (d_1 - K_2 n_1)s^2 + (d_0 - K_2 n_0)s} = 0 \qquad \textbf{(3.13)}$$

Equation (3.13) has zeros at $n_o/n_1$=0.2183. One pole is located at s=0. The other two poles are obtained by solving the denominator of Equation (3.13)

$$s^2 + (d_1 - K_2 n_1)s + (d_0 - K_2 n_0) = 0 \qquad \textbf{(3.14)}$$

Note that Equation (3.14) is strictly a function of $K_2$. An iterative method was used to determine optimum values of $K_1$ and $K_2$, in which values for $K_2$ were first chosen, and corresponding values of $K_1$ were then obtained graphically using an s-domain plot.

A damping ratio ($\zeta$) of 0.707 was chosen as an acceptable goal. For a step input (e.g. applied rudder angle) a damping ratio of 0.707 provides a rise time of four time constants with approximately 5% overshoot. On the s-domain plot, a line that bisects the angle between the real and imaginary axes (45° from the vertical) represents a damping ratio of 0.707.

Figures 3.4 and 3.5 show the s-domain plots for choices of $K_2$=0.5 and 2.5 respectively. The "Xs" on the real axes on both figures represent the locations of the system poles for $K_1$=0. By increasing $K_1$ from zero, the location of the two system poles of Equation (3.14) was changed. For $K_2$=0.5, a damping ratio of 0.707 was obtained for values of $K_1$=0.5 and 2.5. For $K_2$=2.5, a value of $K_1$=6.5 produced a damping ratio of 0.707, and $K_1$=2.95 produced a damping ratio close to 0.707. The simulated performance of the AUV II to a course change of 10° was analyzed for each of the four combination of gains obtained through s-domain analysis. Figure 3.6 is a plot of rudder angle ($\delta$) versus time, and Figure 3.7 shows heading angle ($\psi$) versus time. Time on both these plots is normalized; one unit is the time for the simulated AUV II to travel one shiplength. Figure 3.8 is an X-Y (geographic position) plot of the simulated AUV II through the turn. Table VII summarizes the performance of the four different gain combinations.

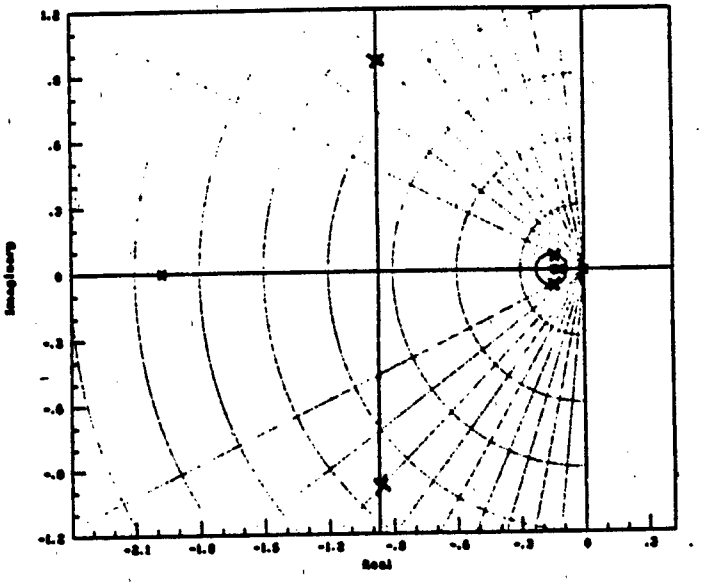

Figure 3.4 S-Domain Plot for $K_2$=0.5

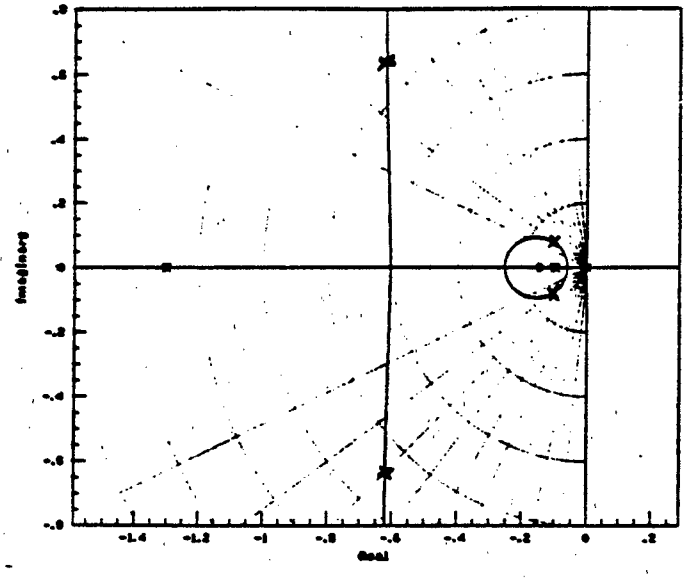

Figure 3.5 S-Domain Plot for $K_2$=2.5

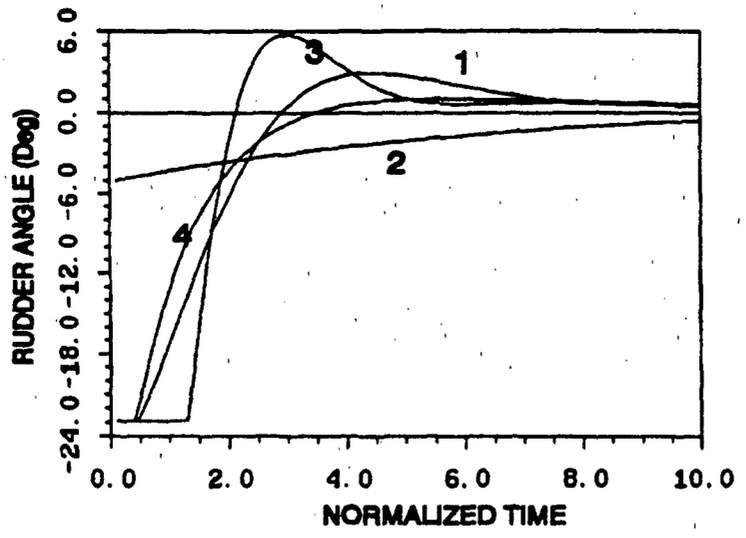


Figure 3.6 Rudder Angle vs. Time for 10° Turn

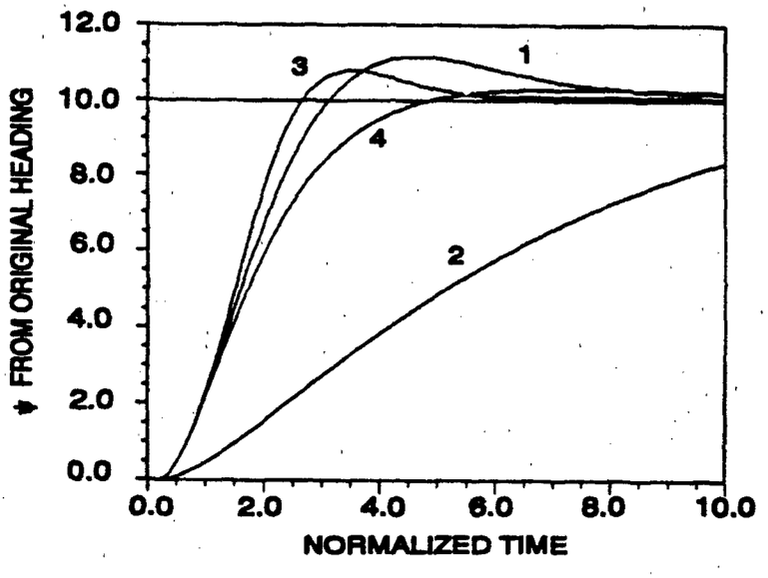


Figure 3.7 Heading versus Time for 10° Turn

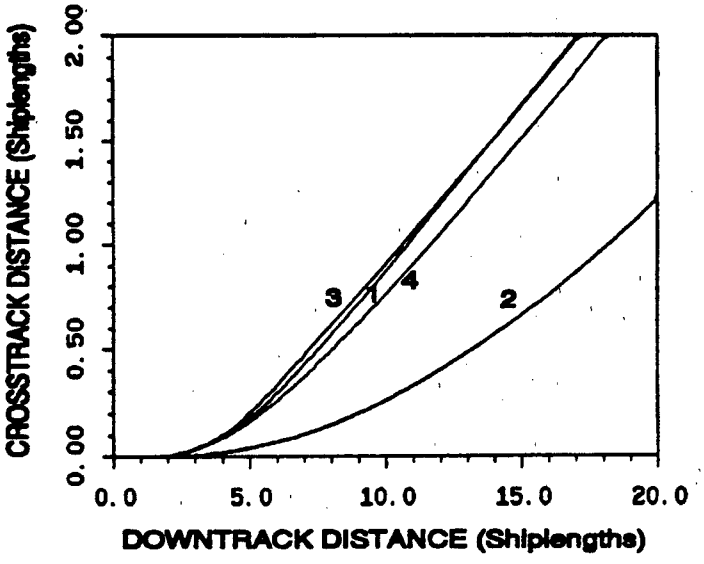


**Figure 3.8** **Simulated AUV II Position During 10° Turn**

**TABLE VII. SIMULATED AUV II PERFORMANCE FOR VARIOUS GAIN COMBINATIONS**

| Option Number | Value of $K_1$ & $K_2$ | | Normalized Rise Time (Vehicle Lengths) | Course % overshoot |
|---|---|---|---|---|
| | $K_1$ | $K_2$ | | |
| 1 | 2.5 | 0.5 | 2.8 | 11 |
| 2 | 0.5 | 0.5 | >10 | N.A. |
| 3 | 6.0 | 2.5 | 2.5 | 8 |
| 4 | 2.95 | 2.5 | 4.1 | 4 |

Analysis of the Figure 3.6 shows that the best rudder performance was obtained using gain options 1 and 4. The full capability of the rudder was not used in gain option 2, and an excessive amount of reverse rudder was used in gain option 3. Figure 3.7 shows the least amount of course overshoot was

obtained with gain option 3, with gain option 1 providing the next best result. Gain option 4 had almost no overshoot, but the time to achieve final course (rise time) was much longer than for either gain option 1 or 3. Gain options 1 and 3 provided the tightest track, though the track obtained with gain option 4 is acceptable. Yielding from the gain option 1 resulted in the best overall performance of the simulated AUV II.

The best overall performance was obtained with gain options 1 and 4. Gain option 1 was chosen as the one to use in the actual AUV II for initial testing because the actual values of $K_1$ and $K_2$ were less than for gain option 4. This translates to less rudder activity and power consumption on the AUV II, an important consideration due to the limited battery life.

## E. COMPARISON WITH ACTUAL AUV II PERFORMANCE

Initial closed loop control, in-water testing of the AUV II was performed in the Naval Postgraduate School swimming pool. This environment was free of outside disturbances, such as currents and high winds. A racetrack pattern was used for initial closed loop testing. Table VIII summarizes the heading commands to the AUV II control system. using a racetrack pattern.

**TABLE VIII. INITIAL AUV II TESTING COURSE COMMANDS**

| Time (seconds) | Course (degrees) |
|---|---|
| 0 | 000 |
| 30 | 180 |
| 90 | 360 |

Figure 3.9 shows a plot of the AUV II heading versus time using data obtained from the onboard heading gyro. Superimposed is the simulated AUV II heading for the same racetrack pattern. The constant offset in heading is caused by model inaccuracies and the speed difference between the simulated AUV II, which was assumed to be a constant 1.6 feet per second, and the actual AUV II, which increased in speed from 0 to approximately 1.6 feet per second during the first 30 seconds. If the first 30 seconds of data are discarded, the heading match between the simulated and actual AUV II's is extremely close (Figure 3.10).

Figure 3.11 is a plot of simulated and actual AUV II turning rate versus time. There is close agreement between both results, though the actual AUV II turning rate increased faster than the computer model. Figure 3.12 shows the rudder performance.

The initial performance of the AUV II was very encouraging. Hydrodynamic coefficients predicted using primarily steady state turning analysis and linearized equations of motion produced good results, noteworthy considering that when turning radii as small as the AUV II's occur (<4 ship lengths) significant non-

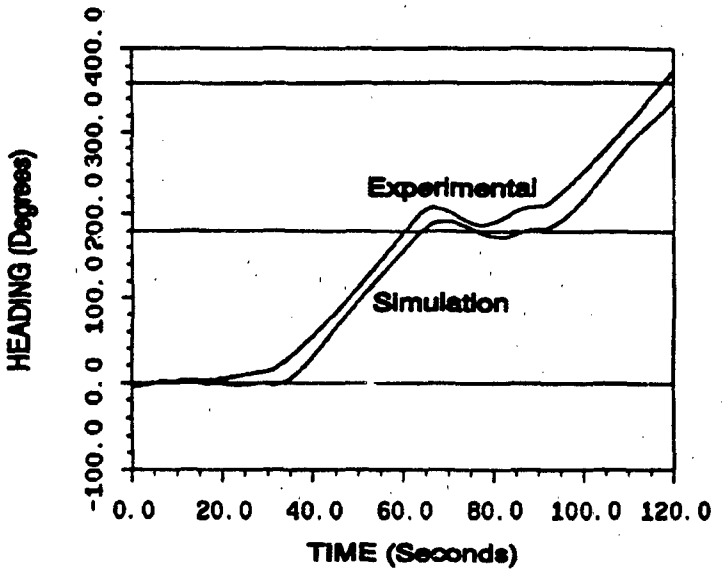


Figure 3.9 AUV II Heading vs. Time

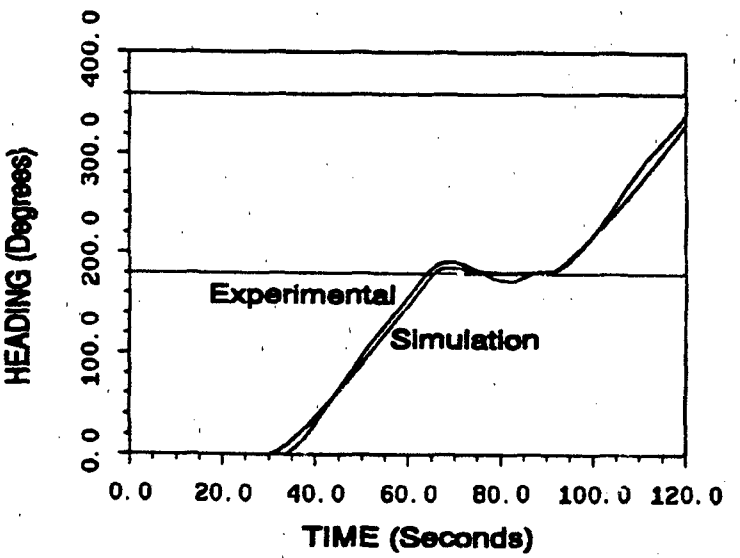


Figure 3.10 AUV II Heading (Actual and Simulated) Start Time @ 30

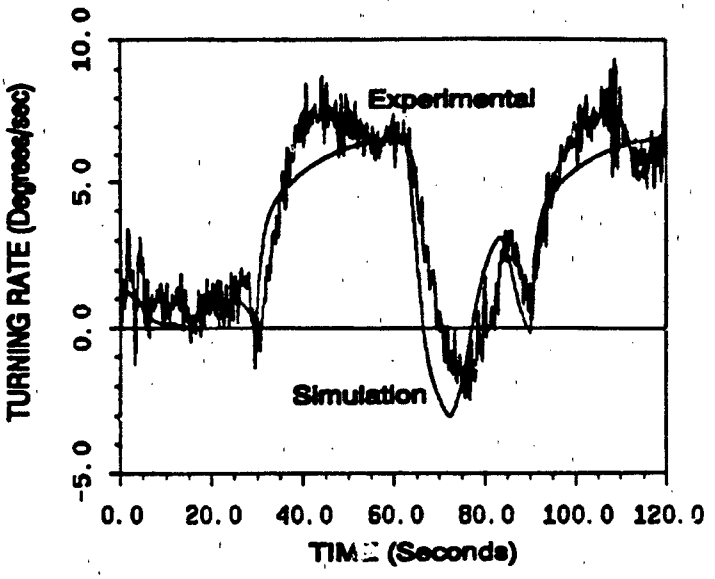


Figure 3.11 Actual and Simulated AUV II Turning Rate vs. Time

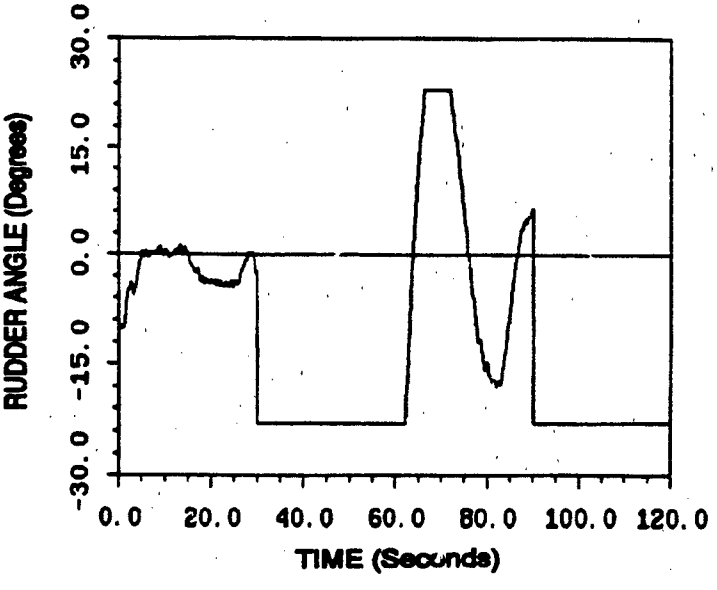


Figure 3.12 AUV Ordered Rudder Angle vs. Time

linearities are encountered in ship modeling. The correlation between actual and simulated results was sufficiently close not to require additional modifications prior to submerged testing of the AUV II.

Information still lacking at this point in the testing program was the accurate measurement of the AUV II speed. Additional analysis and refinement of the AUV II computer model had to wait until the onboard speed sensor was calibrated. Chapter IV will describe submerged AUV II testing, final determination of the lateral motion hydrodynamic coefficients, and the determination of other important hydrodynamic coefficients for the six-degree-of-freedom computer model.

# IV. AUV II SIX-DEGREE-OF-FREEDOM COMPUTER MODEL

## A. EQUATIONS OF MOTION

Further development of the AUV II model required the use of a complete three dimensional, six-degree-of-freedom computer simulation. The six equations of motion for a submerged vehicle [Ref. 10] (surge, sway, heave, yaw, pitch, and roll) were incorporated into the computer code without using any simplifying assumptions. This permitted the maximum flexibility in determining the level of model sophistication. By setting various hydrodynamic coefficients to zero, simpler models could be analyzed. Integrations used to calculate the drag forces in the lateral, heave, pitch, and yaw equations are performed numerically using the trapezoidal rule.

The computer program has the capability to simulate a submerged vehicle using all hydrodynamic coefficients. In developing the AUV II model, a number of simplifying assumptions were made. These assumptions and known physical characteristics of the AUV II are summarized below:

1. The AUV II is neutrally buoyant: W=B
2. The AUV II is symmetrically loaded in the transverse direction ($y_G$=0 and $y_B$=0), and the vertical certer of buoyancy is midway between the top and bottom of AUV II ($z_B$=0).
3. The counter-rotating propellers produce no yaw moment ($N_{prop}$=0).

4. The products of inertia about the body system zero because the AUV II possesses two axes of symmetry.

5. The AUV II acceleration and decelerations rates are small enough so that propeller slip can be neglected.

6. The effect of cross-coupled hydrodynamic coefficients can be neglected in most cases, again because of the AUV II geometric symmetry.

The resulting equations of motion are presented below.

$$\begin{aligned} m\dot{w} - mx_G\dot{q} - Z_{\dot{q}}\dot{q} - Z_{\dot{w}}\dot{w} = \\ muq - mvp - mx_G pr + mz_G(p^2 + q^2) \\ + Z_q uq + Z_w uw + u^2(Z_{\delta_s}\delta_s + Z_{\delta_b}\delta_b) \\ - \int_{x_{nose}}^{x_{tail}} [C_{D_y} h(x)(v + xr)^2 + C_{D_z} b(x)(w - xq)^2] \frac{(w - xq)}{U_{cf}(x)} dx \end{aligned} \tag{4.1}$$

**Heave Equation of Motion**

$$\begin{aligned} m\dot{u} + mz_G\dot{q} - X_{\dot{u}}\dot{u} = \\ mvr - mwq + mx_G q^2 + mx_G r^2 - mz_G pr + X_{rr} r^2 + X_{vv} v^2 \\ + u^2(X_{\delta_s\delta_s}\delta_s^2 + X_{\delta_b\delta_b}\delta_b^2 + X_{\delta_{rb}\delta_{rb}}\delta_{rb}^2 + X_{\delta_{rs}\delta_{rs}}\delta_{rs}^2) + u^2 X_{prop} \end{aligned} \tag{4.2}$$

**Surge Equation of Motion**

$$m\dot{v} + mx_G\dot{r} - mz_G\dot{p} - Y_{\dot{r}}\dot{r} - Y_{\dot{v}}\dot{v} =$$

$$mwp - mur - mx_G pq$$

$$- mz_G qr + Y_r ur + Y_v uv + u^2(Y_{\delta_a}\delta_{rb} + Y_{\delta_a}\delta_{rs}) \qquad \textbf{(4.3)}$$

$$- \int_{x_{tail}}^{x_{nose}} [C_{Dy}h(x)(v+xr)^2 + C_{Dz}b(x)(w-xq)^2]\frac{(v+xr)}{U_{cf}(x)}dx$$

**Sway Equation of Motion**

$$I_x\dot{p} - mz_G\dot{v} - K_{\dot{p}}\dot{p} =$$

$$(I_y - I_z)qr + mz_G ur - mz_G wp + K_p up - (z_G W - z_B B)\cos\theta\sin\phi \qquad \textbf{(4.4)}$$

**Roll Equation of Motion**

$$I_y\dot{q} - mx_G\dot{w} + mz_G\dot{u} - M_{\dot{q}}\dot{q} - M_{\dot{w}}\dot{w} =$$

$$(I_z - I_x)pr - mx_G uq + mx_G vp + mz_G vr - mz_G wq +$$

$$+ M_q uq + M_w uw + u^2(M_{\delta_e}\delta_e + M_{\delta_b}\delta_b) - (z_G W - z_B B)\sin\theta \qquad \textbf{(4.5)}$$

$$- \int_{x_{tail}}^{x_{nose}} [C_{Dy}h(x)(v+xr)^2 + C_{Dz}b(x)(w-xq)^2]\frac{(w-xq)}{U_{cf}(x)}x\,dx$$

**Pitch Equation of Motion**

$$I_z\dot{r} + mx_G\dot{v} - N_{\dot{r}}\dot{r} - N_{\dot{v}}\dot{v} =$$

$$(I_x - I_y)pq - mx_G ur + mx_G wp + N_r ur + N_v uv$$

$$+ u^2(N_{\delta_a}\delta_{rb} + N_{\delta_a}\delta_{rs}) + (x_G W - x_B B)\cos\theta\sin\phi + u^2 N_{prop} \qquad \textbf{(4.6)}$$

$$- \int_{x_{tail}}^{x_{nose}} [C_{Dy}h(x)(v+xr)^2 + C_{Dz}b(x)(w-xq)^2]\frac{(v+xr)}{U_{cf}(x)}x\,dx$$

**Yaw Equation of Motion**

where $U_{cf}(x) = [(v+xr)^2 + (w - xq)^2]^{1/2}$

In addition to these equations, the six-degree-of-freedom computer model includes equations for the euler angle rates ($\dot{\psi}$, $\dot{\phi}$, $\dot{\theta}$) and inertial position rates ($\dot{x}$, $\dot{y}$, $\dot{z}$). These equations are contained in [Ref. 10] and can be easily interpreted from the six-degree-of-freedom computer model in Appendix B.

## B. ESTIMATION OF HYDRODYNAMIC COEFFICIENTS

The determination of the hydrodynamic coefficients in the yaw and sway equations (4.3 and 4.6) was discussed in Chapters II and III. This section will discuss the determination of the hydrodynamic coefficients in the remaining equations of motion.

### 1. Heave and Pitch Equations

The hydrodynamic coefficients in the heave equation (4.1) $Z_w$, $Z_{\dot{w}}$, $Z_q$ and $Z_{\dot{q}}$, and pitch equation (4.5) $M_w$, $M_{\dot{w}}$, $M_q$, $M_{\dot{q}}$ were determined by geometrically scaling the given SDV hydrodynamic coefficients. The hydrodynamic coefficients related to the accelerations are a function of the added mass of the vehicle. Due to the similar, and fairly rectangular shapes of the AUV II and SDV, the coefficients can be considered proportional to the enclosed volume, or mass since both vehicles are neutrally buoyant. For example

$$(Z_{\dot{w}})_{SDV} = \frac{\rho}{2} L^3 (Z'_{\dot{w}})_{SDV} \approx Km_{SDV}$$

where $Z'_{\dot{w}}$ is the dimensionless hydrodynamic coefficient. (For convenience the prime has been left off in other discussions regarding hydrodynamic coefficients,

and will again be left off after this section). Writing a similar expression for $(Z_w)_{AUV}$, and taking the ratio between the two coefficients yields

$$(Z'_w)_{AUV} = (Z'_w)_{SDV}\left(\frac{L_{SDV}}{L_{AUV}}\right)^3\left(\frac{m_{AUV}}{m_{SDV}}\right)$$

By substituting in the appropriate vehicle dimensions and masses

$$(Z'_w)_{AUV} = 0.3718\,(Z'_w)_{SDV}$$

This same ratio applies to the geometric scaling for the other acceleration-related terms.

The velocity-related hydrodynamic coefficients are related to drag forces on the vehicle. For the pitch and heave equations the areas of interest are the vehicle top and bottom. For example

$$(Z_w)_{SDV} = \frac{\rho}{2}L^2(Z'_w)_{SDV} = K\,L_{SDV}\,B_{SDV}$$

Again taking a ratio between AUV II and SDV hydrodynamic coefficients yields

$$(Z'_w)_{AUV} = (Z'_w)_{SDV}\left(\frac{L_{SDV}}{L_{AUV}}\right)\left(\frac{B_{AUV}}{B_{SDV}}\right) = 0.5195(Z'_w)_{AUV}$$

Table IX summarizes the results of geometrically scaling the hydrodynamic coefficients for the pitch and heave equations.

**TABLE IX. PITCH AND HEAVE EQUATION HYDRODYNAMIC COEFFICIENTS**

| Coefficient | SDV Value | Scaling Factor | AUV II Value |
|---|---|---|---|
| $Z_w$ | -0.30200 | 0.5195 | -0.15687 |
| $Z_q$ | -0.13500 | 0.5195 | -0.07013 |
| $M_w$ | 0.09860 | 0.5195 | 0.05122 |
| $M_q$ | -0.06860 | 0.5195 | -0.03563 |
| $Z_w$ | -0.24300 | 0.3718 | -0.09340 |
| $Z_q$ | -0.00681 | 0.3718 | -0.00253 |
| $M_w$ | -0.00681 | 0.3718 | -0.00253 |
| $M_q$ | -0.01680 | 0.3718 | -0.00625 |

### 2. Roll Equation

The primary hydrodynamic coefficients, $K_p$ and $K_{\dot{p}}$, in the roll equation (4.4) were also determined by scaling the given SDV hydrodynamic coefficients. When a vehicle enters a turn the amount and direction of roll is a function of the location of $C_B$ and $C_G$ and the lateral force caused by lateral motion ($Y_v$). Prior to scaling, the effect of the fin on the SDV had to be "removed" from the given values of $K_p$ and $K_{\dot{p}}$. This was done by multiplying the given values of $K_p$ and $K_{\dot{p}}$ by the ratio of the given SDV and Finless SDV values of $Y_v$:

$$(\hat{K}_p')_{finless} = (K_p')_{given}\left(\frac{(Y_v)_{finless}}{(Y_v)_{given}}\right) = -0.01100\left(\frac{-0.03585}{-0.05550}\right) = -0.00711$$

$$(\hat{K}_p')_{finless} = (K_p')_{given}\left(\frac{(Y_v)_{finless}}{(Y_v)_{given}}\right) = -0.00101\left(\frac{-0.03585}{-0.05550}\right) = -0.00065$$

As in the case of the heave and pitch equations, the acceleration coefficient is a function of the added mass term, and is proportional to the masses of the vehicles. Thus

$$(\hat{K}_p')_{AUV} = 0.3718(\hat{K}_p')_{SDV} = (0.3718)(-0.0065) = -0.00024$$

The velocity-related coefficient, $K_p$, is a function of the area of the vehicle side, normal to the lateral velocity vector,

$$(\hat{K}_p)_{SDV} = \frac{\rho}{2}L^2(\hat{K}_p')_{SDV} = K\,T_{SDV}\,L_{SDV}$$

and taking the ratio between AUV II and SDV terms yields

$$(K_p')_{AUV} = (\hat{K}_p')_{SDV}\left(\frac{L_{SDV}}{L_{AUV}}\right)\left(\frac{T_{AUV}}{T_{SDV}}\right) = (-0.00711)(0.7598) = -0.00540$$

### 3. Surge Equation

The acceleration-related hydrodynamic coefficient, $X_{\dot{u}}$, in the surge equation (4.2), was estimated by geometric similarity in the same way as described for other acceleration-related hydrodynamic coefficients.

$$(X'_u)_{AUV} = 0.3718(X'_u)_{SDV} = -0.00282$$

In order to account for nonlinearities in the equations of motion that become significant when turning radii as tight as the AUV II has are encountered, two cross-correlation coefficients were included in the AUV II model. $X_{rr}$, the hydrodynamic force in the x direction as a function of yaw rate, and $X_{vv}$, the hydrodynamic force in the x direction as a function of lateral velocity were estimated for the given SDV values by geometric similarity. The area on the vehicle of concern for these coefficients is the side, thus both $X_{vv}$ and $X_{rr}$ are proportional to the product of vehicle length and draft.

$$(X_{vv})_{SDV} = \frac{\rho}{2} L^2 (X'_{vv})_{SDV} = K L_{SDV} T_{SDV}$$

$$(X_{rr})_{SDV} = \frac{\rho}{2} L^4 (X'_{rr})_{SDV} = K L_{SDV} T_{SDV}$$

Taking ratios of expressions for $X_{vv}$ and $X_{rr}$ for the AUV II and SDV yields

$$(X'_{vv})_{AUV} = (X'_{vv})_{SDV} \left(\frac{L_{SDV}}{L_{AUV}}\right)\left(\frac{T_{AUV}}{T_{SDV}}\right) = (0.05290)(0.7598) = 0.0401$$

$$(X'_{rr})_{AUV} = (X'_{rr})_{SDV} \left(\frac{L_{SDV}}{L_{AUV}}\right)^3\left(\frac{T_{AUV}}{T_{SDV}}\right) = (-0.00401)(4.327) = 0.01735$$

Neglecting propeller slip, $X_{prop}$ is proportional to the overall vehicle drag coefficient, $C_{DO}$. The process begins with the general equation of propulsion force where $\eta = \frac{u_o}{n_o}$, $u_o$ = speed (ft/sec), and $n_o$ = rpm. Rearranging terms, and collecting coefficients results in the following non-linear differential equation:

$$(m - \frac{\rho}{2} l^3 X_u')\dot{u} = \frac{\rho}{2} l^2 u^2 X_{prop}'$$

$$= \frac{\rho}{2} l^2 C_{DO} (\eta n)^2 - \frac{\rho}{2} l^2 C_{DO} u^2$$

$$(m - X_u)\dot{u} + au^2 = a\eta^2 n^2 \qquad \text{where} \quad a = \frac{\rho}{2} l^2 C_{DO} \tag{4.7}$$

This equation can be solved by isolating time and speed-related terms on opposite sides of the equation sign, and then integrating from an initial condition of u=0 at t=0 to u=$u_o$ at t=t. The resulting expression for speed, u, is

$$u = \eta n \frac{e^{At} - 1}{e^{At} + 1}, \qquad \text{where} \quad A = \frac{2a\eta n}{m - X_u} \tag{4.8}$$

To find a value for $C_{DO}$, an expression for a in Equation (4.7) in terms of the other coefficients is required. By assuming u to be a linear fraction ($\alpha$) of $u_o$, when t=T, and n=$n_o$, then

$$\alpha u_o = \eta n_o \frac{e^{AT} - 1}{e^{AT} + 1}$$

Inserting the expression for A from Equation (4.8), and after some algebra, an equation for a is obtained

$$a = \frac{m - X_u}{2u_o T} \ln\left(\frac{1 + \alpha}{1 - \alpha}\right) \tag{4.9}$$

Placing Equation (4.9) into the definition of a in Equation (4.7), and rearranging terms yields an explicit expression for $C_{DO}$

$$C_{DO} = \frac{m - \frac{\rho}{2} l^3 X_{\dot{u}}}{u_o T \rho l^2} \ln\left(\frac{1+\alpha}{1-\alpha}\right) \qquad (4.10)$$

Observations of the AUV II during its maiden voyage indicated the vehicle achieved full speed after a bit more than 20 seconds. By assuming that the AUV II had achieved 90 percent of maximum speed at 20 seconds, using Equation (4.10), an estimated value for $C_{DO}$ of 0.015 was obtained.

## C. ACTUAL AUV II PERFORMANCE COMPARISON WITH MODEL

### 1. Speed

A computer program was written to compute the AUV II speed versus time for various values of $C_{DO}$. Figure 4.1 shows a plot of speed versus time for three different values of $C_{DO}$. Included on the figure is a plot of actual AUV II speed during initial acceleration. The two second offset from zero is due to a data recording problem in the AUV II; shifting the curve to the left shows that it coincides very close to the $C_{DO}$=0.015 curve. Figure 4.2 is a plot of time to reach a certain percentage of top speed versus $C_{DO}$. Curves are plotted for 90%, 95%, and 99% of maximum speed. The AUV II reaches 90% of top speed in approximately 12 seconds.

### 2. Run Profile

The following figures show how close the AUV II model matches the actual AUV II performance. A "Figure 8" run profile was used for this

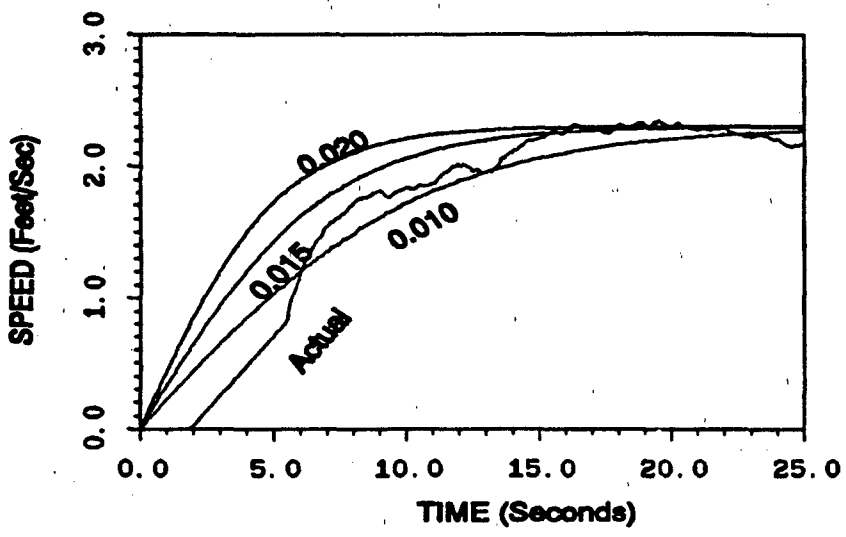


Figure 4.1 AUV II Actual Speed Versus Simulated for Different Values of $C_{DO}$

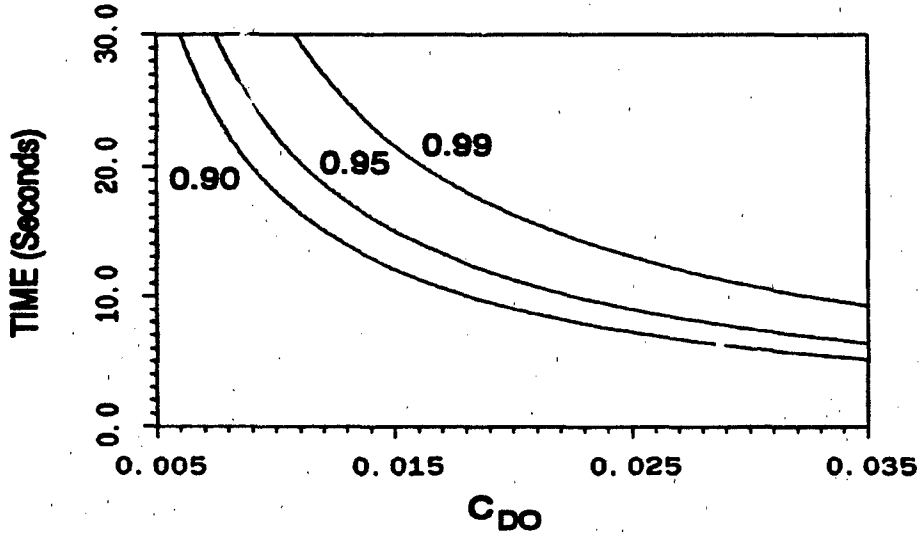


Figure 4.2 Time to Achieve Percentage of Final Speed

comparison. Ordered AUV II speed was two feet/second, and the ordered depth was two feet.

Figure 4.3 shows the rudder commands used to drive the AUV II through the run. After an initial straight run, the ordered rear rudder angles were ±15°; ordered bow rudder angles were the opposite of the stern rudder angles. Figure 4.4 compares measured AUV II turning rate with the computer model. The actual AUV II propeller speeds are shown in Figure 4.5. Note that the rpms are different; the right motor saturates at a lower rpm than the left motor. Fifteen seconds into the run, the speed controller on board the AUV II ordered lower rpms to maintain a speed of two feet per second. Shortly thereafter the first turn began which caused speed to drop, and full speed was ordered on the propellers for the remainder of the run. The gradual drop in rpm during the remainder of the run was due to a drop in battery voltage.

Figure 4.6 compares the computer model and actual AUV II speeds. There is close agreement between the model and actual speeds.

The AUV II model depth performance is shown in Figure 4.7. Figure 4.8 is a plot of the actual stern plane deflection versus time. The actual AUV II planes moved quite a bit to maintain the vehicle on depth through the turns. Comparisons between actual and simulated vehicle pitch rate were not quite as satisfactory as for lateral motion. This is due to a lack of calibration of the hydrodynamic coefficients in the vertical plane as was done for the lateral equations of motion. Nevertheless, the developed computer model provided an

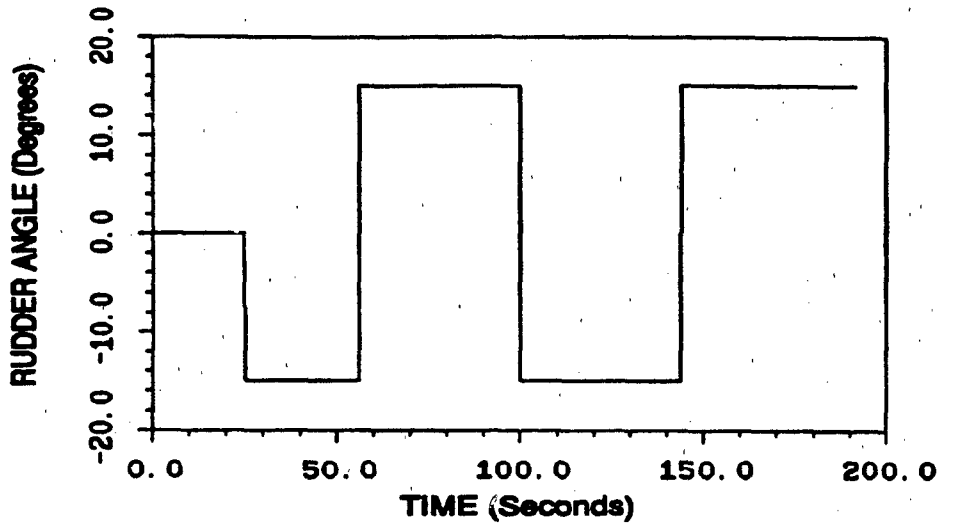


Figure 4.3 Rudder Commands for Figure Eight

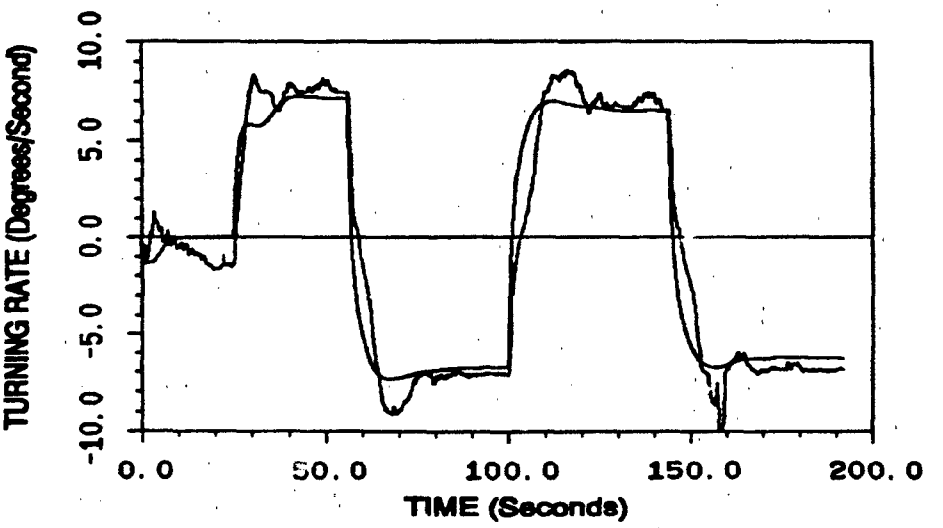


Figure 4.4 AUV II Actual Versus Simulated Turning Rate

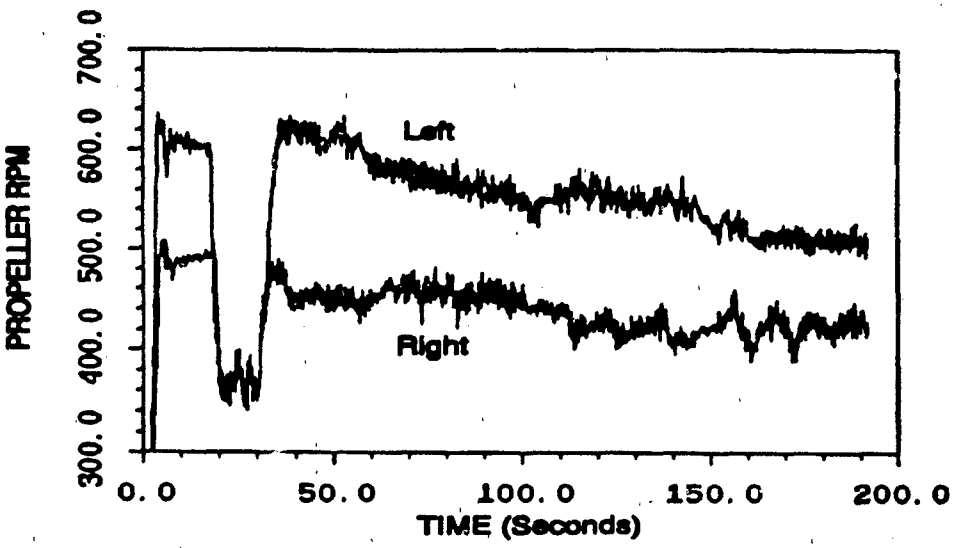


Figure 4.5 Actual AUV II Propeller Speeds

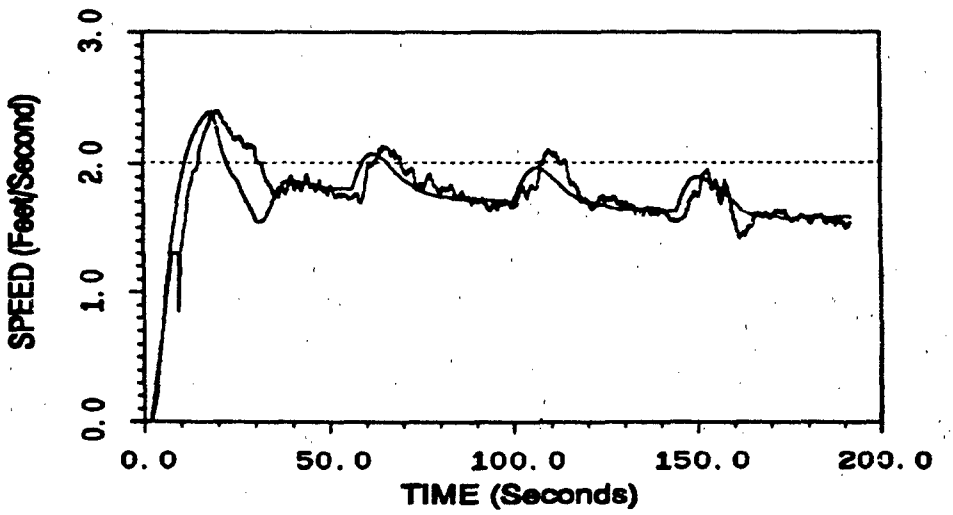


Figure 4.6 Actual Versus Simulated AUV II Speed

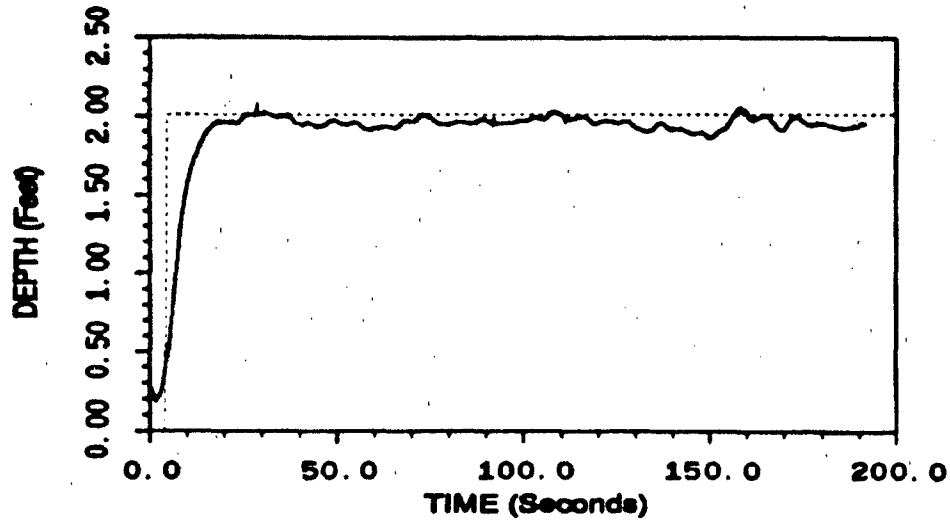


Figure 4.7 Actual AUV II Depth

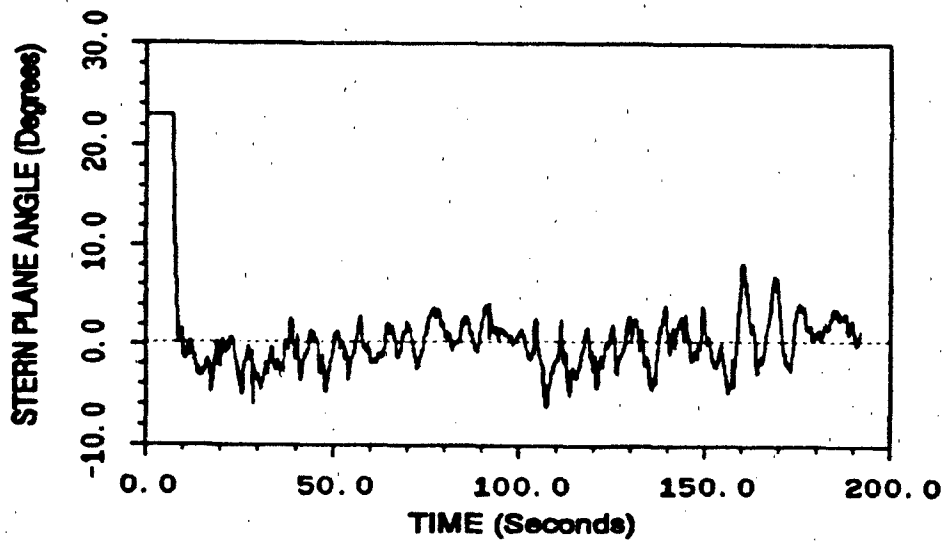


Figure 4.8 Actual AUV II Stern Plane Angle

excellent basis for designing an accurate depth controller, as evidenced by the results of Figure 4.7.

# V. POSITION ESTIMATION AND LATERAL VELOCITY OBSERVER DESIGN AND CALIBRATION

## A. BACKGROUND

The safe operation of a ship and its ability to perform assigned missions requires a continuous knowledge of position. Navigation equipment required in ships has been established by international convention [Ref. 26] and includes a marine radar system, radio direction finder, gyroscopes, and echo sounders. Additional equipments used to fix a ship's position include doppler sonar, satellite positioning receiver, LORAN and Omega.

During the period between fixes a ship's position is estimated using a procedure known as "dead reckoning," in which the ship's position is projected ahead based on ordered course and speed. Ocean currents and errors in estimating or maintaining the ship's course and speed result in the generation of a circle of position uncertainty around the "dead reckoned" position estimate. Naval vessels commonly have an inertial navigator system to accurately estimate position between fixes. The inertial navigator consists of accelerometers mounted such that accelerations in sway, heave and surge are accurately sensed. The accelerations are integrated to determine the vessel's velocity along the three principle axes. The velocities are integrated again to obtain the distance the ship has traveled since the last fix.

Precise knowledge of the AUV II position is just as critical a problem as with any vessel. In fact, the absence of human intervention during a mission requires that navigation and motion control systems provide an extremely accurate estimate of position at all times. The current configuration of the AUV II does not include a system for determining a navigational fix.

The size of the AUV II limits the size and complexity of onboard navigation systems. Within the confines of the NPS swimming pool it is feasible to use the sonar system for position fixing provided accurate sonar ranges to the walls of the swimming pool are available, that information can be used to determine the AUV II position. However, the quality of sonar returns from the walls of the swimming pool are frequently not accurate and consistent enough, especially during turns, to provide continuous and reliable fix information.

The accelerometers on board the AUV II could also be employed as an inertial navigation system to provide a continuous and accurate estimate of the AUV II position. However, the sensitivity of the accelerometers, which must be capable of withstanding gravitational acceleration, is insufficient to accurately measure typical AUV II accelerations which are in the range of .05g.

Data available from instrumentation on board the AUV II includes forward velocity (u), heading ($\psi$), and turning rate (r). Equation (5.1) shows the state space method to determine AUV II velocities in the x and y directions.

$$\dot{x} = u\cos\psi - v\sin\psi$$
$$\dot{y} = u\sin\psi + v\cos\psi \qquad (5.1)$$

Position is then determined by integrating $\dot{x}$ and $\dot{y}$. Note that lateral velocity (v), is not available from instrumentation on board the AUV II. The "dead reckoner" on board the AUV II uses only velocity and heading information to determine position, i.e. v is always assumed to be 0. This results in significant position inaccuracies being built up during the AUV II operation.

With these limitations in mind, three different methods were investigated to provide the AUV II with an accurate position estimator. The first method investigated used the six-degree-of-freedom computer model developed in the previous chapter. A second method used a reduced order observer to estimate lateral velocity. The third method investigated was an explicit determination of lateral velocity based on the turning rate.

## B. SIMULATION POSITION ESTIMATE

The six-degree-of-freedom simulation program was used to provide an estimate of lateral velocity to use in Equation (5.1). The program simulates the rates of change of lateral velocity ($\dot{v}$) and turning rate ($\dot{r}$) using Equation (3.5). After performing a first order integration to determine v

$$v = v + (\Delta t)\dot{v} \qquad (5.2)$$

$\dot{x}$ and $\dot{y}$ are calculated using Equation (5.1). The present AUV II position is then determined by a first order integration of the form of Equation (5.2).

The shortcoming of this method of estimating the AUV II position is that the actual turning rate, $r_{act}$, is not equal to the simulated turning rate, $r_{sim}$. Figure 5.1 shows a comparison of $r_{act}$ and $r_{sim}$ for the first 100 seconds of the "Figure 8" run profile analyzed in the previous chapter. The difference in the simulated r between Figures 4.4 and 5.1 is due to the fact that Figure 5.1 was obtained by using a simulation of the horizontal plane equations only. Since no pitch motions and dive plane activity is present in this case, the model is, as expected, more responsive. Even if the AUV II hydrodynamic coefficients were exactly known, $r_{act}$ and $r_{sim}$ would not always be equal. Over time this difference would result in an ever-increasing error in actual versus estimated positions.

## C. REDUCED ORDER OBSERVER

The development of a closed loop lateral motion control system for the AUV II as described in Chapter III did not require a knowledge of lateral velocity. An accurate estimate of the AUV II position does require knowledge of lateral velocity. Because lateral velocity is not a state variable that can be measured, it must be estimated.

A dynamic system in which state variables are estimated from known (measured) variables is called an observer. It can be shown [Ref. 27] that for an observable system, an observer can be designed such that the difference

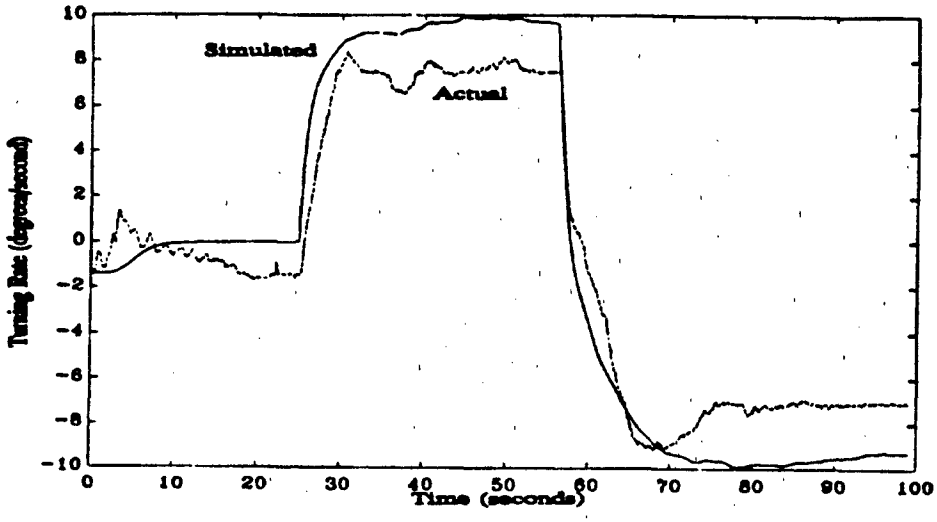


**Figure 5.1.** **Comparison of $r_{act}$ versus $r_{sim}$**

between the state of the actual system and the state of the observer can be made to reach zero as fast as desired through pole placement techniques. If some of the dynamic system state variables can be measured, then a reduced order observer can be developed to estimate the remaining state variables.

The development of a reduced order observer for lateral velocity begins with the equations for $\dot{r}$ and $\dot{v}$ presented in Equation (3.3), and reproduced below.

$$\dot{v} = a_{11}uv + a_{12}ur + b_{11}u^2\delta_{rs} + b_{12}u^2\delta_{rb}$$
$$\dot{r} = a_{21}uv + a_{22}ur + b_{21}u^2\delta_{rs} + b_{22}u^2\delta_{rb} \qquad \textbf{(5.3)}$$

In Equation (5.3) r is known, but v must be estimated by

$$\hat{\dot{v}} = a_{11}u\hat{v} + a_{12}uC_1^{-1}y + b_{11}u^2\delta_{ra} + b_{12}u^2\delta_{rb}$$

By defining

$$\hat{v} = Ly + z \tag{5.4}$$

where

$$\dot{z} = Fz + Gy + Hu \tag{5.5}$$

the estimation error can be defined as

$$\dot{e} = \dot{v} - \hat{\dot{v}} = a_{12}ur + a_{11}uv + b_{11}u^2\delta_a + b_{12}u^2\delta_b - L\dot{y} - \dot{z}$$

After a few algebraic steps, and grouping terms associated with r, v, $\delta_b$ and $\delta_a$, the estimation error can be expressed as

$$\begin{aligned}\dot{e} = Fe &- [a_{12}u - LC_1a_{22}u + FLC_1 - GC_1]r \\ &+ [a_{11}u + LC_1a_{21}u - F]v \\ &+ [b_{11}u^2 - LC_1b_{21}u^2 - H_1]\delta_a \\ &+ [b_{12}u^2 - LC_1b_{22}u^2 - H_2]\delta_b\end{aligned} \tag{5.6}$$

For the error to be independent of r, v, $\delta_b$, and $\delta_a$, the matrices multiplying them must vanish (i.e. equal 0). Therefore, matrices F, G and H can be defined as

$$F = a_{11}u - LC_1a_{22}u$$

$$G = [a_{12}u - LC_1a_{22}u]C^{-1} + F$$

$$H = [b_{11}u^2 - LC_1b_{21}u^2 \quad b_{12}u^2 - LC_1b_{22}u^2]^T$$

and,

$$\dot{e} = Fe$$

For the system to be stable, the eigenvalues of F must lie in the left half of the s-plane. Since F in this problem is a scalar, appropriate eigenvalues, equivalent to the observer time constants, can be directly determined without computing the determinant of a matrix.

The observer gain matrix, L, also a scalar in this problem, is found by solving

$$F = a_{11}u - La_{21}u = \frac{-u}{T_o l} \qquad (5.7)$$

where $\frac{-u}{T_o l}$ represents the eigenvalue of F. The AUV II vehicle length is l, and $T_o$ is expressed in time to travel a certain number of vehicle lengths. Different values of the observer time constant, $T_o$, result in different values of the observer gain matrix. Once a value for L has been found, Equations (5.4) and (5.5) are used to calculate an estimated value for v which is then used in Equations (5.1) and (5.2) to calculate the AUV II velocities and the present AUV II position.

Figure 5.2 is a plot of lateral velocity versus time for the first 100 seconds of the Figure 8 run profile. Note the variation of estimated lateral velocity versus

time constant. Varying the time constant of a linear observer should only affect the speed with which the estimate converges to the exact value. However, in this instance varying the time constant also affected the steady state value of lateral velocity. The reasons for this will be discussed after the next section which describes the development of the "explicit" lateral velocity curve shown in Figure 5.2.

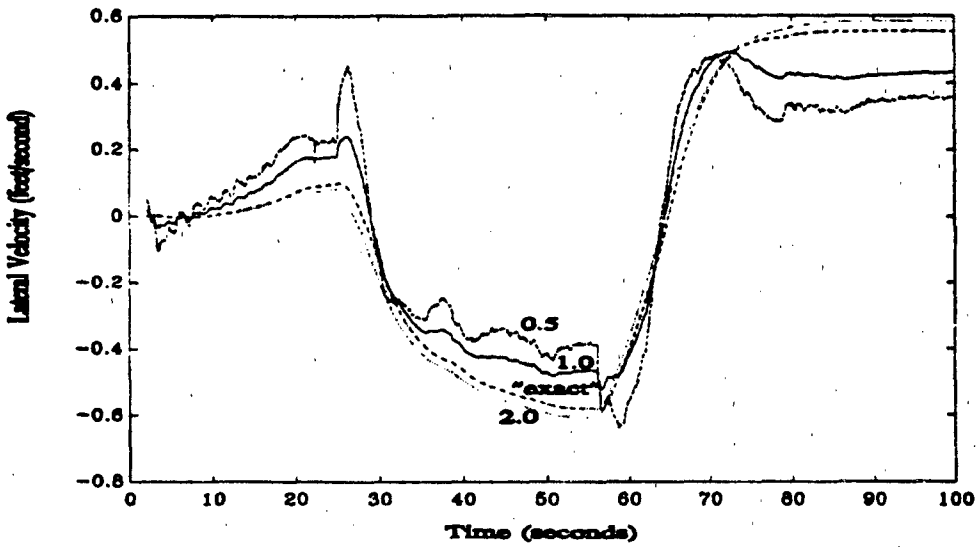


**Figure 5.2** **AUV II Lateral Velocity versus Time for Different Observer Time Constants**

## D. EXPLICIT DETERMINATION OF LATERAL VELOCITY

The expressions for $\dot{v}$ and $\dot{r}$ with the bow and stern rudders not operating independently are contained in Equation (3.5), and printed below in equation vice matrix form.

$$\dot{v} = a_{11}uv + a_{12}ur + b_1u^2\delta$$
$$\dot{r} = a_{12}uv + a_{22}ur + b_2u^2\delta \qquad \textbf{(5.8)}$$

The rudder angle, $\delta$, can be eliminated by rearranging the equations, yielding an equation that is a function of v, $\dot{v}$, r and $\dot{r}$ only,

$$b_2\dot{v} + (b_1a_{21} - b_2a_{11})uv = b_1\dot{r} + (a_{12}b_2 - b_1a_{22})ur$$

or, in the s domain

$$KT_3sv + Kv = K_vr + K_vT_4sr$$
$$\text{where} \quad K = (b_1a_{21} - b_2a_{11})u$$
$$T_3 = b_2/K \qquad \textbf{(5.9)}$$
$$K_v = (a_{12}b_2 - b_1a_{22})u$$
$$T_4 = b_1/K_v$$

K and $K_v$ are constants and $T_3$ and $T_4$ can be treated as time constants of v and r respectively.

Equation (5.9) can be rearranged to clearly show the explicit transfer function that exists between v and r

$$\frac{v}{r} = \frac{K_v(1 + T_4s)}{K(1 + T_3s)} \qquad \textbf{(5.10)}$$

from which an explicit solution for $\dot{v}$ can be derived

$$\dot{v} = -\frac{1}{T_3}v + \frac{K_vT_4}{KT_3}\dot{r} + \frac{K_v}{KT_3}r \qquad \textbf{(5.11)}$$

The "explicit" lateral velocity curve of Figure 5.2 was obtained by using Equation (5.10) to determine $\dot{v}$.

A possible problem exists with Equation (5.11) in that the derivative of r is used to calculate $\dot{v}$. Any noise in the value of r is amplified by taking its derivative, and this amplified noise has the potential to degrade the computed value of $\dot{v}$. Therefore, it is desirable to eliminate the zero associated with $\dot{r}$. This is accomplished by writing the reciprocal of Equation (5.10) and performing a Taylor series expansion of the right hand side. The resulting "first order" transfer function between v and r is

$$\frac{v}{r} = \frac{K_v}{K + K(T_3 - T_4)s}$$

in which, in the time domain, Equation (5.12), $\dot{v}$ is a function of only v and r

$$\dot{v} = -\frac{1}{T_3 - T_4}v + \frac{K_v}{K(T_3 - T_4)}r \qquad \textbf{(5.12)}$$

Figure 5.3 shows the explicitly determined lateral velocity as computed by the exact expression (Equation (5.11)) and the first order approximation (Equation (5.12)). Also shown, for comparison, is the 0-th order approximation obtained from Equation (5.10) by substituting s=0. In the case of the AUV II the effect of noise in the value of $\dot{r}$ is minimal. Though the amplitude of all the terms in Equation (5.11) are within the same order of magnitude, it appears that any noise introduced into the estimation of $\dot{v}$ is minimized by the subsequent integration to obtain v.

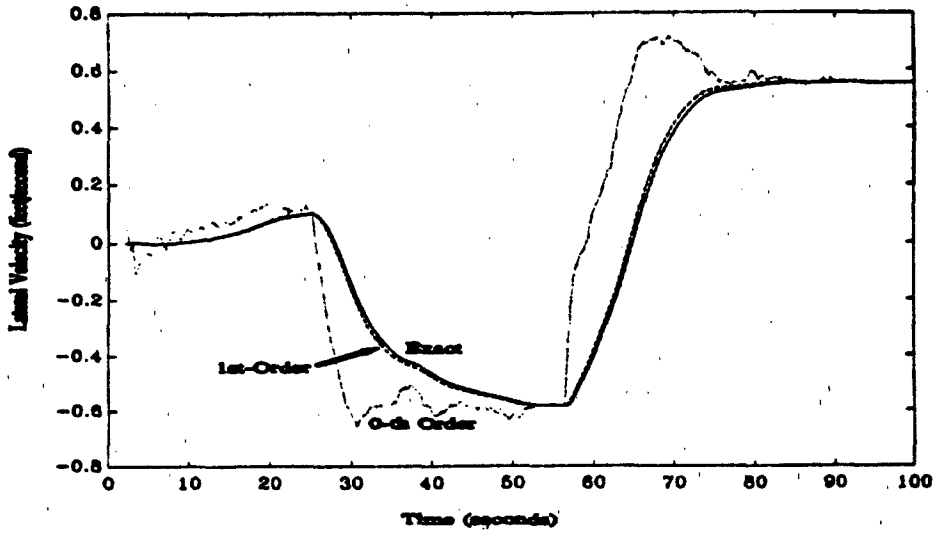


**Figure 5.3** **Explicitly Determined AUV II Lateral Velocity, Exact and First Order Approximations**

The explicitly determined lateral velocity behaves as an observer with a time constant between 1 and 2. This "natural time constant" can be computed directly from Equation (5.7). This time constant is a function of the AUV II hydrodynamic coefficients which make up the various coefficients of the **a** and **b** matrices. Substituting numbers into the equation yields a value of $T_o$ of approximately 1.8. This is consistent with the location of the explicit curve on Figure 5.2.

## E. OBSERVER CHARACTERISTICS AND CALIBRATION

The analysis so far has only compared different methods of estimating the AUV II lateral velocity. Still unknown is the actual AUV II lateral velocity, which is the benchmark against which the different estimation methods must be judged.

Since there is no way to determine the actual AUV II lateral velocity, the six-degree-of-freedom computer simulation was used to determine the appropriate lateral velocity observer time constant.

### 1. Six-Degree-of-Freedom Calibration of Lateral Velocity Observer

Generating a track using the six-degree-of-freedom computer model of the AUV involved no estimates of sensor errors. Recognizing that the model is not yet a perfect representation of the AUV II, it could still be used to generate a track against which the performance of the enhanced position estimator could be evaluated. The inputs to the simulation were actual AUV II rpm and rudder angles as recorded during an oval run profile performed by the AUV II. Actual rpm and rudder commands were fed into the simulation. The results of the simulation were treated as the truth against which the different lateral velocity observers were compared. Figure 5.4 is a plot of lateral velocity versus time. In addition to the real lateral velocity as determined by the six-degree-of-freedom computer model, results for observers with time constants of 1, 1.5, 2, and 2.5 vehicle lengths are plotted.

Analysis of Figure 5.4 reveals that the best time constant for the lateral velocity observer is approximately 2.0. The reason for the difference in the results for different observer time constants can be attributed to the non-linearities of the equations of motion used in the six-degree-of-freedom computer simulation. The lateral motion observers were developed based on linear, simplified equations of motion. Any non-linearities not accounted for in the observer design would result

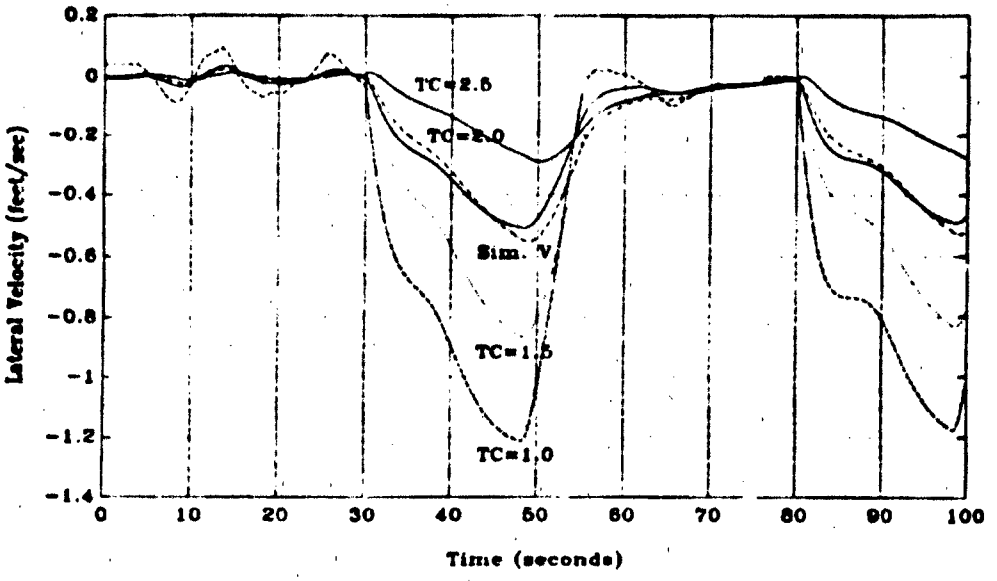


**Figure 5.4** **Comparison of Simulated AUV II Lateral Velocity with Estimated Lateral Velocities**

in the error in estimating lateral velocity not being independent of r, $\dot{r}$, v and $\dot{v}$. Thus, the observer would "believe" the estimation error was zero, when it in fact was not. These "hidden" non-linearities are responsible for the variation in steady state lateral velocities seen in Figures 5.2 and 5.4.

In order to verify the variation in steady state lateral velocities during the turns was in fact caused by non-linearities and that the observer was working properly, the same speed and rudder commands from the oval run of the AUV II were used in a simulation program based solely on the simplified, linear equations of motion. Figure 5.5 is a plot of the difference between the simulated lateral velocity and the explicit and estimated lateral velocities. The differences are

almost insignificant, thus verifying the proper performance of the lateral velocity observer.

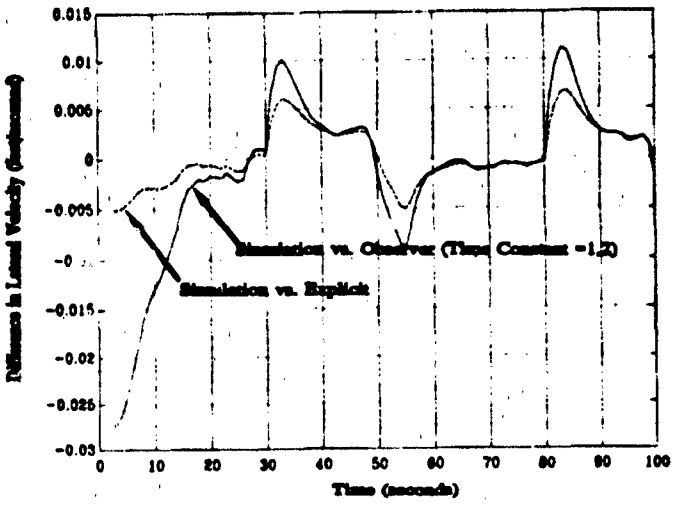


**Figure 5.5** **Difference Between Simulated and Estimated AUV II Lateral Velocities Using Linear, Simplified Equations of Motion**

Figure 5.6 shows the results of using the six-degree-of-freedom computer model using a version of program OBSERVE (Appendix C). The solid line is the actual simulated track, the "truth" which the enhanced position estimator had to match. The dashed line shows the position estimate that would have been calculated by the AUV II without lateral velocity information. The dotted line shows the estimated position of the AUV II using time constants of 1.5, 2.0, and 2.5. It appears that the best time constant lies between 2.0 and 2.5.

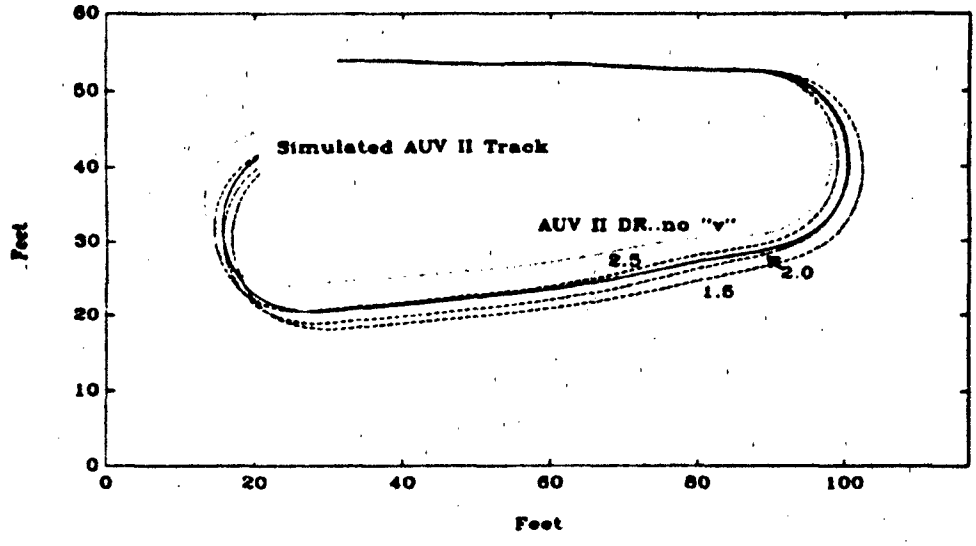


**Figure 5.6 Geographic Plot of Simulated AUV II Run**

The improvement in position estimation using the reduced order observer for lateral velocity is clearly seen. Figure 5.7 shows the difference between the simulated and estimated x and y positions for a time constant of 2.3. Nowhere is the error more than two feet. More importantly, since the position estimator is being driven by the lateral velocity observer, the cross track error is never greater than one foot.

As pointed out before, the six-degree-of-freedom computer model of the AUV II is not yet perfect. Consequently, there will be some differences between an actual and simulated track. In particular, any error in lateral velocity will be integrated into the estimate of position. As time progresses, this error will continually increase.

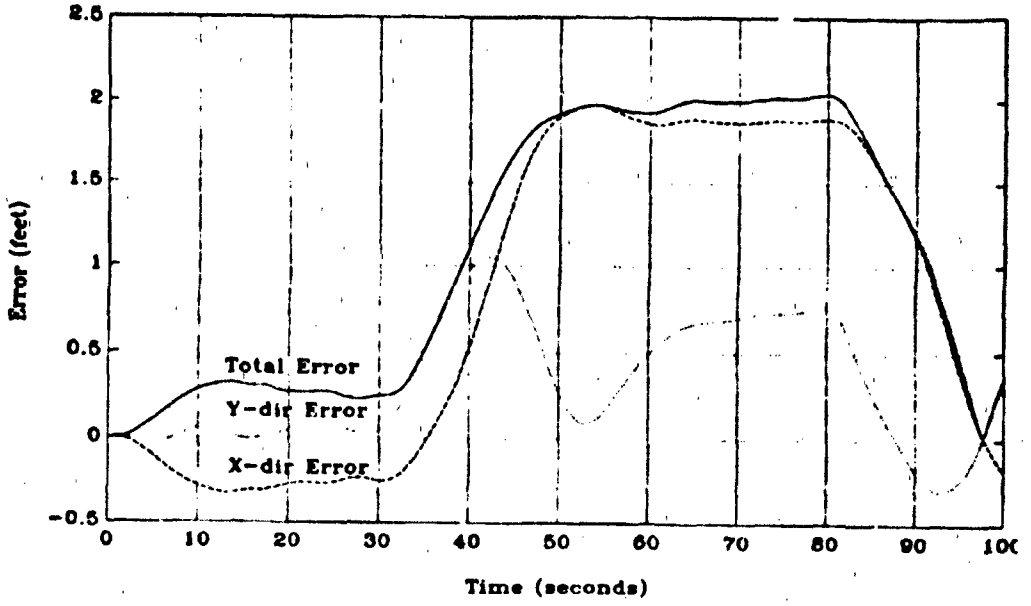


**Figure 5.7** **Position Estimate Range Error**

### 2. "Constant Pool Width" Verification

It has been shown that the reduced order lateral velocity observer and the enhanced position estimator can accurately estimate the AUV II geographic position when using the six-degree-of-freedom computer model. The ability of the lateral velocity observer and enhanced position estimator to estimate actual AUV II position from an actual AUV II run provided a second, independent means of proving the validity of this technique to obtain a real-time position estimate of the AUV II.

The actual track of the AUV II would have to be determined from sonar range data to the sides of the swimming pool. Fairly good sonar range data to the edges of the swimming pool were available in the data file from the oval run used in the previous section. In particular, this run contained two straight legs

over 25 seconds long which provided a good lateral position of the AUV II in the pool. The range data from the forward-looking sonar was also very good. Both of these ranges could be combined to provide track data on the long legs of the oval.

Figure 5.8 shows the geometry and terms associated with the "constant pool width" method. Because the swimming pool is a constant width of 60 feet, the sum of the initial distance the AUV II was from the left edge of the swimming pool, the lateral distance traveled, and the range to the right side of the pool should be 60 feet, as described in Equation (5.13).

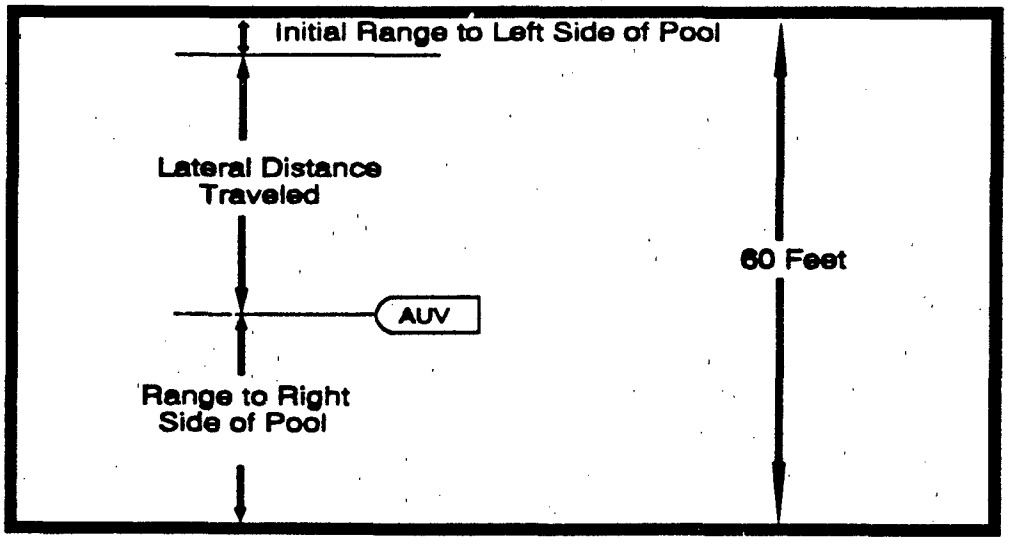


Figure 5.8 "Constant Pool Width" Geometry

$$\underset{\text{left pool wall}}{\text{Initial range from}} + \underset{\text{traveled}}{\text{Lateral distance}} + \underset{\text{pool wall}}{\text{Range to right}} = 60 \text{ feet} \qquad (5.13)$$

Figure 5.9 shows the raw range data from the AUV II data file corrected for the actual vehicle heading angle. During the time period shown, the range shown is the range to the right wall of the swimming pool. The erroneous range spikes had to be deleted, or smoothed, prior to using the data file for further analysis. A routine was written to smooth the data that used a threshold of .3 feet of difference between successive sonar returns. If the range changed by more than the threshold value the range was kept at the previous value until the actual range returned to a value within the threshold. The dotted line in Figure 5.9 shows the areas in which the range information was smoothed.

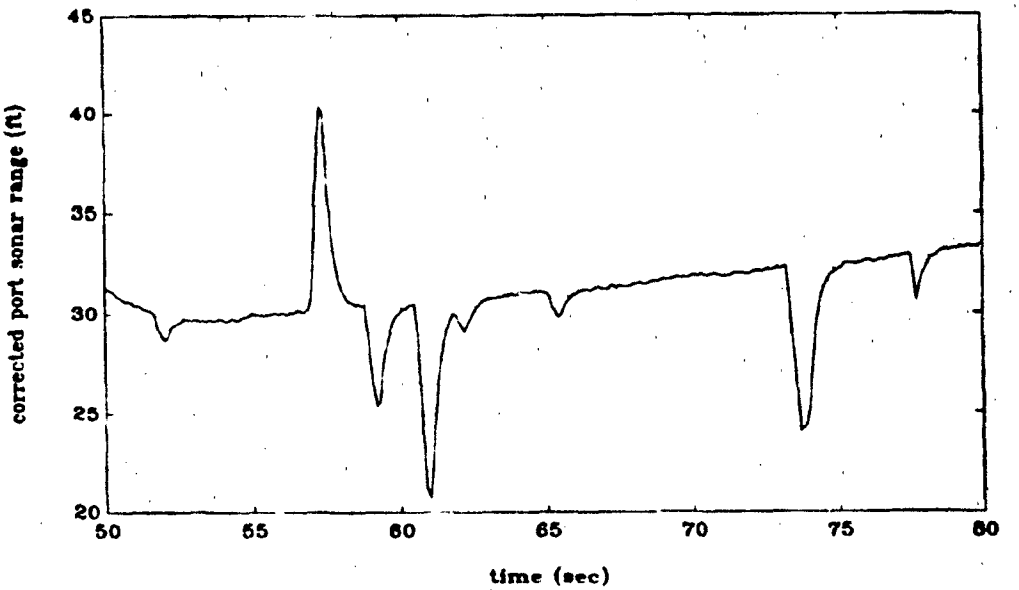


**Figure 5.9** **Rough and Smooth Ranges to Right Side of Pool, 50-80 Seconds**

The initial distance from the left wall was obtained by analyzing Figure 5.10, which is a graph of the first six seconds of the oval trial run. The average range appeared to be 6.1 feet. Even if the choice of average range was in error by 0.1 feet, the effect on the overall constant width calculation was very small.

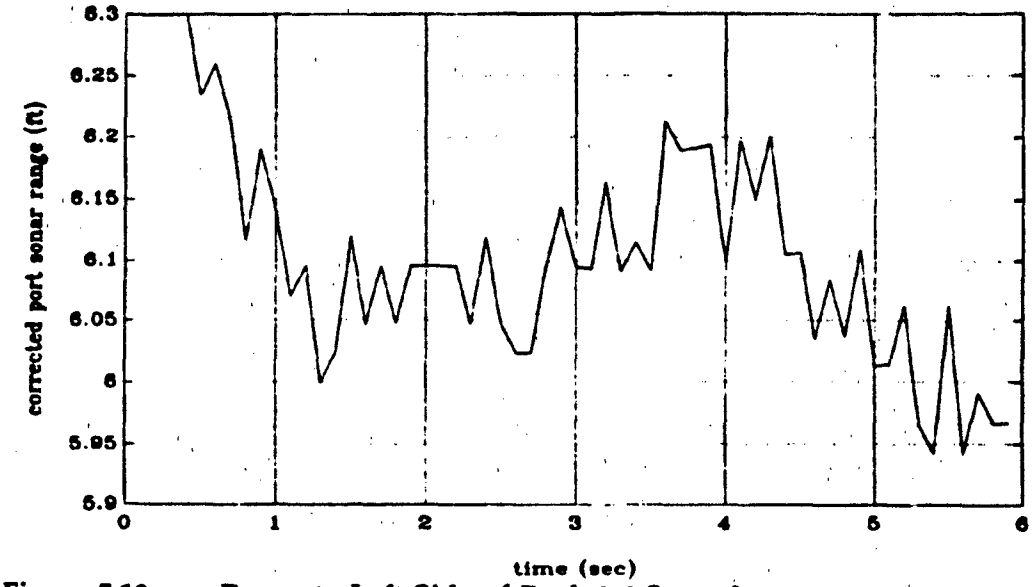


**Figure 5.10 Range to Left Side of Pool, 0-6 Seconds**

Figure 5.11 shows the initial results of the constant pool width calibration using a horizontal plane dead reckoning program with a time constant of 2.0. Though the horizontal dead reckoning program uses only the lateral motion, its response is very close to the six-degree-of-freedom computer model. The curves in Figure 5.11 represent the width of the pool as calculated by Equation (5.13). Both range terms in Equation (5.13) are known, hence any errors are due to an incorrect estimation of lateral distance traveled.

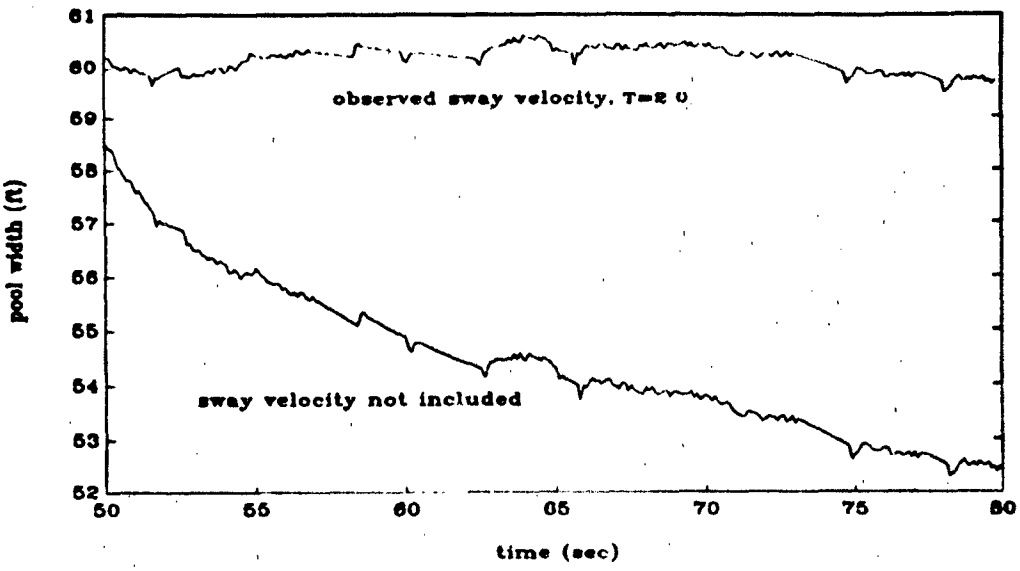


Figure 5.11 "Constant Pool Width" Verification

Figure 5.12 is a geographic plot of the AUV II oval track and range data. The solid line represents the position of the AUV II as dead-reckoned by the AUV II. The AUV II computes down and cross track velocity using Equation (5.1), with v=0.0. The dashed line is the enhanced position estimate of the AUV II using a time constant of 2.0. The straight lines along each side of the oval tracks are the ranges to the side of the pool obtained by the AUV II during the run.

A quick analysis of Figure 5.12 indicates that the enhanced position estimate did a much better job of determining the actual position of the AUV II. Closer observation of Figure 5.12 reveals some problems with the onboard sensors which affect the validity of the results presented.

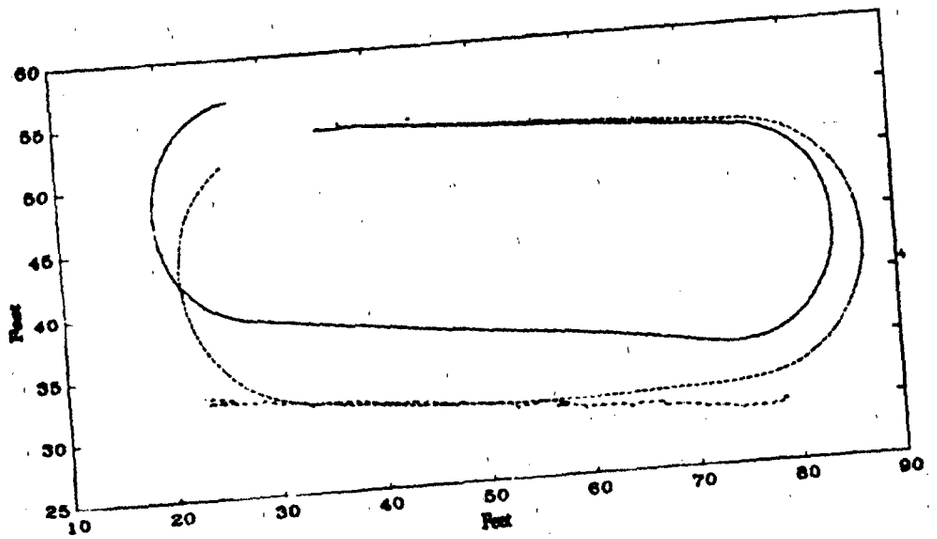


**Figure 5.12 Geographic Plot of AUV II Oval Run**

Both edges of the oval were supposed to be parallel to the pool sides. It can be seen that neither leg of the AUV II is parallel to the pool sides. This was caused by a drifting problem with the heading gyro. Initial pool side tests of the heading gyro drift indicated an approximate drift rate of 0.014 radians/sec. Subsequent testing indicated that drift rate varied as the supply voltage varied. The supply voltage varied depending upon the rpm of the shafts. To a lesser degree, the turning rate gyro also drifted during this run. Both of these drift rates had to be approximated to produce Figure 5.12.

It can also be seen that the AUV II track turns prior to the end of the straight range line. This is due to an inaccuracy in the calibration of the speed sensor on the AUV II. The solid line in Figure 5.13 shows the range to the far

end of the pool during the initial leg of the oval. The dotted line during the first nine seconds is a smoothed range computed by integrating the recorded AUV II speed. The constantly decreasing range from 10-33 seconds indicates the AUV II speed was approximately 2.3 feet/sec, though the onboard data file reported speed approximately 1.6 feet/sec.

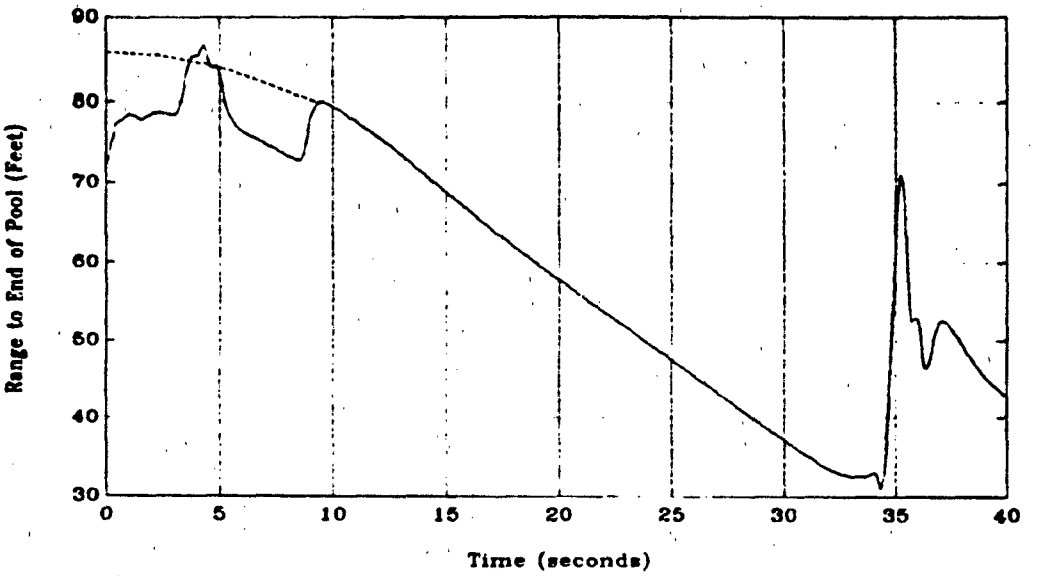


**Figure 5.13 Range to Far End of Pool, 0-40 Seconds**

Nevertheless, compensation for the combination of sensor errors is difficult. The sensor errors notwithstanding, Figure 5.12 does show that the enhanced position estimator can be used to produce a better estimate of the AUV II position.

It is noteworthy that the best lateral velocity observer time constant for both the six-degree-of-freedom computer model and horizonal dead reckoning

methods was approximately 2.0. These independent methods of determining the performance of the lateral velocity observer and enhanced position estimator prove the method is sound. Improvements to the estimation of position in the six-degree of freedom simulation computer model will occur when the AUV II hydrodynamic coefficients are more accurately known. When the problems of sensor errors in the AUV II itself are solved, the accuracy of the estimated position will be much better. This research has demonstrated that the reduced order lateral velocity observer and enhanced position estimator can be used to obtain a more accurate estimate of the AUV II position.

# VI. CONCLUSIONS AND RECOMMENDATIONS

## A. CONCLUSIONS

This thesis describes various aspects of research directly related to supporting the initial phases of in-water testing of the NPS AUV II. For the first time in this project the hydrodynamic coefficients of the AUV II vehicle were estimated. Table X summarizes the hydrodynamic coefficients and significant geometric properties of the AUV II as determined by this research.

A proportional-derivative controller was designed for initial closed loop testing of the AUV II in the NPS swimming pool. The performance of the vehicle was as predicted by computer simulations. Initial turning response of the vehicle proved to be very satisfactory.

Labor, equipment, and time constraints limit the amount of in-water testing that can be performed with the AUV II. A number of components within the AUV II have limited lifetimes, e.g., the gyros have a service life of only 200 hours. For these reasons, it is important to conduct computer simulations of the AUV II to test various guidance and control schemes. To this end, a six-degree-of-freedom computer model of the AUV II was developed.

Space limitations on board the AUV II restrict the amount of navigational equipment that can be installed. To provide the AUV II with an accurate means by which to estimate current position, a reduced order observer for lateral

velocity was developed and validated. By using the estimated lateral velocity with actual AUV II speed and heading it was demonstrated that the AUV II position can be accurately estimated. The enhanced position estimator was tested using both simulated and actual AUV II trial runs.

## B. RECOMMENDATIONS FOR FUTURE RESEARCH

The hydrodynamic coefficients for the AUV II must be refined. Research being conducted by Bahrke [Ref. 28] in the estimation of hydrodynamic coefficients using parameter identification techniques should yield a more accurate set of hydrodynamic coefficients. The coefficients will then result in improved accuracy of the six-degree-of-freedom computer model and enhanced position estimator.

The controllers and guidance schemes investigated for the AUV I and SDV Mark 9 vehicles should be tested with the AUV II. The six-degree-of-freedom computer model is ideally suited to perform this testing.

The enhanced position estimator should be incorporated into the guidance methods, and research conducted as to the best method by which to generate heading commands based on the current estimated portion and next waypoint generated by the mission planning software.

The speed measurement of the AUV II should be improved. As a minimum, the paddle wheel speed sensor should again be calibrated. The performance of the paddle wheel during a turn, where the actual vehicle velocity is not normal to the

paddles, needs to be evaluated. Perhaps an improved speed sensor, such as a pitot tube should be installed.

The effect of improvements to the AUV II should be studied using the six-degree-of-freedom computer model. Topics of immediate concern include:

1. The installation of thrusters. Thrusters will add additional terms to the equations of motion; the reduced order observer and enhanced position estimator can be easily modified to account for the thruster effects.

2. Separate control of bow and stern rudders. Analysis of the NACA 0015 plane characteristics would indicate that the bow rudder might stall during the sharp turns conducted by the AUV II. Separate control of the rudders would prevent stalling, and might even improve the performance of the AUV II in a turn.

3. Separate control of the shafts. Independent operation of the shafts will enhance maneuvering and position keeping at slow speeds

With the incorporation of any of the above improvements to the motion control systems of the AUV II, the governing equations of motion become more complex. Fortunately with the design of the reduced order observer, the enhanced position estimator is quickly adaptable to an increased number of parameters. With an accurate set of hydrodynamic coefficients, the six-degree-of-freedom computer model and enhanced position estimator will significantly improve future AUV II performance.

**TABLE X. SUMMARY OF HYDRODYNAMIC COEFFICIENTS AND SIGNIFICANT GEOMETRIC PROPERTIES**

| Coefficient | Value | Coefficient | Value |
|---|---|---|---|
| $X_{rr}$ | -0.01735 | $M_q$ | -0.03565 |
| $X_{\dot{u}}$ | 0.00282 | $M_w$ | 0.05122 |
| $X_{vv}$ | -0.04019 | $M_{\delta s}$ | $-0.337*L*Y_{\delta rs}$ |
| $X_{\delta s\delta s}$ | 0.02345 | $M_{\delta b}$ | $0.283*L*Y_{\delta rb}$ |
| $X_{\delta b\delta b}$ | 0.02345 | $N_r$ | -0.00047 |
| $X_{\delta r\delta r}$ | 0.02345 | $N_{\dot{v}}$ | -0.00178 |
| $X_{prop}$ ($C_{DO}$) | 0.015 | $N_r$ | -0.01022 |
| $Y_r$ | -0.00178 | $N_v$ | -0.00769 |
| $Y_{\dot{v}}$ | -0.03430 | $N_{\delta rs}$ | $-0.337*L*Y_{\delta rs}$ |
| $Y_r$ | 0.01187 | $N_{\delta rb}$ | $0.283*L*Y_{\delta rb}$ |
| $Y_v$ | -0.03896 | $I_x$ ($ft^4$) | 2.7 |
| $Y_{\delta rs}$ | 0.02345 | $I_y$ ($ft^4$) | 42.0 |
| $Y_{\delta rb}$ | 0.02345 | $I_z$ ($ft^4$) | 45.0 |
| $Z_q$ | -0.00253 | $X_{rs}$ (ft) | -0.377*L |
| $Z_{\dot{w}}$ | -0.09340 | $X_{rb}$ (ft) | 0.283*L |
| $Z_q$ | -0.07013 | Weight (lbs) | 435 |
| $Z_w$ | -0.15687 | Length 'ft) | 7.3 |
| $Z_{\delta s}$ | -0.02345 | $\rho$ ($slugs/ft^3$) | 1.94 |
| $Z_{\delta b}$ | -0.02345 | $X_G$ (ft) | 0.0104 |
| $K_p$ | -0.00024 | $Z_G$ (ft) | .05 |
| $K_p$ | -0.00540 | $X_B$ (ft) | 0.0104 |
| $M_q$ | -0.00625 | $C_{DY}$ | 0.5 |
| $M_{\dot{w}}$ | -0.00253 | $C_{DZ}$ | 0.6 |

## APPENDIX A: SDV FIN HYDRODYNAMIC COEFFICIENTS

A fixed fin attached to a vessel contributes to the overall vessel hydrodynamic coefficients. The Y force and N-moment produced by the fin are[1]

$$Y_f = \pm(L_f \cos\beta_f + D_f \sin\beta_f)$$
$$N_f = Y_f x_f \qquad \textbf{(A1)}$$

where $\beta_f$ = fin angle of attack ($v_f/u_f$)
$L_f$ = fin lift
$D_f$ = fin drag
$x_f$ = distance to the fin centroid from the body center axis origin

The derivative of $Y_f$ with respect to $v_f$ taken at $v_f = 0$ is the fin velocity-dependent hydrodynamic coefficient:

$$(Y_v)_f = -\left|(Y_\beta)_f\left(\frac{\partial\beta}{\partial v}\right)_f\right| \qquad \textbf{(A2)}$$

By using the definition of $\beta_f$, algebraic manipulation of equations 1 and 2, and expressing $L_f$ and $D_f$ in terms of non-dimensional drag coefficients

$$L_f = \left(\frac{\rho}{2}\right)A_f u^2 C_L$$
$$D_f = \left(\frac{\rho}{2}\right)A_f u^2 C_D$$

[1]Equations presented in this appendix are taken from section 10.2 of [Ref. 24].

the final expression for $Yr_f$ is obtained:

$$(Y_v)_f = -\left|\left(\frac{\rho}{2}\right)A_f u\left[\left(\frac{\partial C_L}{\partial \beta}\right)_f + (C_D)_f\right]\right| \qquad \textbf{(A3)}$$

For small angles of attack $(C_D)_f$ is small in relation to $\left(\frac{\partial C_L}{\partial \beta}\right)_f$ and can be ignored. By expressing $(Yv)_f$ in normalized, nondimensional form equation A3 becomes

$$(Y_v)_f = -\left|A_f'\left(\frac{\partial C_L}{\partial \beta}\right)_f\right| \qquad \textbf{(A4)}$$

Note that the prime in equation A4 indicates that the fin area has been normalized by dividing the actual area ($a_f$) by $l^2_{ref}$. For the rest of this appendix only normalized dimensions will be used in equations, and, for simplification, the prime will be left deleted.

The total area and centroid of the SDV fin was determined by graphical integration. Figure A1 shows the SDV rear fin, and the eight areas in to which it was divided to determine the area and centroid. Table AI summarizes calculations performed.

$$x_f = \frac{\sum Ax}{\sum A} = \frac{113977.5\,\text{in}^3}{1406.1\,\text{in}^2} = 81\,\text{in.}$$

Figure A2 shows the equivalent rectangular fin for the SDV together with the actual and normalized dimensions.

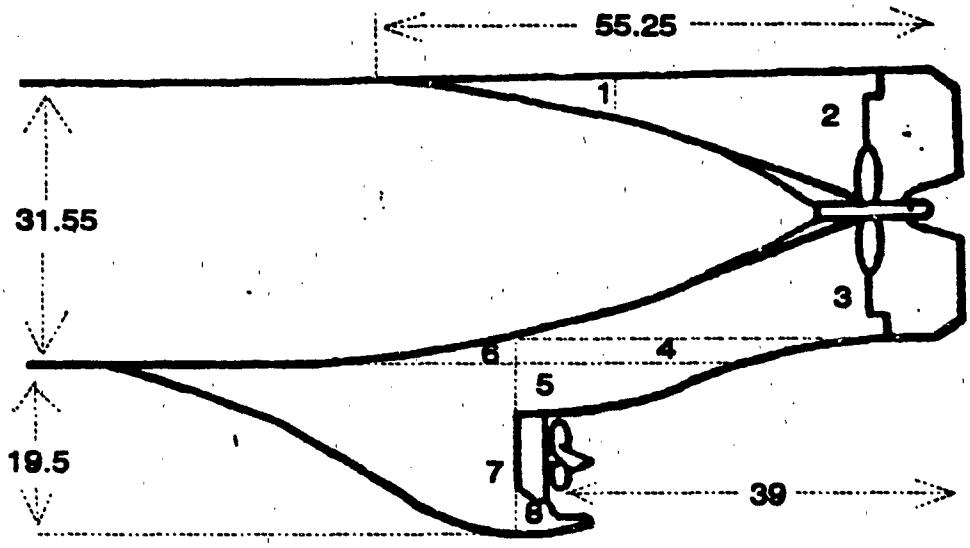


**Figure A1** **SDV Fin**

**TABLE AI. SDV FIN GRAPHICAL INTEGRATION VALUES**

| Section | Area[1] ($in^2$) | x (in) | Ax ($in^3$) |
|---|---|---|---|
| 1 | 39.6 | 96.8 | 3883.3 |
| 2 | 363.1 | 96.8 | 35148.1 |
| 3 | 253.5 | 100.0 | 25350.0 |
| 4 | 116.2 | 91.3 | 10609.1 |
| 5 | 84.5 | 80.5 | 6802.3 |
| 6 | 47.5 | 64.3 | 3054.3 |
| 7 | 491.1 | 57.8 | 28385.6 |
| 8 | 10.6 | 75.0 | 795.0 |
| TOTAL | 1406.1 | | 113977.5 |

[1] Dimensions based on 3.25 in./side of a square on the graph paper

[2] Measured from origin of SDV body-centered axes.

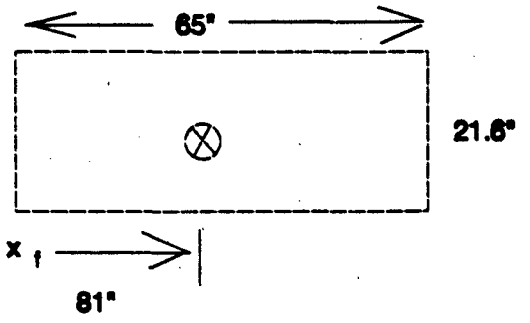


length $l_f$ = 65"

span b = 21.6"

$$b' = \frac{21.6}{210.1} = .103$$

aspect ratio $a = \frac{b_f}{l_f} \frac{21.6}{65} = .33$

geometric aspect ratio

$$a = \frac{b_f^2}{A_f} \frac{(216)^2}{1406.1} = .33$$

**Figure A2 SDV Equivalent Fin Dimensions**

The value of $\frac{\partial C_L}{\partial \beta}$ was estimated using Jones' formula

$$\frac{\partial C_L}{\partial \beta} = \frac{\pi}{2} a = \frac{3.14}{2}(0.33) = 0.518$$

Using the values derived above, the values for $(Y_v)_f$, $(N_v)_f$, $(Y_r)_f$, and $(N_r)_f$ were calculated as follows:

$$(Y_v)_f = -\left|A_f\left(\frac{\partial C_L}{\partial \beta}\right)_f\right| = -\left|(0.032)(0.518)\right| = -0.01660$$

$$(N_v)_f = (Y_v)_f x_f = (-0.0166)(-0.385) = 0.00639$$

$$(Y_r)_f = x_f (Y_v)_f = (-0.385)(-0.0166) = 0.00639$$

$$(N_r)_f = x^2 (Y_v)_f = (-0.385)^2(-0.0166) = -0.00246$$

The contribution of the fixed fin to the acceleration-related hydrodynamic coefficients can be approximated by

$$(Y_v)_f = \frac{-2\pi b A_f}{\sqrt{(a_C^2 + 1)}} \qquad \textbf{(A5)}$$

Substituting the normalized geometric properties of the SDV equivalent fin into Equation (A5), the values for $(Y_v)_f$, $(N_v)_f$, $(y_t)_f$, and $(N_t)_f$ were calculated as follows:

$$(Y_v)_f = \frac{-2\pi b A_f}{\sqrt{a_C^2 + 1}} = \frac{(-2)(3.14)(0.103)(0.032)}{\sqrt{0.332^2 + 1}} = -0.01965$$

$$(N_v)_f = x_f(Y_v)_f = (-0.385)(-0.01965) = 0.00756$$

$$(Y_t)_f = x_f(Y_v)_f = (-0.385)(-0.01965) = 0.00756$$

$$(N_t)_f = x_f^2(Y_v)_f = (-0.385)^2(-0.01965) = -0.00291$$

# APPENDIX B: SIMULATION MODEL

```
C     PROGRAM SIMAUV
C
C     Fotis A. Papoulias/David C. Warner
C     NAVAL POSTGRADUATE SCHOOL
C     November 1991
C
C     NPS AUV II Six-Degree-of-Freedom Simulation Model
C
C As written, this program uses data files produced by the AUV II
C  during experimental runs. With slight modification the program
C  can use input rudder and speed commands supplied by the
C  programmer to predict AUV II performance for different run
C  profiles
C
C DECLARATIONS
C
      REAL L,MASS,IX,IY,IZ,IXZ,IYZ,IXY,NU,LRPM,KPDOT,KRDOT,KPQ,KQR
      REAL KVDOT,KP,KR,KVQ,KWP,KWR,KV,KVW,KPN,KDB
      REAL MQDOT,MPP,MPR,MRR,MWDOT,MQ,MVP,MVR,MW,MVV,MDS,MDB,NDRB
      REAL NPDOT,NRDOT,NPQ,NQR,NVDOT,NP,NR,NVQ,NWP,NWR,NV,NVW,NDRS
      REAL MM(6,6),INDX(100)
      DIMENSION X(15),BR(15),HH(15),VECH1(15),VECH2(15),XMMINV(6,6)
      DIMENSION VECV1(15),VECV2(15),F(12),FP(6)
C
C NPS AUV II GEOMETRIC PROPERTIES (Basic Length Dimension is Feet)
C
      WEIGHT= 435.0
      IX    =   2.7
      IY    =  42.0
      IZ    =  45.0
      IXY   =   0.0
      IYZ   =   0.0
      IXZ   =   0.0
      L     =   87.625/12.0
      RHO   =   1.94
      G     =  32.2
      XG    =   0.125/12.0
      YG    =   0.0
      ZG    =   0.05
      XB    =   0.125/12.0
      YB    =   0.0
      ZB    =   0.0
      ZARM  =   2.287
      MASS  =WEIGHT/G
```

```
      BOY   =WEIGHT
      XRS   =-0.377*L
      XRB   =+0.283*L
C
C DRAG COEFFICIENTS AND SPEED CALIBRATION DATA
C
      CD0   =   0.015
      CDY   =   0.5
      CDZ   =   0.6
      RPM0  = 500.0
      U0    =   2.3
C
C SURGE HYDRODYNAMIC COEFFICIENTS
C
      XPP   = 0.00000*0.5*RHO*L**4
      XQQ   = 0.00000*0.5*RHO*L**4
      XRR   =-0.01735*0.5*RHO*L**4
      XPR   = 0.00000*0.5*RHO*L**4
      XUDOT =-0.00282*0.5*RHO*L**3
      XWQ   = 0.00000*0.5*RHO*L**3
      XVP   = 0.00000*0.5*RHO*L**3
      XVR   = 0.00000*0.5*RHO*L**3
      XQDS  = 0.00000*0.5*RHO*L**3
      XQDB  = 0.00000*0.5*RHO*L**3
      XRDRS = 0.00000*0.5*RHO*L**3
      XRDRB = 0.00000*0.5*RHO*L**3
      XVV   =-0.04019*0.5*RHO*L**2
      XWW   = 0.00000*0.5*RHO*L**2
      XVDRS = 0.00000*0.5*RHO*L**2
      XVDRB = 0.00000*0.5*RHO*L**2
      XWDS  = 0.00000*0.5*RHO*L**2
      XWDB  = 0.00000*0.5*RHO*L**2
      XDSDS =-0.02345*0.417*0.5*RHO*L**2
      XDBDB =-0.02345*0.417*0.5*RHO*L**2
      XDRDR =-0.02345*0.417*0.5*RHO*L**2
      XRES  = CD0*0.5*RHO*L**2
      XPROP = XRES*(U0/RPM0)**2
C
C LATERAL HYDRODYNAMIC COEFFICIENTS
C
      YPDOT = 0.00000*0.5*RHO*L**4
      YRDOT =-0.00178*0.5*RHO*L**4
      YPQ   = 0.00000*0.5*RHO*L**4
      YQR   = 0.00000*0.5*RHO*L**4
      YVDOT =-0.03430*0.5*RHO*L**3
      YP    = 0.00000*0.5*RHO*L**3
      YR    =+0.01187*0.5*RHO*L**3
      YVQ   = 0.00000*0.5*RHO*L**3
      YWP   = 0.00000*0.5*RHO*L**3
      YWR   = 0.00000*0.5*RHO*L**3
```

```
      YV     =-0.03896*0.5*RHO*L**2
      YVW    = 0.00000*0.5*RHO*L**2
      YDRS   =+0.02345*0.5*RHO*L**2
      YDRB   =+0.02345*0.5*RHO*L**2
C
C HEAVE HYDRODYNAMIC COEFFICIENTS
C
      ZQDOT =-0.00253*0.5*RHO*L**4
      ZPP    = 0.00000*0.5*RHO*L**4
      ZPR    = 0.00000*0.5*RHO*L**4
      ZRR    = 0.00000*0.5*RHO*L**4
      ZWDOT =-0.09340*0.5*RHO*L**3
      ZQ     =-0.07013*0.5*RHO*L**3
      ZVP    = 0.00000*0.5*RHO*L**3
      ZVR    = 0.00000*0.5*RHO*L**3
      ZW     =-0.15687*0.5*RHO*L**2
      ZVV    = 0.00000*0.5*RHO*L**2
      ZDS    =-0.02345*0.5*RHO*L**2
      ZDB    =-0.02345*0.5*RHO*L**2
C
C ROLL HYDRODYNAMIC COEFFICIENTS
C
      KPDOT =-0.00024*0.5*RHO*L**5
      KRDOT = 0.00000*0.5*RHO*L**5
      KPQ    = 0.00000*0.5*RHO*L**5
      KQR    = 0.00000*0.5*RHO*L**5
      KVDOT = 0.00000*0.5*RHO*L**4
      KP     =-0.00540*0.5*RHO*L**4
      KR     = 0.00000*0.5*RHO*L**4
      KVQ    = 0.00000*0.5*RHO*L**4
      KWP    = 0.00000*0.5*RHO*L**4
      KWR    = 0.00000*0.5*RHO*L**4
      KV     = 0.00000*0.5*RHO*L**3
      KVW    =-0.00000*0.5*RHO*L**3
C
C PITCH HYDRODYNAMIC COEFFICIENTS
C
      MQDOT =-0.00625*0.5*RHO*L**5
      MPP    = 0.00000*0.5*RHO*L**5
      MPR    = 0.00000*0.5*RHO*L**5
      MRR    = 0.00000*0.5*RHO*L**5
      MWDOT =-0.00253*0.5*RHO*L**4
      MQ     =-0.03565*0.5*RHO*L**4
      MVP    = 0.00000*0.5*RHO*L**4
      MVR    = 0.00000*0.5*RHO*L**4
      MW     =+0.05122*0.5*RHO*L**3
      MVV    = 0.00000*0.5*RHO*L**3
      MDS    =-0.377*L*YDRS
      MDB    =+0.283*L*YDRB
C
```

```
C YAW HYDRODYNAMIC COEFFICIENTS
C
      NPDOT = 0.00000*0.5*RHO*L**5
      NRDOT =-0.00047*0.5*RHO*L**5
      NPQ   = 0.00000*0.5*RHO*L**5
      NQR   = 0.00000*0.5*RHO*L**5
      NVDOT =-0.00178*0.5*RHO*L**4
      NP    = 0.00000*0.5*RHO*L**4
      NR    =-0.01022*0.5*RHO*L**4
      NVQ   = 0.00000*0.5*RHO*L**4
      NWP   = 0.00000*0.5*RHO*L**4
      NWR   = 0.00000*0.5*RHO*L**4
      NV    =-0.00769*0.5*RHO*L**3
      NVW   = 0.00000*0.5*RHO*L**3
      NDRS  =-0.377*L*YDRS
      NDRB  =+0.283*L*YDRB
C
C OPEN DATA AND RESULTS FILES. THE INPUT FILE (5) IS CHANGED BY
C THE RESEARCHER DEPENDING UPON THE AUV RUN BEING SIMULATED
C
      OPEN ( 5,FILE='MODOVAL.DAT',STATUS='OLD')
      OPEN (11,FILE='U.RES',STATUS='NEW')
      OPEN (12,FILE='V.RES',STATUS='NEW')
      OPEN (13,FILE='W.RES',STATUS='NEW')
      OPEN (14,FILE='P.RES',STATUS='NEW')
      OPEN (15,FILE='Q.RES',STATUS='NEW')
      OPEN (16,FILE='R.RES',STATUS='NEW')
      OPEN (17,FILE='DRB.RES',STATUS='NEW')
      OPEN (18,FILE='SSAS.RES',STATUS='NEW')
      OPEN (19,FILE='SSAB.RES',STATUS='NEW')
      OPEN (20,FILE='PHI.RES',STATUS='NEW')
      OPEN (21,FILE='THETA.RES',STATUS='NEW')
      OPEN (22,FILE='PSI.RES',STATUS='NEW')
      OPEN (23,FILE='DRS.RES',STATUS='NEW')
      OPEN (24,FILE='DS.RES',STATUS='NEW')
      OPEN (25,FILE='XY.RES',STATUS='NEW')
      OPEN (26,FILE='XZ.RES',STATUS='NEW')
      OPEN (27,FILE='YZ.RES',STATUS='NEW')
      OPEN (28,FILE='ZCELL.RES',STATUS='NEW')
      OPEN (31,FILE='DRSS.RES',STATUS='NEW')
      OPEN (32,FILE='DRBS.RES',STATUS='NEW')
      OPEN (33,FILE='SIMTODR.RES',STATUS='NEW')
C
C MASS MATRIX INITIALIZATION AND DEFINITION
C
      DO 15 J=1,6
       DO 10 K=1,6
       XMMINV(J,K)=0.0
       MM(J,K)=0.0
10     CONTINUE
```

```
15    CONTINUE
C
      MM(1,1)= MASS-XUDOT
      MM(1,5)= MASS*ZG
      MM(1,6)=-MASS*YG
C
      MM(2,2)= MASS-YVDOT
      MM(2,4)=-MASS*ZG-YPDOT
      MM(2,6)= MASS*XG-YRDOT
C
      MM(3,3)= MASS-ZWDOT
      MM(3,4)= MASS*YG
      MM(3,5)=-MASS*XG-ZQDOT
C
      MM(4,2)=-MASS*ZG-KVDOT
      MM(4,3)= MASS*YG
      MM(4,4)= IX-KPDOT
      MM(4,5)=-IXY
      MM(4,6)=-IXZ-KRDOT
C
      MM(5,1)= MASS*ZG
      MM(5,3)=-MASS*XG-MWDOT
      MM(5,4)=-IXY
      MM(5,5)= IY-MQDOT
      MM(5,6)=-IYZ
C
      MM(6,1)=-MASS*YG
      MM(6,2)= MASS*XG-NVDOT
      MM(6,4)=-IXZ-NPDOT
      MM(6,5)=-IYZ
      MM(6,6)= IZ-NRDOT
C
C MASS MATRIX INVERSION
C
      DO 12 I=1,6
        DO 11 J=1,6
        XMMINV(I,J)=0.0
11      CONTINUE
      XMMINV(I,I)=1.0
12    CONTINUE
      CALL INVTA(MM,6,INDX,D)
      DO 13 J=1,6
       CALL INVTB(MM,6,INDX,XMMINV(1,J))
13    CONTINUE
C
C VARIABLE INITIALIZATION
C
      TWOPI =8.0*ATAN(1.0)
      PI    =0.5*TWOPI
      IECHO =10
```

```
      IPRNT =1
      JPRNT =0
      IJ    =0
      JE    =0
      DELTA =0.1
      ISIM  =10000
C
C DEFINE THE LENGTH (X), BREADTH (BR), AND HEIGHT (HH) TERMS
C
      X(1)  = -43.9/12.0
      X(2)  = -39.2/12.0
      X(3)  = -35.2/12.0
      X(4)  = -31.2/12.0
      X(5)  = -27.2/12.0
      X(6)  = -10.0/12.0
      X(7)  =   0.0/12.0
      X(8)  =  10.0/12.0
      X(9)  =  26.8/12.0
      X(10) =  32.0/12.0
      X(11) =  37.8/12.0
      X(12) =  40.8/12.0
      X(13) =  42.3/12.0
      X(14) =  43.3/12.0
      X(15) =  43.7/12.0
C
      HH(1) =   0.0/12.0
      HH(2) =   2.7/12.0
      HH(3) =   5.2/12.0
      HH(4) =   7.6/12.0
      HH(5) =  10.1/12.0
      HH(6) =  10.1/12.0
      HH(7) =  10.1/12.0
      HH(8) =  10.1 12.0
      HH(9) =  10.1/12.0
      HH(10)=   9.6/12.0
      HH(11)=   7.6/12.0
      HH(12)=   5.6/12.0
      HH(13)=   4.2/12.0
      HH(14)=   2.3/12.0
      HH(15)=   0.0/12.0
C
      BR(1) =  16.5/12.0
      BR(2) =  16.5/12.0
      BR(3) =  16.5/12.0
      BR(4) =  16.5/12.0
      BR(5) =  16.5/12.0
      BR(6) =  16.5/12.0
      BR(7) =  16.5/12.0
      BR(8) =  16.5/12.0
      BR(9) =  16.5/12.0
```

```
      BR(10)=  15.5/12.0
      BR(11)=  12.4/12.0
      BR(12)=   9.5/12.0
      BR(13)=   7.0/12.0
      BR(14)=   4.0/12.0
      BR(15)=   0.0/12.0
C
C RUDDER STALL ANGLES
C
      STL1=25.0*PI/180.0
      STL2=30.0*PI/180.0
      STL3=45.0*PI/180.0
C
C     SIMULATION BEGINS
C
      DO 100 I=1,ISIM
C
C Some early AUV II files had an ERR1 field after RANGE1, and
C  an ERR2 field after RANGE2. If the file being used has these
C  fields, the following statement must be modified.
C
      READ (5,*,END=500) TIME,XPOSE,YPOSE,ZPOSE,PHIE,THETAE,PSIE,
     &                   PE,QE,RE,DRE,DSE,RANGE1,RANGE2,
     &                   SPEEDE,RPMORD,RRPM,LRPM
      IF (I.NE.1) GO TO 111
C
      XPOS  = XPOSE
      YPOS  = YPOSE
      ZPOS  = ZPOSE
      PHI   = PHIE
      THETA = THETAE
      P     = PE
      Q     = QE
      R     = RE
C
111   DRS = DRE
      DRB =-DRE
      DS  = DSE
      DB  =-DSE
      RPM=(LRPM+RRPM)/2.
C
C CALCULATE THE DRAG FORCE, INTEGRATE THE DRAG OVER THE VEHICLE
C
      DO 600 K=1,15
       UCF=(V+X(K)*R)**2+(W-X(K)*Q)**2
       UCF=SQRT(UCF)
       IF (UCF.LT.1.E-6) GO TO 601
       CFLOW   =CDY*HH(K)*(V+X(K)*R)**2+CDZ*BR(K)*(W-X(K)*Q)**2
       VECH1(K)=CFLOW*(V+X(K)*R)/UCF
       VECH2(K)=CFLOW*(V+X(K)*R)*X(K)/UCF
```

```
        VECV1(K)=CFLOW*(W-X(K)*Q)/UCF
        VECV2(K)=CFLOW*(W-X(K)*Q)*X(K)/UCF
600     CONTINUE
        CALL TRAP(15,VECV1,X,HEAVE)
        CALL TRAP(15,VECV2,X,PITCH)
        CALL TRAP(15,VECH1,X,SWAY )
        CALL TRAP(15,VECH2,X,YAW  )
        HEAVE=-0.5*RHO*HEAVE
        PITCH=+0.5*RHO*PITCH
        SWAY =-0.5*RHO*SWAY
        YAW  =-0.5*RHO*YAW
        BETA =ATAN(ABS(V)/U)
        IF (R.NE.0.0) RADIUS=SQRT(U**2+V**2)/R
        IF (R.EQ.0.0) RADIUS=200.0*L
        ARS  =ABS(XRS)*COS(BETA)/(RADIUS+ABS(XRS)*SIN(BETA))
        ARB  =ABS(XRB)*COS(BETA)/(RADIUS+ABS(XRB)*SIN(BETA))
        ARS  =ATAN(ABS(ARS))
        ARB  =ATAN(ABS(ARB))
        ARS  =0.0
        ARB  =0.0
        SSAS =ATAN(V/U)+ARS
        SSAB =ATAN(V/U)-ARB
        UV   =U
C
        SSAS=0.0
        SSAB=0.0

        GO TO 602
601     HEAVE=0.0
        PITCH=0.0
        SWAY =0.0
        YAW  =0.0
        SSAS =0.0
        SSAB =0.0
        UV   =U
602     CONTINUE
C
C FORCE EQUATIONS
C
C SURGE FORCE
C
      FP(1) = MASS*V*R-MASS*W*Q+MASS*XG*Q**2+MASS*XG*R**2-
     &      MASS*YG*P*Q-MASS*ZG*P*R+XPP*P**2+XQQ*Q**2+XRR*R**2+
     &      XPR*P*R+XWQ*W*Q+XVP*V*P+XVR*V*R+U*Q*(XQDS*DS+XQDB*DB)+
     &      U*R*(XRDRS*(DRS-SSAS)+XRDRB*(DRB-SSAB))+XVV*V**2+
     &      XWW*W**2+U*V*(XVDRS*(DRS-SSAS)+XDRB*(DRB-SSAB))+
     &      U*W*(XWDS*DS+XWDB*DB)+(XDSDS*DS**2+XDBDB*DB**2+
     &      XDRDR*((DRS-SSAS)**2+(DRB-SSAB)**2))*UV**2-
     &      (WEIGHT-BOY)*SIN(THETA)+XPROP*RPM*RPM-XRES*U*U
C
```

```
C SWAY FORCE
C
      SFDRS=YDRS*UV**2*DRSS
      SFDRB=YDRB*UV**2*DRBS
      FP(2) = -MASS*U*R-MASS*XG*P*Q+MASS*YG*R**2-MASS*ZG*Q*R+
     &      YPQ*P*Q+YQR*Q*R+YP*U*P+YR*U*R+YVQ*V*Q+YWP*W*P+YWR*W*R+
     &      YV*U*V+YVW*V*W+SFDRS+SFDRB+(WEIGHT-BOY)*
     &      COS(THETA)*SIN(PHI)+MASS*W*P+MASS*YG*P**2+SWAY
C
C HEAVE FORCE
C
      FP(3) = MASS*U*Q-MASS*V*P-MASS*XG*P*R-MASS*YG*Q*R+
     &      MASS*ZG*P**2+MASS*ZG*Q**2+ZPP*P**2+ZPR*P*R+ZRR*R**2+
     &      ZQ*U*Q+ZVP*V*P+ZVR*V*R+ZW*U*W+ZVV*V**2+HEAVE+
     &      U**2*(ZDS*DS+ZDB*DB)+(WEIGHT-BOY)*COS(THETA)*COS(PHI)
C
C  ROLL MOMENT
C
      FP(4) = -IZ*Q*R+IY*Q*R-IXY*P*R+IYZ*Q**2-IYZ*R**2+IXZ*P*Q+
     &      MASS*YG*U*Q-MASS*YG*V*P-MASS*ZG*W*P+KPQ*P*Q+KQR*Q*R+
     &      KP*U*P+KR*U*R+KVQ*V*Q+KWP*W*P+KWR*W*R+KV*U*V+KVW*V*W+
     &      (YG*WEIGHT-YB*BOY)*COS(THETA)*COS(PHI)-(ZG*WEIGHT-
     &      ZB*BOY)*COS(THETA)*SIN(PHI)+MASS*ZG*U*R
C
C PITCH MOMENT
C
      FP(5) = -IX*P*R+IZ*P*R+IXY*Q*R-IYZ*P*Q-IXZ*P**2+IXZ*R**2-
     &      MASS*XG*U*Q+MASS*XG*V*P+MASS*ZG*V*R-MASS*ZG*W*Q+
     &      MPP*P**2+MPR*P*R+MRR*R**2+MQ*U*Q+MVP*V*P+MVR*V*R+MW*U*W+
     &      MVV*V**2+U**2*(MDS*DS+MDB*DB)-(XG*WEIGHT-
     &      XB*BOY)*COS(THETA)*COS(PHI)-
     &      (ZG*WEIGHT-ZB*BOY)*SIN(THETA)+PITCH
C
C YAW MOMENT
C
      YMDRS=NDRS*UV**2*DRSS
      YMDRB=NDRB*UV**2*DRBS
      FP(6) = -IY*P*Q+IX*P*Q+IXY*P**2-IXY*Q**2+IYZ*P*R-IXZ*Q*R-
     &      MASS*XG*U*R+MASS*XG*W*P-MASS*YG*V*R+MASS*YG*W*Q+NPQ*P*Q+
     &      NQR*Q*R+NP*U*P+NR*U*R+NVQ*V*Q+NWP*W*P+NWR*W*R+NV*U*V+
     &      NVW*V*W+YMDRS+YMDRB+(XG*WEIGHT-XB*BOY)*
     &      COS(THETA)*SIN(PHI)+(YG*WEIGHT-YB*BOY)*SIN(THETA)+YAW
C
C COMPUTE THE RIGHT HAND SIDE OF XDOT=F(X)
C
      DO 610 J = 1,6
       F(J) = 0.0
       DO 611 K = 1,6
        F(J) = XMMINV(J,K)*FP(K) + F(J)
611     CONTINUE
```

```
610   CONTINUE
C
C COMPUTE INERTIAL POSITION RATES
C
      F(7) = U*COS(PSI)*COS(THETA)+V*(COS(PSI)*SIN(THETA)*
     &       SIN(PHI)-SIN(PSI)*COS(PHI))+W*(COS(PSI)*SIN(THETA)*
     &       COS(PHI)+SIN(PSI)*SIN(PHI))
C
      F(8) = U*SIN(PSI)*COS(THETA)+V*(SIN(PSI)*SIN(THETA)*
     &       SIN(PHI)+COS(PSI)*COS(PHI))+W*(SIN(PSI)*SIN(THETA)*
     &       COS(PHI)-COS(PSI)*SIN(PHI))
C
      F(9) = -U*SIN(THETA)+V*COS(THETA)*SIN(PHI)+W*COS(THETA)*
     &       COS(PHI)
C
C COMPUTE EULER ANGLE RATES
C
      F(10)= P+Q*SIN(PHI)*TAN(THETA)+R*COS(PHI)*TAN(THETA)
C
      F(11)= Q*COS(PHI)-R*SIN(PHI)
C
      F(12)= Q*SIN(PHI)/COS(THETA)+R*COS(PHI)/COS(THETA)
C
C ASSIGN VALUES TO THE "XDOT" VECTOR
C
      UDOT   = F(1)
      VDOT   = F(2)
      WDOT   = F(3)
      PDOT   = F(4)
      QDOT   = F(5)
      RDOT   = F(6)
      XDOT   = F(7)
      YDOT   = F(8)
      ZDOT   = F(9)
      PHIDOT = F(10)
      THEDOT = F(11)
      PSIDOT = F(12)
C
C FIRST ORDER INTEGRATION
C
      U    = U    + DELTA*UDOT
      V    = V    + DELTA*VDOT
      W    = W    + DELTA*WDOT
      P    = P    + DELTA*PDOT
      Q    = Q    + DELTA*QDOT
      R    = R    + DELTA*RDOT
      XPOS = XPOS + DELTA*XDOT
      YPOS = YPOS + DELTA*YDOT
      ZPOS = ZPOS + DELTA*ZDOT
      PHI  = PHI  + DELTA*PHIDOT
```

```
      THETA = THETA + DELTA*THEDOT
C
C DEPTH CELL READING
C
      ZCELL = ZPOS + ZARM*SIN(THETA)
C
C PRINT AND ECHO RESULTS
C
      JE=JE+1
      IF (JE.NE.IECHO) GO TO 99
      WRITE (*,*) TIME,PSI
      JE=0
99    JPRNT=JPRNT+1
      IF (JPRNT.NE.IPRNT) GO TO 100
      WRITE (11,*) TIME,U
      WRITE (12,*) TIME,ATAN(V/U)*180.0/PI
      WRITE (13,*) TIME,ATAN(W/U)*180.0/PI
      WRITE (14,*) TIME,P*180.0/PI
      WRITE (15,*) TIME,Q*180.0/PI
      WRITE (16,*) TIME,R*180.0/PI
      WRITE (17,*) TIME,DRB*180.0/PI
      WRITE (18,*) TIME,(DRS-SSAS)*180.0/PI
      WRITE (19,*) TIME,(DRB-SSAB)*180.0/PI
      WRITE (20,*) TIME,PHI*180.0/PI
      WRITE (21,*) TIME,THETA*180.0/PI
      WRITE (22,*) TIME,PSI*180.0/PI,PSI1*180.0/PI
      WRITE (23,*) TIME,DRS*180.0/PI
      WRITE (24,*) TIME,DS*180.0/PI
      WRITE (25,*) XPOS,YPOS
      WRITE (26,*) XPOS,ZPOS
      WRITE (27,*) YPOS,ZPOS
      WRITE (28,*) TIME,ZCELL
      WRITE (31,*) TIME,DRSS*180.0/PI
      WRITE (32,*) TIME,DRBS*180.0/PI
      WRITE (33,900),TIME,XPOS,YPOS,PSI,U,DR,R
900   FORMAT (7F10.5)
      JPRNT=0
100   CONTINUE
500   STOP
      END
C=======================================================================
      SUBROUTINE TRAP(N,A,B,OUT)
C
C NUMERICAL INTEGRATION ROUTINE USING THE TRAPEZOIDAL RULE
C
      DIMENSION A(1),B(1)
      N1=N-1
      OUT=0.0
      DO 1 I=1,N1
       OUT1=0.5*(A(I)+A(I+1))*(B(I+1)-B(I))
```

```
       OUT =OUT+OUT1
1      CONTINUE
       RETURN
       END
C=======================================================================
       SUBROUTINE INVTA(MM,N,INDX,D)
C
C MATRIX INVERSTION ROUTINE FOR MATRIX A
C
       PARAMETER (NMAX=100,TINY=1.0E-20)
       DIMENSION INDX(6),VV(NMAX)
       REAL MM(6,6)
       D=1
       DO 12 I=1,N
        AAMAX=0.
        DO 11 J=1,N
         IF(ABS(MM(I,J)).GT.AAMAX) AAMAX=ABS(MM(I,J))
11      CONTINUE
        IF (AAMAX.EQ.0.) PAUSE 'SINGULAR MATRIX'
        VV(I)=1./AAMAX
12     CONTINUE
       DO 19 J=1,N
        DO 14 I=1,J-1
         SUM=MM(I,J)
         DO 13 K=1,I-1
          SUM=SUM-MM(I,K)*MM(K,J)
13       CONTINUE
         MM(I,J)=SUM
14      CONTINUE
        AAMAX=0.
        DO 16 I=J,N
         SUM=MM(I,J)
         DO 15  K=1,J-1
          SUM=SUM-MM(I,K)*MM(K,J)
15       CONTINUE
         MM(I,J)=SUM
         DUM=VV(I)*ABS(SUM)
         IF (DUM.GE.AAMAX) THEN
          IMAX=I
          AAMAX=DUM
         ENDIF
16      CONTINUE
        IF (J.NE.IMAX)THEN
         DO 17 K=1,N
          DUM=MM(IMAX,K)
          MM(IMAX,K)=MM(J,K)
          MM(J,K)=DUM
17       CONTINUE
         D=-D
         VV(IMAX)=VV(J)
```

```
        ENDIF
        INDX(J)=IMAX
        IF(MM(J,J).EQ.0.)MM(J,J)=TINY
        IF(J.NE.N)THEN
         DUM=1./MM(J,J)
         DO 18 I=J+1,N
          MM(I,J)=MM(I,J)*DUM
18       CONTINUE
        ENDIF
19     CONTINUE
       RETURN
       END
C=======================================================================
       SUBROUTINE INVTB(MM,N,INDX,B)
C
C MATRIX INVERSION ROUTINE FOR MATRIX B
C
       DIMENSION INDX(N),B(N)
       REAL MM(6,6)
       II=0.
       DO 12 I=1,N
        LL=INDX(I)
        SUM=B(LL)
        B(LL)=B(I)
        IF (II.NE.0)THEN
         DO 11 J=II,I-1
          SUM=SUM-MM(I,J)*B(J)
11       CONTINUE
        ELSE IF (SUM.NE.0) THEN
         II=I
        ENDIF
        B(I)=SUM
12     CONTINUE
       DO 14 I=N,1,-1
        SUM=B(I)
        IF (I.LT.N)THEN
         DO 13 J=I+1,N
          SUM=SUM-MM(I,J)*B(J)
13       CONTINUE
        ENDIF
        B(I)=SUM/MM(I,I)
14     CONTINUE
       RETURN
       END
```

# APPENDIX C: PROGRAM OBSERVE

```
C     PROGRAM OBSERVE
C
C     Fotis A Papoulias/David Warner
C     NAVAL POSTGRADUATE SCHOOL
C     28 October 1991
C
C This program uses the results of SIMCH6 for the AUV simulation of
C  the September MODOVAL computer run. The only inputs are TIME,
C  XPOSE, YPOSE, PSIE, UE, DRE, RE. Outputs are a simulated track
C  ("Truth") plotted from the given XPOS and YPOS, a track that the
C  AUV II would use as its DR (without V), and the Enhanced
C  Position obtained by using a reduced order observer to estimate
C  value of lateral motion, V.
C
      REAL L,MASS,NRDOT,NVDOT,NR,NV,NDRS,NDRB,IZ
      REAL KK,KV
      DIMENSION X(15),HH(15),BR(15),VEC1(15),VEC2(15)
C
C     GEOMETRIC PROPERTIES
C
      WEIGHT=435.0
      IZ    =45.0
      L     =87.625/12.0
      RHO   =1.94
      G     =32.2
      XG    =0.0/12.0
      CD0   =0.015
      CDY   =0.5
      CDZ   =0.6
      RPM0  =550
      U0    =2.5
      MASS  =WEIGHT/G
      XRS   =-0.377*L
      XRB   =+0.238*L
C
C SURGE HYDRODYNAMIC COEFFICIENTS
C
      XRR  =-0.01735*0.5*RHO*L**4
      XUDOT=-0.00282*0.5*RHO*L**3
      XVV  =-0.04019*0.5*RHO*L**2
      XDSDS=-0.02345*0.417*0.5*RHO*L**2
      XDRDB=-0.02345*0.417*0.5*RHO*L**2
      XDRDR=-0.02345*0.417*0.5*RHO*L**2
      XRES =CDO*0.5*RHO*L**2
```

```
      XPPOP=XRES*(U0/RPM0)**2
C
C LATERAL HYDRODYNAMIC COEFFICIENTS
C
      YRDOT=-0.00178*0.5*RHO*L**4
      YVDOT=-0.03430*0.5*RHO*L**3
      YR    =+0.01187*0.5*RHO*L**3
      YV    =-0.03896*0.5*RHO*L**2
      YDRS =+0.02345*0.5*RHO*L**2
      YDRB =+0.02345*0.5*RHO*L**2
C
C YAW HYDRODYNAMIC COEFFICIENTS
C
      NRDOT=-0.00047*0.5*RHO*L**5
      NVDOT=-0.00178*0.5*RHO*L**4
      NR    =-0.01022*0.5*RHO*L**4
      NV    =-0.00769*0.5*RHO*L**3
      NDRS =-0.377*YDRS*L
      NDRB =+0.283*YDRB*L
C
C THE FILE USED IN THE FIRST STATEMENT WILL VARY DEPENDING UPON
C  THE RUN BEING ANALYZED AND THE SOURCE OF DATA
C
      OPEN (10,FILE='SIMTODR.RES',STATUS='OLD')
      OPEN (11,FILE='XY1.RES',STATUS='NEW')
      OPEN (12,FILE='XY2.RES',STATUS='NEW')
      OPEN (13,FILE='XY3.RES',STATUS='NEW')
      OPEN (14,FILE='LAT.RES',STATUS='NEW')
      OPEN (20,FILE='TRUAUV1.RES',STATUS='NEW')
      OPEN (21,FILE='TRUAUV2.RES',STATUS='NEW')
C
C     VARIABLE INITIALIZATION
C
      ISIM=10000
      TWOPI =8.0*ATAN(1.0)
      PI    =0.5*TWOPI
      IECHO =10
      IPRNT =1
      JPRNT =0
      IJ    =0
      JE    =0
      DELTA =0.1
      V=0.0
C

C THE INITIAL AUV II POSITION IN THE POOL MUST BE ENTERED BASED
C  ON KNOWN RANGE INFORMATION FROM THE DATA FILE OR OTHER SOURCE.
C  DWELL TIME AT THE BEGINNING OF THE RUN MUST ALSO BE ENTERED TO
C  PROPERLY CORRECT PSI FOR GYRO DRIFT.
C  ONCE THE INITIAL RANGES ARE ENTERED THE INITIAL AUV II POSITION
```

```
C  IN THE POOL IS COMPUTED BASED ON THE LENGTH (LPOOL) AND WIDTH
C  (WPOOL) OF THE POOL.
C
      WRITE (*,*) 'ENTER INITIAL RANGE FROM LEFT SONAR SENSOR
      READ (*,*) RLRNG
      WRITE (*,*) 'ENTER INITIAL RANGE FROM FORWARD SONAR SENSOR
      READ (*,*) RFRNG
      WRITE (*,*) 'ENTER DWELL TIME
      READ (*,*) TDWELL
      WPOOL=60
      LPOOL=117
      XSTART=LPOOL-RFRNG
      YSTART=WPOOL-RLRNG
C
C COMPUTE THE COEFFICIENTS OF THE A AND B MATRICIES
C
      A1=MASS-YVDOT
      A2=MASS*XG-YRDOT
      A3=YR-MASS
      A4=YV
      A5=YDRS
      A6=YDRB
      B1=MASS*XG-NVDOT
      B2=IZ-NRDOT
      B3=NR-MASS*XG
      B4=NV
      B5=NDRS
      B6=NDRB

      DEN=A1*B2-A2*B1
C
      AA11=(A4*B2-A2*B4)/DEN
      AA12=(A3*B2-A2*B3)/DEN
      AA21=(A4*B1-A1*B4)/(-DEN)
      AA22=(A3*B1-A1*B3)/(-DEN)
      BB11=(A5*B2-A2*B5)/DEN
      BB12=(A6*B2-A2*B6)/DEN
      BB21=(A5*B1-A1*B5)/(-DEN)
      BB22=(A6*B1-A1*B6)/(-DEN)
      BB1=BB11-BB12
      BB2=BB21-BB22
C
C ENTER THE TIME CONSTANT OF THE LATERAL MOTION OBSERVER
C
      WRITE (*,*) ' ENTER V-OBSERVER TIME CONSTANT'
      READ  (*,*) TVOBS
      GAIN=(AA11+1.0/(TVOBS*L))/AA21
      WRITE (*,*) GAIN
C
      IJ=0
```

```
      JE=0
C
C     SIMULATION BEGINS
C
      DO 100 I=1,ISIM
C
C THIS PROGRAM BE USED TO EITHER USE DATA FILES WRITTEN DURING
C AUV II TRIAL RUNS, OR A SEPARATELY GENERATED DATA FILE.
C Some early AUV II files had an ERR1 field after RANGE1, and
C  an ERR2 field after RANGE2. If the file beingg used has these
C  fields, the following statement must be modified.
C
C      READ (10,*,END=500) TIME,XPOSE,YPOSE,ZPOSE,PHIE,THETAE,PSIE,
C     &                    PE,QE,RE,DRE,DSE,RANGE1,RANGE2,
C     &                    SPEEDE,RPMORD,RRPM,LRPM
C
C THIS STATEMENT IS USED TO READ A SEPARATELY GENERATED FILE OF
C  DATA FROM SIMAUV
C
      READ (10,*,END=500) TIME,XPOSE,YPOSE,PSIE,SPEEDE,DRE,RE
C
C The following statements transfer the actual AUV II data to
C  variables used in the computation of various positions. The 111
C  jump statement is used to establish initial positions for only
C  the first time step.
C  X1POS,Y1POS,PSIMX,PSIMY: Track position for simulated AUV II
C  X2POS,Y2POS,PNOVX,PNOVY: Track position for track without V
C  X3POS,Y3POS,POSDRX,POSDRY: Track position as determined using
C                     Reduced order observer
C
      IF (I.NE.1) GO TO 111
      X1POS = XPOSE
      Y1POS = YPOSE
      X2POS = XPOSE
      Y2POS = YPOSE
      X3POS = XPOSE
      Y3POS = YPOSE
111   PSI   = PSIE
      U     = SPEEDE
      R     = RE
C
C These statements apply actual rudder positions to the DR proram
C
      DRS = DRE
      DRB =-DRE
C
C These statements calculate the reduced order observer "constants"
C
      IF (U .EQ. 0.0) GO TO 1009
      KK    = (BB1*AA21-BB2*AA11)*U
```

```
      T3     = BB2/KK
      KV     = (BB2*AA12-BB1*AA22)*U
      T4     = BB1/KV
C
C The Simulated AUV II position is provided from the input data
C
      X1POS=XPOSE
      Y1POS=YPOSE
C
C REDUCED ORDER OBSERVER FOR V
C
      OVDOT=(AA11*U-GAIN*AA21*U)*OV+(AA12*U-GAIN*AA22*U+
     &         (AA11*U-GAIN*AA21*U)*GAIN)*R+(BB11-GAIN*BB21)*
     &         U*U*DRS+(BB12-GAIN*BB22)*U*U*DRB
      OV    =OV+DELTA*OVDOT
      VHAT  =GAIN*R+OV
      V1    =VHAT
      X3DOT=U*COS(PSIE)-V1*SIN(PSIE)
      Y3DOT=U*SIN(PSIE)+V1*COS(PSIE)
      X3POS=X3POS+DELTA*X3DOT
      Y3POS=Y3POS+DELTA*Y3DOT
C
C Calculate the Simulated AUV II postion without V information
C
      X2DOT  =U*COS(PSIE)
      Y2DOT  =U*SIN(PSIE)
      X2POS=X2POS+DELTA*X2DOT
      Y2POS=Y2POS+DELTA*Y2DOT
1009  CONTINUE
C
C NOW THAT ALL THE X & Y POSITIONS HAVE BEEN CALCULATED, TRANSFORM
C  THE POSITIONS INTO POOL COORDINATES
C
C "TRUE" SIMULATED POSITION
C
      PSIMX=XSTART+X1POS
      PSIMY=YSTART-Y1POS
C
C  SIMULATED AUV II POSITION, WITHOUT V INFORMATION
C
      PNOVX=XSTART+X2POS
      PNOVY=YSTART-Y2POS
C
C ENHANCED POSITION ESTIMATE
C
      POSDRX=XSTART+X3POS
      POSDRY=YSTART-Y3POS
      JE=JE+1
      IF (JE.NE.IECHO) GO TO 99
      WRITE (*,*) TIME
```

```
      JE=0
99    J=J+1
      IF (J.NE.IPRNT) GO TO 100
      IJ=IJ+1
      TIME=I*DELTA
      WRITE (11,*) X1POS,Y1POS
      WRITE (12,*) X2POS,Y2POS
      WRITE (13,*) XXPOS,Y3POS
      WRITE (14,*) V,V1
      WRITE (20,*) TIME,PSIMX,PSIMY,PNOVX,PNOVY
      WRITE (21,*) POSDRX,POSDRY,PSI,PSIE
      J=0
100   CONTINUE
500   STOP
      END
```

## APPENDIX D: BIBLIOGRAPHY

This appendix contains a chronological listing of all theses written through the end of 1991 dealing with the NPS Autonomous Underwater Vehicle Project.


Putman, R. "Conceptual Design of an Inertial Navigation system for an Autonomous Underwater Vehicle," Master's Thesis, Naval Postgraduate School, Monterey, California, September 1987.

Boncal, R.J. "A Study of Model Based Maneuvering Controls for Autonomous Underwater Vehicles," Master's Thesis, Naval Postgraduate School, Monterey, California, December 1987.

Thompson, C.A. "A Conceptual Design of a Hovering System Controller for an Autonomous Underwater Vehicle," Engineer's Thesis, Naval Postgraduate School, Monterey, California, December 1987.

Brunner, G.M., "Experimental Verification of AUV Performance," Engineer's Thesis, Naval Postgraduate School, Monterey, California, December 1987.

Delaplane, S.W., "Preliminary Design and Cycle Verificatioon of a Digital Autopilot for Autonomous Underwater Vehicles," Master's Thesis, Naval Postgraduate School, Monterey, California, March 1988

Farren, M., "Some Experiments with Acoustic Signal Returns Relative to Obstacle Identification for AUV Operations," Master's Thesis, Naval Postgraduate School, Monterey, California, March 1988.

MacPherson, D.L., "Computer Simulation Study of Rule-Based Control of an Autonomous Underwater Vehicle," Master's Thesis, Naval Postgraduate School, Monterey, California, June, 1988.

Smith, W. "Local Path Planning Using Optimal Control Techniques," Master's Thesis, Naval Postgraduate School, Monterey, California, June 1988.

Larsen, K.P., "Reduced Hydrodynamic Modelling for a Submersible Vehicle," Master's Thesis, Naval Postgraduate School, Monterey, California, September 1988.

Sanders, D.W., "A Feasibility Study in Path Planning using Optimization Techniques," Master's Thesis, Naval Postgraduate School, Monterey, California, December 1988.

Reina, G.J., "AUV Dive Control Development Including Sensor Bias Compensation and Parameter Estimation," Master's Thesis, Naval Postgraduate School, Monterey, California, December 1988.

Schwartz, M., "Kalman Filtering for Adaptive Depth, Steering, and Roll Control of an AUV," Master's Thesis, Naval Postgraduate School, Monterey, California, March 1989.

McDonald, G.S., "Model Based Design and Verification of a Rapid Dive Controller for an Autonomous Underwater Vehicle," Engineer's Thesis, Naval Postgraduate School, Monterey, California, March 1989

Nordman, D.B., "A Computer Simulation Study of Mission Planning and Control for the NPS Autonomous Underwater Vehicle," Master's Thesis, Naval Postgraduate School, Monterey, California, September 1989.

Lorhammer, D., "An Experimental Study of an Acoustic Ranging System for AUV Obstacle Avoidance," Master's Thesis, Naval Postgraduate School, Monterey, California, September 1989.

Davis, M., "Real-time Adaptive Control of an AUV," Master's Thesis, Naval Postgraduate School, Monterey, California, September 1989.

Joo-No Sur, "Design and Investigation of a Dive Plane Sliding Mode Compensator for an Autonomous Underwater Vehicle," Master's Thesis, Naval Postgraduate School, Monterey, California, September 1989.

Good, M.R., "Design and Construction of the Second Generation AUV," Master's Thesis, Naval Postgraduate School, Monterey, California, December 1989.

Rogers, R.C., "A Study of 3-D Visualization and Knowledge Based Mission Planning and Control for the NPS Model 2 Autonomous Underwater Vehicle," Master's Thesis, Naval Postgraduate School, Monterey, California, December 1989.

Friend, J. "Design of a Navigator for a Testbed Underwater Vehicle," Master's Thesis, Naval Postgraduate School, Monterey, California, December 1989.

Williams, M. "Real-Time Implementation of an Adaptive Depth Controller for a Submersible," Master's Thesis, Naval Postgraduate School, Monterey, California, September 1989.

Saunders, T. "Performance of Small Thrusters and Propulsion Systems," Master's Thesis, Naval Postgraduate School, Monterey, California, March 1990.

Riling, D., "Real-Time Implementation of an Autopilot and Signal Processor for an Autonomous Underwater Vehicle," Master's Thesis, Naval Postgraduate School, Monterey, California, March 1990.

Lienard, D., "Multivariable Sliding Mode Control for AUV Autopilots," Engineer's Thesis, Naval Postgraduate School, Monterey, California, June 1990.

Ong, S.M., "A Mission Planning Expert System with 3-Dimensional Path Optimization for the NPS AUV II Autonomous Underwater Vehicle," Master's Thesis, Naval Postgraduate School, Monterey, California, June 1990.

Cloutier, M.J. "Guidance and Control System for an Autonomous Vehicle," Master's Thesis, Naval Postgraduate School, Monterey, California, June 1990.

Chism, S., "Robust Path Tracking of Autonomous Underwater Vehicles Using Sliding Modes," Engineer's Thesis, Naval Postgraduate School, Monterey, California, September 1990.

Hawkinson, T., "Multiple Input Sliding Mode control for Autonomous Diving and Steering of Underwater Vehicles," Engineer's Thesis, Naval Postgraduate School, Monterey, California, December 1990.

Jurewicz, T., "Graphical Simulation of the NPS AUV II," Master's Thesis, Naval Postgraduate School, Monterey, California, December 1990.

McLean, M., "Dynamic Response of Small Thrusters," Master's Thesis, Naval Postgraduate School, Monterey, California, March 1991.

Zaring, R., "Damping of Schuler Oscillations," Master's Thesis, Naval Postgraduate School, Monterey, California, March 1991.

Leatherman, B., "An Approach to the Integration of Real Time Software for the NPS AUV II," Master's Thesis, Naval Postgraduate School, Monterey, California, June, 1991.

Murphy, B., "Segmentation and Estimation of Images," Master's Thesis, Naval Postgraduate School, Monterey, California, June 1991.

Swanadee, P. "Orientation Guidance and Control for Marine Vehicles in the Horizontal Plane," Master's Thesis, Naval Postgraduate School, Monterey, California, June 1991.

Floyd, C., "Design and Implementation of a Collision Avoidance System for the NPS AUV II Utilizing Ultrasonic Sensors," Master's Thesis, Naval Postgraduate School, Monterey, California, September 1991.

Papasotiriou, A., "Three Dimensional Pursuit, Guidance and Control for Submersibles," Master's Thesis, Naval Postgraduate School, Monterey, California, September 1991.

Magrino, C., "A 3-Dimension Guidance System for the NPS AUV II," Master's Thesis, Naval Postgraduate School, Monterey, California, September 1991.

Marsilio, A., "Use of Hopfield Networks in Parameter Identification," Master's Thesis, Naval Postgraduate School, Monterey, California, September 1991.

Bonsignore, J., "Underwater Multidimensional Path Planning Using Real World Constraints for the NPS AUV II," Master's Thesis, Naval Postgraduate School, Monterey, California, September 1991.

Caddell, T.W., "Three Dimensional Path Planning Using Real World Constraints for the NPS AUV II," Master's Thesis, Naval Postgraduate School, Monterey, California, September 1991.

Wilkinson, W.P., "An Onboard Expert System for the NPS AUV II," Master's Thesis, Naval Postgraduate School, Monterey, California, September 1991.

Warner, D.C., "Design, Simulation, and Experimental Verification of a Computer Model and Enhanced Position Estimator for the NPS AUV II," Engineer's Thesis, Naval Postgraduate School, Monterey, California, December 1991.

## LIST OF REFERENCES


1. Polmar, W., "Robot Submarines," *Proceedings*, Naval Institute Press, September 1991, pp. 122-123.

2. Pappas, G., *et al.*, *The Darpa/Navy Unmanned Undersea Vehicle Program*, *Unmanned Systems*, Spring 1991, pp. 24-30.

3. "Proceedings of the Symposium on Autonomous Underwater Vehicle Technology," IEEE Catalog No. 90CH2856-3, June 5-6, 1990, Washington, D.C.

4. *Proceedings*, IARP 1st Workshop on Mobile Robots for Subsea Environments, MBARI, Monterey, California, October 23-26, 1990.

5. Healey, A.J., Cristi, R., Smith, D.L., McGhee, R.B., "Navigation, Path Planning, Dynamics and Control of Generic Autonomous Underwater Vehicles Proposal," Research Proposal to Naval Postgraduate School Direct Research Fund, Monterey, California, April 1988.

6. Healey, A.J., *et al.*, "Mission Planning, Execution, and Data Analysis for the NPS Autonomous Vehicle," *Proceedings*, IART 1st Workshop on Mobile Robots for Subsea Environments, MBARI, Monterey, California, pp. 177-186, October 23-26, 1990.

7. Brunner, G.M., "Experimental Verification of AUV Performance," Engineer's Thesis, Naval Postgraduate School, Monterey, California, March 1988.

8. Good, M., "Design and Construction of a Second Generation Autonomous Underwater Vehicle," Master's Thesis, Naval Postgraduate School, Monterey, California, December 1989.

9. Boncal, R.J., "A Study of Model Based Maneuvering Controls for Autonomous Underwater Vehicles," Master's Thesis, Naval Postgraduate School, Monterey, California, December 1987.

10. Smith, N.S., Crane, J.W., Summey, D.C., SDV Simulator Hydrodynamic Coefficients (U), Technical Memorandum NCSC-TM231-78, Naval Coastal Systems Center, Panama City, Florida, June 1978.

11. McDonald, G.S., "Model Based Design and Verification of a Rapid Dive Controller for an Autonomous Underwater Vehicle," Engineer's Thesis, Naval Postgraduate School, Monterey, California, March 1989.

12. Sur, J.N., "Design of a Dive Plane Sliding Mode Compensator for an Autonomous Underwater Vehicle," Master's Thesis, Naval Postgraduate School, Monterey, California, September 1989.

13. Lienard, D., "Sliding Mode Control for Multivariable AUV Autopilots," Engineer's Thesis, Naval Postgraduate School, Monterey, California, June 1990.

14. Papoulias, F.A., and Healey, A.J., "Path Tracking of Surface Ships Using Multivariable Sliding Mode Control," *Proceedings*, 9th Ship Control Systems Symposium, Washington, D.C., September 10-14, 1990.

15. Chism, S., "Robust Control of Guidance Laws," Engineer's Thesis, Naval Postgraduate School, Monterey, California, December 1990.

16. Hawkinson, T.D., "Multiple Input Sliding Mode Control for Autonomous Diving and Steering of Underwater Vehicles," Master's Thesis, Naval Postgraduate School, Monterey, California, December 1990.

17. Papasotiriou, A., "Three Dimensional Pursuit, Guidance and Control for Submersibles," Master's Thesis, Naval Postgraduate School, Monterey, California, September 1991.

18. Clothier, M., "Guidance and Control System for an Autonomous Vehicle," Master's Thesis, Naval Postgraduate School, Monterey, California, June 1990.

19. Farren, M., "Some Experiments with Acoustic Signal Returns Relative to Obstacle Identification for AUV Operations," Master's Thesis, Naval Postgraduate School, Monterey, California, March 1988.

20. Lorhammer, D., "An Experimental Study of an Acoustic Ranging System for AUV Obstacle Avoidance," Master's Thesis, Naval Postgraduate School, Monterey, California, September 1989.

21. Floyd, C., "Design and Implementation of a Collision Avoidance System for the NPS AUV II Utilizing Ultrasonic Sensors," Master's Thesis, Naval Postgraduate School, Monterey, California, September 1991.

22. Saunders, T., "Performance of Small Thrusters and Propulsion Systems," Master's Thesis, Naval Postgraduate School, Monterey, California, March 1990.

23. McLean, M., "Dynamic Response of Small Thrusters," Master's Thesis, Naval Postgraduate School, Monterey, CA,, March 1991.

24. Comstock, John P., ed., *Principles of Naval Engineering*, The Society of Naval Architects and Marine Engineers, New York, NY, 1967.

25. Clarke, D., Gedling, P., and Hine G., "The Application of Manoeuvering Criteria in Hull Design Using Linear Theory," *The Royal Institute of Naval Architects*, pp. 45-68, March, 1983.

26. Taggert, R., ed., *Ship Design and Construction*, The Society of Naval Architects and Marine Engineers, New York, NY 1980.

27. Friedland, B., *Control System Design, An Introduction to State-Space Methods*, McGraw-Hill, New York, NY 1986.

28. Bahrke, Fred, "Parameter Identification and Sliding Mode Control for the NPS AUV II," research in progress for Engineer's Degree, Naval Postgraduate School, Monterey, California, March 1992.

## INITIAL DISTRIBUTION LIST

| | | No. of Copies |
|---|---|---|
| 1. | Defense Technical Information Center<br>Cameron Station<br>Alexandria, Virginia 22304-6145 | 2 |
| 2. | Library, Code 52<br>Naval Postgraduate School<br>Monterey, California, 93943-5002 | 2 |
| 3. | Dr. A.J. Healey, Code ME<br>AUV Project<br>Department of Mechanical Engineering<br>Naval Postgraduate School<br>Monterey, California 93940 | 2 |
| 4. | Prof. Fotis Papoulias, Code ME/Pa<br>Department of Mechanical Engineering<br>Naval Postgraduate School<br>Monterey, California 93940 | 1 |
| 5. | David C. Warner<br>20 Starr St.<br>New London, Connecticut 06320 | 1 |
| 6. | Paul Heckman, Code 943<br>Naval Ocean Systems Center<br>San Diego, California 92152 | 1 |
| 7. | Robert Wilson<br>Head, Systems Engineering Branch<br>David Taylor Research Center<br>Carderock, Bethesda, Maryland 20084-5000 | 1 |
| 8. | Dan Steiger, Marine Systems Group<br>Naval Research Laboratory<br>Washington, D.C. 20032 | 1 |
| 9. | Mr. Kirk Dye<br>Naval Coastal Systems Center<br>Panama City, Florida 32407-5000 | 1 |

10. Technical Library
Naval Surface Warfare Center
Silver Spring, Maryland 20901 — 1

11. Radm. Evans, Code SEA-92
Naval Sea Systems Command
Washington, D.C. 20362 — 1